# On the design of a hybrid actuated hand prosthesis

## Master Thesis


A.L. Hoek

**Supervisor:**
Dr. ir. Dick Plettenburg


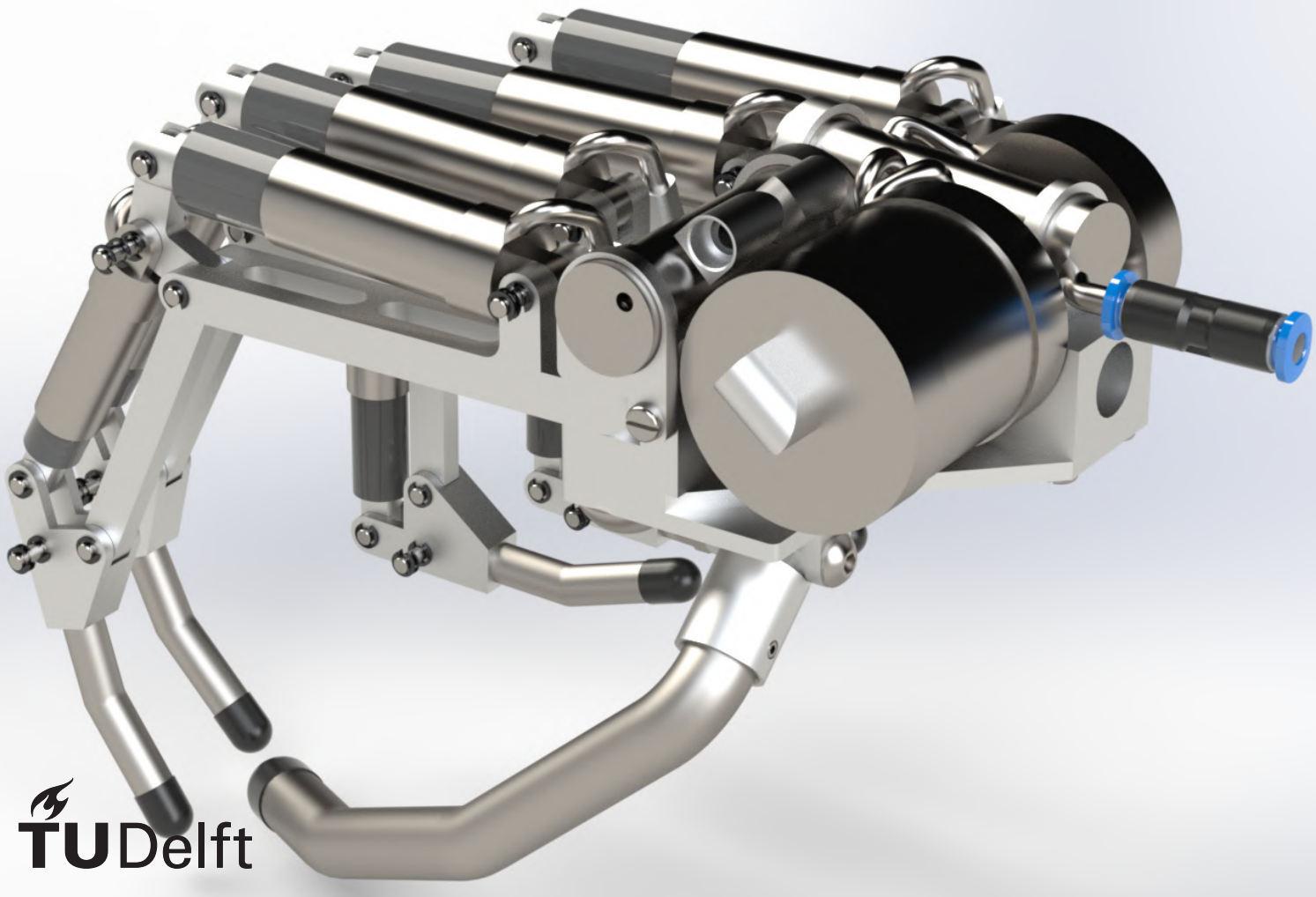

TU Delft

# On the design of a hybrid actuated hand prosthesis

## Master Thesis

by

A.L. Hoek

to obtain the degree of Master of Science
at the Delft University of Technology,
to be defended publicly on Friday September 25, 2020 at 10:00 AM.

| | | |
|---|---|---|
| Student number: | 4445058 | |
| Project duration: | November 11, 2019 – September 25, 2020 | |
| Thesis committee: | Dr. ir. D. H. Plettenburg, | TU Delft, supervisor |
| | Prof. dr. F. C. T. van der Helm, | TU Delft |
| | Dr. ir. T. Horeman-Franse, | TU Delft |

An electronic version of this thesis is available at http://repository.tudelft.nl/.

TU Delft

# Preface

Before starting out with this graduation project I performed a literature study on pneumatically powered hand prostheses. This literature study is titled “Advances in Pneumatically Powered Hand Prostheses since 2000” and the paper that I wrote can be found in appendix A. This paper builds upon the inventory of pneumatically powered hand prostheses by Dick Plettenburg from 2002 [7], called “Pneumatically Powered Prostheses: An Inventory”. Together these two inventories give an overview of the efforts that have been made by researchers to develop pneumatically powered hand prostheses ever since the first design dating back to 1877. Modern advances in the field of pneumatically powered hand prostheses are making them an ever more attractive option for people in need of a hand prosthesis. This graduation project is, therefore, focuses on the field of a pneumatically powered hand prostheses.

After five years as a student, the end is now in sight. This thesis details the efforts made during my graduation research and, therefore, the last step towards my graduation. Throughout my Bachelor, Honours and Master program I have worked on many projects, each one more fun and challenging than the last one, however, this graduation project has both been the nicest and most challenging project of them all. It is a shame that this period in my life is coming to an end, but it is time to take the next step.

I would like to thank Dick Plettenburg for his supervision and invaluable input throughout this whole project. Furthermore, I would like to thank Jan van Frankenhuyzen for his input on the design of the prototype and help with realizing it. Moreover, I would like to thank Frans van der Helm for his feedback on the draft version of this report. I would also like to thank Reinier van Antwerpen for producing the parts of the prototype and helping with the assembly. Finally, I would like to thank my dad Arie Hoek, my mom Leonor Arrebola Aranda, my brother Leo Hoek and my girlfriend Alexis Cuevas Landeros for their support and motivation throughout my whole career. I could not have done this without a single one of you!

*A.L. Hoek*
*Delft, September 2020*

# Abstract

Hand prostheses commonly advertise on three main selling points: strength, speed and lightweight. Most conventional hand prostheses are only able to combine two of these three attributes. Therefore, combining all three attributes into a single device can result in a commercially attractive hand prosthesis. Another interesting point, particularly for pneumatic prostheses, is the usage time, as historically many have run into problems here and an extended usage time makes it attractive to the user. The goal of this graduation research is, therefore, to design a pneumatically powered hand prosthesis, that combines a high grip strength, a high opening/closing speed and lightweight into a single device, whilst maintaining a reasonable usage time. A hybrid actuated hand prosthesis is designed that combines a finger design based upon the Delft Cylinder Hand, with dual-mode actuation. This dual-mode actuation increases the efficiency of the hand and consist of a $CO_2$ supply with a hydraulic transmission to the fingers. A final prototype of the dual-mode actuation transmission is fabricated and evaluated. Although there is room for improvement in the resistance and timing of the system, the hand has a relatively high pinch force of an estimated 56 N. Furthermore, a grip speed of less than a second makes the hand attractive to be used. With a mass of only 235 grams, the hand weighs less than most of its competitors and is comfortable in use. The dual-mode actuation significantly increases the efficiency of the hand and gives it a usage time of over 400 cycles.

# Contents

# 1

# Introduction

In this chapter the topic of this master thesis will be introduced and its goal will be made clear. Section 1.1 will detail the initial research idea and section 1.2 will build on this with a second source of inspiration. Finally, section 1.3 will describe the goal of this graduation project and provides an overview of the structure of this report.

## 1.1. 1919 hand

Initially this graduation project started out with the idea to perform research on the pneumatically actuated “1919 hand” [1], which is shown in figure 1.1, and to see if this prosthesis could be recreated or used to create a new design for a pneumatically actuated hand prosthesis.

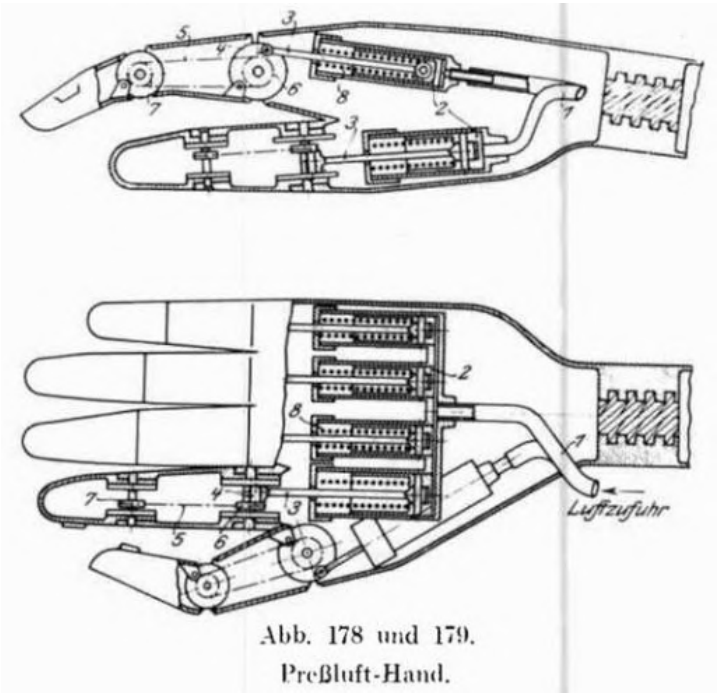


Figure 1.1: Design of an adaptive pneumatically powered hand prosthesis from the year 1919 [1]. The hand features five pneumatic actuators with built-in return springs, that each actuate one finger through a rod and crank mechanism. The pneumatic pressure is divided over the actuators evenly, as they are connected to a single air supply, making the hand underactuated.

The 1919 hand consists of five fingers, consisting of two phalange links each, that each have their own pneumatic actuator. This pneumatic actuator consists of a fixed cylinder in which a piston, that is kept in place by a compression spring, slides. A rod is attached on one end to an axis that runs

throughout the piston, which allows the rod to rotate with respect to the piston, and the other end is attached to a pulley that is attached to the first link of the finger. Therefore, the pneumatic actuator acts as a rod and crank mechanism; When the pneumatic actuator is pressurized the piston will slide outwards, overcoming the force exerted by its return spring, and it will push the rod forward, which in turn will rotate the pulley around its axis. As the pulley is attached to the finger, the finger will bend once the pneumatic actuator is pressurized. The movement of the distal link of the finger is coupled to the movement of the proximal link of the finger through a belt. This belt runs around the pulley that is connected to the proximal link with its axis in the palm of the hand, and the other pulley that is connected to the distal link with its axis in the proximal link. Due to this belt and pulley system, the distal link will bend with respect to the proximal link once the proximal link bends with respect to the palm of the hand, thus closing the hand. When the pneumatic actuator is depressurized, the built-in return spring will return the hand to its initial, opened position.

The pneumatic actuators of the hand are all connected to the same pneumatic supply, which means that the pressure within them is equal. This means that if the hand is closed and for example one finger hits an object, causing the pressure inside its actuator to rise, the other fingers will keep closing until they too hit an object or their limit, as the pressure is the same inside them all. This makes this hand prosthesis adaptive, as it uses a single pneumatic supply to control five fingers that are able to grasp a wide range of objects, as they are able to adapt to it.

The integrated return springs and the adaptive movement of this hand make it a very attractive hand prosthesis, especially for its time, as it allows the hand to grasp a wide range of objects and returns the hand to its initial position passively. However, there are no records of the hand ever actually being built or tested. Therefore, it is unknown whether the hand works as intended and if the attributes that make it interesting actually result in an attractive performance. That is why this looked like an interesting topic for this graduation project, and the goal was set to:

*Design a hand prosthesis based upon the blueprints of the “1919 hand”, and fabricate and test this pneumatically powered hand prosthesis to uncover its performance.*

The very first step that was taken was to recreate the exact design of the 1919 hand in SOLIDWORKS. Figure 1.2 shows an overview of the model that was created. The belt and return spring are not visible in the model but are added virtually through “mates”. This turned out to be a good step, because when the actuator was moved, it turned out that only the whole finger bends, and not the links with respect to each other. When looking into further detail, this makes sense; The first pulley appears to be rigidly attached to the proximal link, which means that they cannot rotate with respect to each other. The axis of the other pulley is attached to the proximal link and as this pulley is coupled to the first pulley by a belt, it will also not be able to rotate with respect to the proximal link. Therefore, the finger cannot bend at all, it can only be moved downwards by the pneumatic actuator.

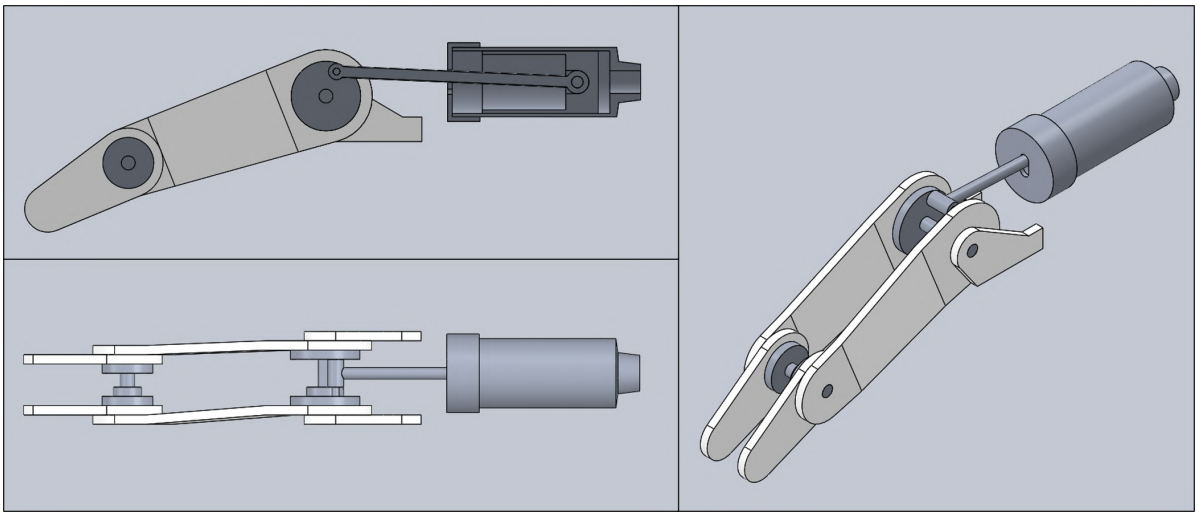

Figure 1.2: Recreation of an actuated finger of the 1919 hand prosthesis in SOLIDWORKS. Top left: Cross section of the finger and actuator. Bottom left: Top view of the finger and actuator. Right: overview of the finger and actuator.

As it turns out the design of the 1919 hand as shown in figure 1.1 does not work as intended for a hand prosthesis, and this could be the reason why it was never made or tested.

## 1.2. Delft Cylinder Hand

As the aforementioned 1919 hand did not turn out to work as intended, the topic of this graduation project was re-evaluated. Another possible interesting direction could be to redesign the body powered Delft Cylinder Hand in order to power it pneumatically. The Delft Cylinder Hand [9], as shown in figure 1.3 is a very promising hand prosthesis, as it is very lightweight compared to its competitors, while simultaneously offering competitive grip forces.

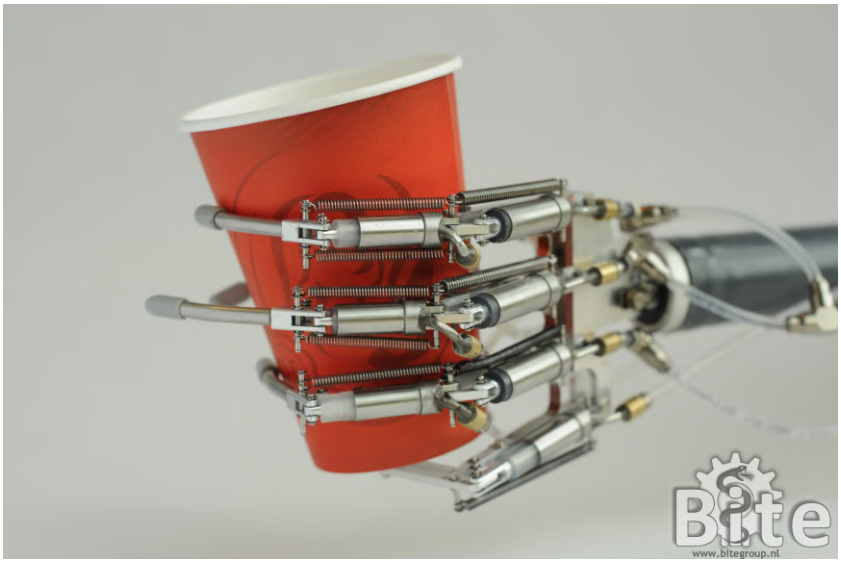


Figure 1.3: Image of the Delft Cylinder Hand [9] without its cosmetic cover and holding a coffee cup.

This topic, however, was deemed to be too specific, as I might be able to come up with other designs for pneumatically powered hand prostheses, that work even better than when being restrained to the Delft Cylinder Hand. On the other hand, like the 1919 hand, the Delft Cylinder Hand shows many promising aspects, and could therefore be used as a source of inspiration.

## 1.3. Assignment

Hand prostheses commonly advertise on three main selling points, namely:

- *Strength* How much force the hand can exert on an object. A high grip strength means that a larger range of objects can be grasped, and more different tasks can be performed using the prosthetic hand.
- *Speed* How fast the hand can be opened and closed. If the hand closes or opens too slow, the user might get annoyed by this delayed response. A high opening and closing speed increases the interaction between the user and the prosthetic hand.
- *Lightweight* How low the overall weight of the prosthetic hand is. A lower mass means that less effort from the user is required when moving the prosthetic hand or the user's arm.

Most conventional hand prostheses are, however, only able to combine two of these three attributes. Figure 1.4 shows a Venn diagram of these attributes, including four overlapping areas, and most conventional hand prostheses are located in areas A, B and C.

**A** These hand prostheses combine strength and speed but are heavy. An example of this are hand prostheses using conventional pneumatic cylinders. These cylinders are very strong and fast acting; however, they are bulky and relatively heavy.

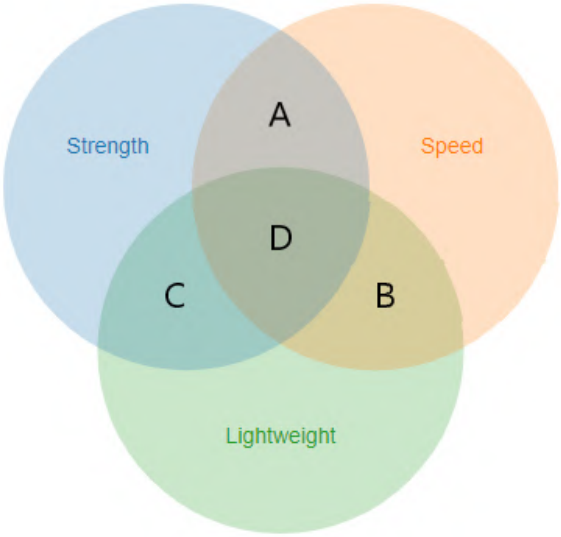


Figure 1.4: Venn diagram of common hand prosthesis selling points.

**B** These hand prostheses combine speed and lightweight but are weak. An example of this are soft pneumatic hand prostheses, which are discussed in the literature review in appendix A. These hands are hollow and made of soft material which inflates when pressurized. The hollow construction and soft materials make these prostheses lightweight and they close fast once pressurized and inflated. However, the soft materials and low allowable pressures severely reduce the strength of the hand.

**C** These hand prostheses combine strength and lightweight but are relatively slow. An example of this are hand prostheses using lightweight electric DC motors. These motors require a large transmission in order to convert their high angular velocity into a high torque. The big transmission ratio that is needed to achieve strength, however, severely reduces the speed of the hand.

For a new design of a hand prosthesis it would, therefore, be an interesting selling point to combine all the three aforementioned categories into a single device and thus belong in area **D**. Another interesting point, particularly for pneumatic prostheses, is the usage time. Pneumatic prostheses rely on a gas cartridge to supply the gas needed for actuation, however, only a limited amount of gas can be brought along. Therefore, the prosthesis needs to be efficient enough to be used for a sufficient amount of time, without running out of gas. Historically, many pneumatic hand prostheses have run into problems with usage time and, therefore, this should be taken into account for this new design. Combining this attribute with the aforementioned attributes in area **D**led to the goal for this graduation project, namely to:

***Design a pneumatically powered hand prosthesis, that combines a high grip strength, a high opening/closing speed and lightweight into a single device, whilst maintaining a reasonable usage time.***

The next chapter will detail exactly which (quantitative) requirements are set for this new design, indicating what needs to be achieved in order to reach this goal.

Due to the limited time available for this project, this research will focus on the mechanical design of the hand prosthesis itself, and therefore the control of the hand and the gas supply to the hand were deemed to be out of scope for this project.

This research was performed under the supervision of Dick Plettenburg and as part of the Delft Institute of Prosthetics and Orthotics (DIPO) group, which is part of the BioMechanical Engineering Department of the Faculty of Mechanical, Maritime, and Materials Engineering at the Delft University of Technology.

### 1.3.1. Looking forward

Chapter 2 will describe the requirements that were set on the design of the pneumatically powered hand prosthesis. Next, chapter 3 will detail the concepts made to fulfill these requirements and the selection thereof. Chapter 4 builds on the selected concept and details the complete design for the pneumatically powered hand prosthesis. Hereafter, chapter 5 describes the process of creating a prototype for this hand prosthesis and the manufacturing thereof. Next, chapter 6 goes in on the tests performed with this prototype and the results that were obtained with them. Thereafter, chapter 7 discusses the results that were found and the observations made during the project. Finally, chapter 8 will conclude this project.

# 2

# Requirements

Before starting to design the pneumatically powered hand prosthesis, the requirements for it need to be clear. This chapter will, therefore, detail the requirements set for the prosthetic hand and how they were determined. Even though, the requirements are numbered they are all considered to be equally important. The definition of the list of requirements was an iterative process as a balance needed to be found between wishes and reality. Furthermore, it is hard to make an exact list of requirements when it is not yet known what the prosthesis will look like or how it will work. Therefore, the requirements are generalized as much as possible. At the end of this report I will reflect back on this list of requirements, to compare the actual performance to what was required.

The first requirement is on the total mass of the hand prosthesis (excluding the controller or gas supply). An adult male hand weighs around 400-450 grams [2]. A hand prosthesis, however, should weigh less than this, as the weight of a human hand is well distributed over the arm, as it is attached with muscles, tendons and skin, while the weight of the hand prosthesis is concentrated at the socket that connects it to the residual limb. Kay and Rakic, and Pons et al. [4, 8], therefore, state that a hand prosthesis should weigh less than 375 grams. This is, however, still quite a lot of weight, and as there are already many lighter designs for hand prostheses it is also not really a challenge. One of the lightest pneumatically actuated adult hand prostheses, is the Delft Cylinder Hand that was mentioned earlier [9], which has a mass of 273 grams. To make it a challenge, the requirement of the mass for the hand prosthesis was therefore set at a maximum of 250 grams.

> **Req. 1: Mass.** *The total mass of the prosthetic hand (excluding control and supply) should not exceed 250 grams.*

The second requirement is on the grip strength of the hand prosthesis. As the grip strength depends on the position and orientation of the hand, the grip strength was defined for a precision grip using one finger and is thus measured as the maximum force at the tip of a finger. According to Weir [10], a maximum precision grip strength of 68 N is needed in everyday life. For a hand prosthesis this a very high force, and the Delft Cylinder Hand, for example, can only exert 30 N using a precision grip with *two* fingers. For the current design of a pneumatically powered hand prosthesis the strength requirement was set at 60 N, as this is more than enough for most everyday tasks and is much more than current pneumatic hand prostheses offer.

> **Req. 2: Grip strength.** *The maximum grip force at the tip of a finger should be at least 60 N.*

The third requirement is on the size of the hand prosthesis. In order to be cosmetically similar to a real human hand, the hand prosthesis should be able to fit within the contours of a human hand, and in case a cosmetic glove will be used, slightly smaller even. Human hands come in many shapes and sizes depending on sex, age, gender, height, and even then, hands still vary in size. It is, therefore, hard to set one size for a hand prosthesis. Since I will be designing the hand, I therefore chose to use my own hand as a reference.

**Req. 3: Size.** *The prosthetic hand should fit completely inside the contours of an adult male human hand.*

The fourth requirement is on the range of motion of the hand prosthesis. The objects we grasp on a daily basis come in all kinds of shapes and sizes; they can be as small as a grain of sand, or as large as a mattress. Furthermore, they can be as light as a feather or as heavy as gym equipment. Preferably a hand prosthesis would be able to grasp them all, however, this is not realistic as even real human hands cannot grasp everything. Furthermore, hand prosthesis users frequently use an indirect grip, where they place the object in their prosthetic hand using their functional limb. For the design of the hand prosthesis the range of objects that it needs to be able to grasp, was therefore limited to objects commonly found in an office, such as a pen or a cup, but also a laptop.

**Req. 4: Motion.** *The prosthetic hand should be able to grasp differently shaped and sized common office objects, using different kinds of grip.*

The fifth requirement is on the grip speed (the time it takes to close the hand) of the hand prosthesis. The speed with which one can open or close a hand depends on many factors, such as age or training. For a hand prosthesis this depends heavily on the actuators and transmission that are used. A grip speed that is too slow can be frustrating for a prosthesis user, as he needs to wait for it to move. According to Peerdeman et al. [6], grip speeds currently range from a half to one second on average. Therefore, the design for the pneumatically powered hand prosthesis needs to be at least within this range, but preferably even lower.

**Req. 5: Grip speed.** *The prosthetic hand should be able to switch from the completely opened to completely closed position in less than one second.*

The sixth requirement is on the type of gas that is used for the hand prosthesis. As shown in the advancement of “Propellant” in my literature study in appendix A. Different kinds of gas have been used for pneumatic hand prostheses. The oldest one is air, which was used as it is commonly available, however, due to its low energy density it is not used much anymore. The most commonly used gas for pneumatic hand prostheses is at the moment carbon dioxide ($CO_2$), as it has a relatively high energy density, is non-toxic in reasonable amounts, and $CO_2$ cartridges are commonly available in stores nowadays. There are also other kinds of gasses being tested with pneumatic prostheses, however, for the design of the pneumatically powered hand prosthesis $CO_2$ will be used as this is currently the most available and proven option.

**Req. 6: Gas.** *The gas used for the pneumatic actuation of the prosthesis is carbon dioxide, $CO_2$.*

The seventh requirement is on the pressure of the aforementioned $CO_2$ that is used for the hand prosthesis. As stated in the advancement of “Pressure” in my literature study in appendix A, many different pressure levels are used for $CO_2$ in prostheses, and there is not one standard level. In his work, Doedens [3] shows, however, that using a pressure of 1.2 MPa for the $CO_2$ supply, results in the highest energy efficiency for the system. Therefore, this is also the pressure level that will be used for the design of the pneumatically powered hand prosthesis.

**Req. 7: $CO_2$ pressure.** *The pressure of the $CO_2$ supplied to the prosthetic hand should be 1.2 MPa.*

The eighth requirement is on the usage time of the hand prosthesis. Hand prostheses are used the whole day; however, the gas supply slowly depletes with each use. When the gas storage is finished, it needs to be refilled or replaced, and even though this does not take as long as it did in the past, it is still inconvenient. Therefore, the amount of times this needs to be done, needs to be minimized. It would seem reasonable to limit this to moments when the user is already taking a break and would not be bothered by taking a minute to change or refill the gas storage. Therefore, three times a day seems reasonable, as most people take breaks for breakfast, lunch and dinner. According to Limehouse and Farnsworth [5], a person performs on average 1200 grasping cycles a day and therefore a single cartridge should last at least 400 cycles.

**Req. 8: Usage time.** *The prosthetic hand should be able perform at least 400 cycles with a single $CO_2$ cartridge.*

The ninth requirement is on the loudness of the hand prosthesis. Pneumatic devices always produce some level of sound when operating, as the gas creates vibrations when moving through the components, or when it is expelled. A low level of sound is not a problem as there is always some amount of ambient noise, but your brain just filters it away. It does become problematic, however, when the noise becomes too loud, because then it will not be filtered away and when you hear it the whole day it will become annoying for you and the people around. A quiet office, which most people experience as a pleasant environment, has a loudness of about 45 dB and, therefore, this seems like an appropriate upper limit for the loudness of the pneumatically powered hand prosthesis.

**Req. 9: Loudness.** *The loudness of the sound produced by the prosthetic hand should stay below 45 dB at a distance of one meter.*

The tenth requirement is on the appearance of the hand prosthesis. Cosmetics play an important part in the choice of a prosthesis: The user wants it to look as close to the real thing as possible. Hand prostheses do not always look like human hands, as there are for example a wide range of hook prostheses available. The design of the pneumatically powered hand prosthesis, however, should be close in resemblance to a real hand and thus have four individual fingers and a thumb, connected to the palm of the hand. The movement of the hand should also be similar to that of a human hand, as otherwise the hand will still look unnatural.

**Req. 10: Cosmetic.** *The prosthetic hand should consist of four fingers and a thumb, connected to a hand palm. Furthermore, the prosthetic hand should be similar both in dimensions and movement to a real human hand.*

The eleventh requirement is on the integration of the parts of the hand prosthesis. A pneumatic hand prosthesis consists of many parts, such as the hand palm, phalanges, actuators, tubing, transmissions, etc. The pneumatically powered hand prosthesis should be a standalone device and not require many components to be worn externally (except the controller and gas supply). Therefore, all the components needed for the hand, need to be integrated within the hand itself, to make it one whole and not individual components.

**Req. 11: Integration.** *All parts of the prosthetic hand system, except the control unit and the $CO_2$ supply, should be incorporated within the hand itself.*

The twelfth requirement is on the resistance to environmental factors of the hand prosthesis. People use their hands in all kinds of different environments, including many that are not ideal for prostheses, such as corrosive environments or environments with small particles, such as sand or dust. Many hand prostheses are not resistant to such environments and rely on a cosmetic glove to keep particles or liquids out. The design of the pneumatically powered hand prosthesis should, however, be resistant to most of the common environments that a person encounters, without needing external protection. This means that the prosthesis should be water and dust proof, and thus have an IP67 or IP68 rating, and furthermore, the hand should be resistant to most everyday chemicals, such as alcohol or hydrocarbons.

**Req. 12: Environment.** *The hand prosthesis should be water and dust proof (IP67/68) and non-reactive to common chemicals and substances.*

The thirteenth requirement is on the durability of the hand prosthesis. When one buys a hand prosthesis, or any other kind of device, they expect it to keep working well for a long time. However, all devices with moving parts will at some point need maintenance or repairs to keep working well. This is generally not a problem, as long as this is not required too often. As hand prostheses are mechanisms with a lot of small moving parts, these are prone to damage or wear and thus need maintenance relatively often. Most actively powered hand prostheses, and in particular electrically powered hand prostheses, cannot even go a month without needing some form of maintenance. This seems like it would be too often and will bother the user. Therefore, maintenance should only be required a couple of times a year. For the pneumatically powered hand prosthesis a durability was chosen of at least one season, so three months, as this seems like enough time to go without being bothered and not too long to become unrealistic. Three months of usage comes down to around 100,000 cycles.

**Req. 13: Durability.** *The hand prosthesis should last at least 100,000 cycles without needing maintenance or repairs.*

The fourteenth and final requirement is on the control of the hand prosthesis. Although the control of the hand prosthesis was deemed to be out of scope for this graduation project, I wanted to make it as simple as possible for someone making the controller, which could for example be an EMG controller. Therefore, the pneumatic actuators of the hand prosthesis should be easily controllable, and if possible, using only one single valve. This means that a control module will only need to control a single valve to control the whole hand, which prevents that a lot of time and effort are needed to create a controller for the hand.

**Req. 14: Control.** *The operation of the hand prosthesis should be as simple as possible, preferably by a single valve.*

# 3

# Concepts

To go from a list of requirements to a detailed design, concepts are made first to see which direction is the most promising one to go for the design. This chapter will detail the generation and selection of the concepts made based on the requirements from chapter 2. Section 3.1 will describe all the concepts that were made, section 3.2 will describe the selection procedure of these concepts, section 3.3 will then describe the concept that was chosen in more detail, and finally section 3.4 will detail the actuation of this concept.

## 3.1. Concept generation

There are many different technologies available that can be incorporated into the concept for a pneumatically powered hand prosthesis. To narrow down the list of technologies used for generating concepts, the hand was split up into four separate attributes, namely: actuation, finger movement, joints and return mechanism. For each of the attributes the advantages and disadvantages of different technologies that could be a solution for this attribute, were listed. By comparing the (dis)advantages of different technologies with each other, the most attractive one(s) could be chosen for being used for generating concepts. Tables 3.1, 3.2, 3.3 and 3.4 show the overviews of the technologies and the (dis)advantages of each one. The most attractive technology for each of the attributes is underlined in the tables.

Table 3.1: Overview of the advantages and disadvantages of the different possible technologies for the actuation of a concept for a pneumatically powered hand prosthesis.

| **Attribute** | **Actuation** | | |
|---|---|---|---|
| **Technology** | *Soft Robotics* | *PAM* | *Cylinder* |
| **Pros** | Highly flexible/adaptive<br>Single part | Large force | Compact<br>Large force |
| **Cons** | Low pressure<br>Prone to rupture/tearing | Antagonistic pair needed<br>Low stroke | Rigid |

Table 3.2: Overview of the advantages and disadvantages of the different possible technologies for the movement of the fingers of a concept for a pneumatically powered hand prosthesis.

| **Attribute** | **Finger movement** | | |
|---|---|---|---|
| **Technology** | *Underactuated* | *Coupled* | *Individual control* |
| **Pros** | Highly flexible/adaptive<br>Simple control<br>Force distribution | Simple control<br>Predefined motion | High level of control |
| **Cons** | Unpredictable behavior | Sub-optimal grip<br>Not adaptive | Very complex<br>Many parts |

Table 3.3: Overview of the advantages and disadvantages of the different possible technologies for the joints of a concept for a pneumatically powered hand prosthesis.

| **Attribute** | **Joints** | | | |
|---|---|---|---|---|
| **Technology** | *Ball bearing* | *Plain bearing* | *Bending* | Rolling contact |
| **Pros** | Low friction | Simple | No friction<br>Single part | No friction |
| **Cons** | Large size | Moderate friction<br>Wear | Elasticity<br>Fatigue | Slip<br>Keep together |

Table 3.4: Overview of the advantages and disadvantages of the different possible technologies for the return mechanism of a concept for a pneumatically powered hand prosthesis.

| **Attribute** | **Return mechanism** | |
|---|---|---|
| **Technology** | *Normally closed* | *Normally opened* |
| **Pros** | Hold object at rest | Precise control of grip force<br>Energy only to hold object |
| **Cons** | Inverse control of grip force<br>Energy to keep open | Drop object at rest |

Using the list of requirements from chapter 2 and the chosen solutions for the attributes of the hand, a total of 8 concepts were generated. Below each of the concepts it is indicated where the inspiration came from. Each of the following paragraphs will briefly describe one of the eight concepts and show a simplified schematic drawing.

## Concept 1

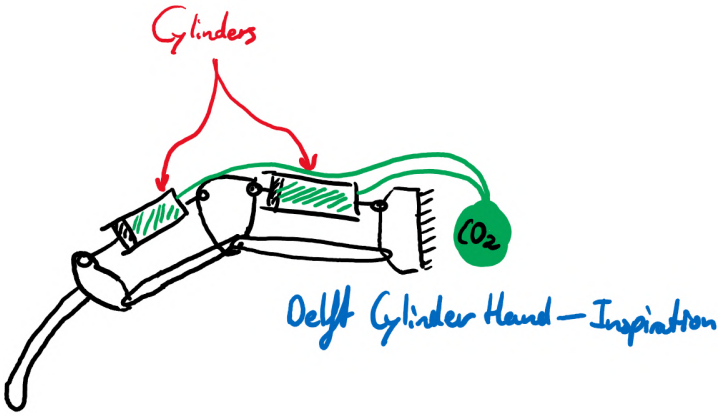


Figure 3.1: Simplified schematic drawing of concept 1. This concept is based upon the Delft Cylinder Hand and features two pneumatic cylinders that are operated by a single $CO_2$ supply.

This concept is based upon the design of the Delft Cylinder Hand and is shown in figure 3.1. It consists of two connected four bar mechanism. The first four bar mechanism is fixed on the right side (shaded), has a pneumatic cylinder as the top link, the bottom link acts as the proximal phalange, and it shares a link with the second four bar mechanism on the left. The second four bar mechanism also has a pneumatic cylinder as the top link, the bottom link acts as the medial phalange, and its left link acts as the distal phalange. When the cylinder in the first four bar mechanism is extended the proximal phalange will bend downwards and the second four bar mechanism will furthermore be rotated counterclockwise, resulting in bending of the medial phalange with respect to the proximal phalange, but not of the distal phalange with respect to the medial phalange. When the cylinder in the second four bar mechanism is extended, the medial phalange will bend even more, and the distal phalange will bend with respect to the medial phalange, thus closing the hand. Both of the pneumatic cylinders are connected to the same gas supply, which means that the pressure within them is the same. This

makes the cylinders adaptive, as when one cylinder is blocked due to the phalange hitting an object, the other cylinder will keep moving until it is blocked too. Therefore, this significantly eases the control as the cylinders do not have to be controlled separately, and furthermore this also distributes the contact forces more evenly over an object.

## Concept 2

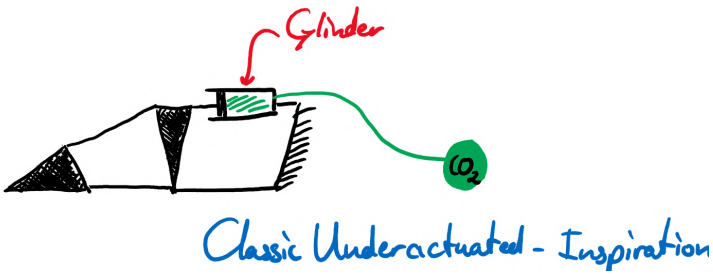


Figure 3.2: Simplified schematic drawing of concept 2. This concept is based upon the classic design of an underactuated finger and a single pneumatic cylinder that is operated by a $CO_2$ supply.

This concept is based upon the classic design of an underactuated (more degrees of freedom than actuators) finger and is shown in figure 3.2. Just like concept 1 this concept consists of two adjacent four bar mechanisms. This concept, however, only features one pneumatic cylinder except of two, which could decrease the overall gas usage. When the cylinder is extended, the proximal phalange bends downwards, but at the same time the link that is shared by the two four bar mechanisms rotates counterclockwise, resulting in both the bending of the medial phalange with respect to the proximal phalange, as the bending of the distal phalange with respect to the medial phalange. The underactuation of the finger means that even though the finger only has a single actuator, the movement of the phalanges is not coupled, i.e. their movement is not dependent on the movement of the other phalanges.

## Concept 3

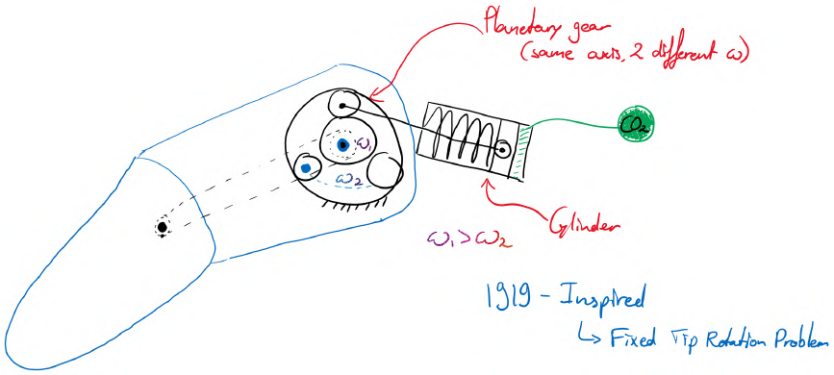


Figure 3.3: Simplified schematic drawing of concept 3. This concept is based upon the 1919 hand and is actuated by a combination of a single pneumatic cylinder that is operated by a $CO_2$ supply, and a planetary gear mechanism.

This concept is based upon the 1919 hand. However, the movement problem described in section 1.1 is solved by using a planetary gear mechanism. The concept is shown in figure 3.3. The ring gear is fixed (shaded), the axes of two of the planet gears are connected to respectively the actuator and the proximal phalange which acts as the carrier, and the sun gear is connected to the axis of the distal phalange through a belt transmission. When the actuator extends, it bends the proximal phalange downwards, but at the same time the planet gears will roll in the ring gear and rotate clockwise. This causes the sun gear to rotate counterclockwise with a higher angular velocity than the carrier ($\omega_1 > \omega_2$). As the sun gear is connected to the axis of the distal phalange with a belt, this means that the distal phalange will bend with respect to the proximal phalange. Extending the actuator thus causes the hand

to close, although the bending angle of the two phalanges is coupled.

## Concept 4

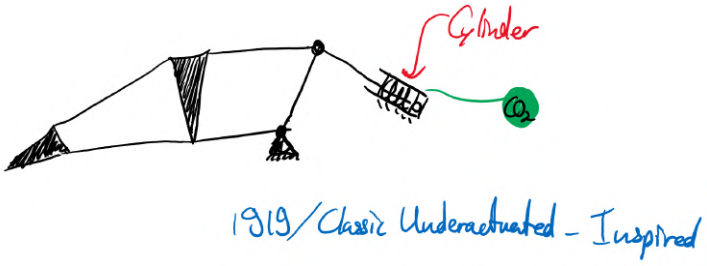


Figure 3.4: Simplified schematic drawing of concept 4. This concept is based upon the classic design of an underactuated finger in combination with a pneumatic actuator of the 1919 hand.

This concept is based upon the classic design of an underactuated finger in combination with the pneumatic actuator of the 1919 hand and is shown in figure 3.4. Like concepts 1 and 2, this concept consists of two connected four bar mechanisms. However, here the pneumatic actuator as used in the 1919 hand design is not one of the links, but rather it is connected externally. This means that the fingers will be less bulky as the cylinder is moved outside of the finger itself. When the actuator is extended, the right link of the first four bar mechanism is rotated counterclockwise. This not only causes the whole finger to bend downwards, but it also causes the link that is shared by the two four bar mechanism to rotate counterclockwise with respect to the proximal phalange. As described in concept 2, this also causes the medial phalange to bend with respect to the proximal phalange, and the distal phalange with respect to the medial phalange. Therefore, extending the pneumatic actuator causes the hand to close.

## Concept 5

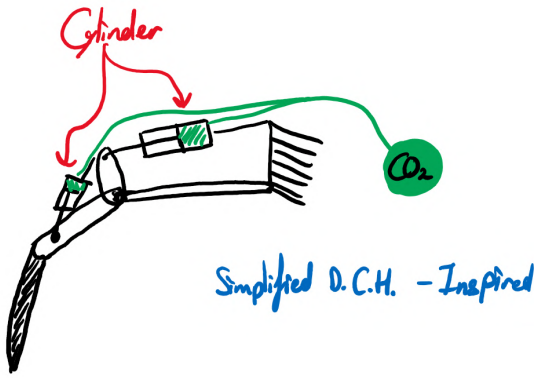


Figure 3.5: Simplified schematic drawing of concept 5. This concept is based upon the Delft Cylinder Hand and features a single pneumatic cylinder that is operated by a $CO_2$ supply.

This concept is based upon the design of the Delft Cylinder Hand and is shown in figure 3.5. This concept is similar to concept 1, however, in this concept the left link of the second four bar mechanism is removed and the distal phalange and medial phalanges are rigidly connected, therefore it only has two bending phalanges instead of three. This reduces both the complexity of the design and the size of the finger itself. As in concept 1, when the pneumatic cylinder in the first four bar mechanism is extended, the proximal phalange bends downwards and the shared link rotates counterclockwise with respect to the proximal phalange. When the second pneumatic cylinder is extended, the medial/distal phalange link bends even more with respect to the proximal phalange, thus closing the hand.

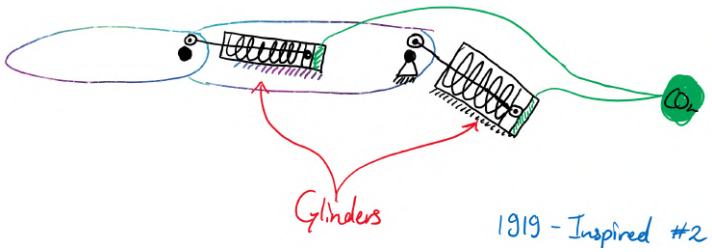


Figure 3.6: Simplified schematic drawing of concept 6. This concept is based upon the 1919 hand and features two pneumatic cylinders that are operated by a single $CO_2$ supply.

## Concept 6

This concept is based upon the 1919 hand and is shown in figure 3.6. However, it uses two pneumatic actuators per finger instead of a single one. The extra pneumatic cylinder increases the force that can be exerted at the tip of the finger. The pneumatic actuator that rotates the proximal phalange is connected in the same way as in the 1919 hand. The other pneumatic actuator, is rigidly attached to the proximal phalange and rotates the distal phalange with respect to the proximal phalange through a rod and crank mechanism once the actuator is extended, thus closing the hand.

## Concept 7

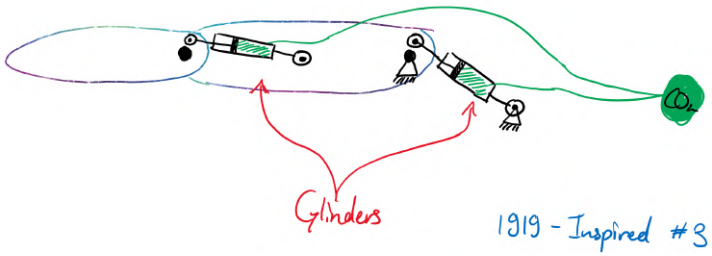


Figure 3.7: Simplified schematic drawing of concept 7. This concept is based upon the 1919 hand and features two conventional pneumatic cylinders that are operated by a single $CO_2$ supply.

This concept is based upon the 1919 hand and is shown in figure 3.7. It is very similar to concept 6. However, this concept uses two conventional pneumatic cylinders instead of the pneumatic actuators of the 1919 hand. Conventional cylinders are more commonly available then the ones used in the 1919 hand and furthermore, they can be made more compact as there is no spring inside the cylinder.

## Concept 8

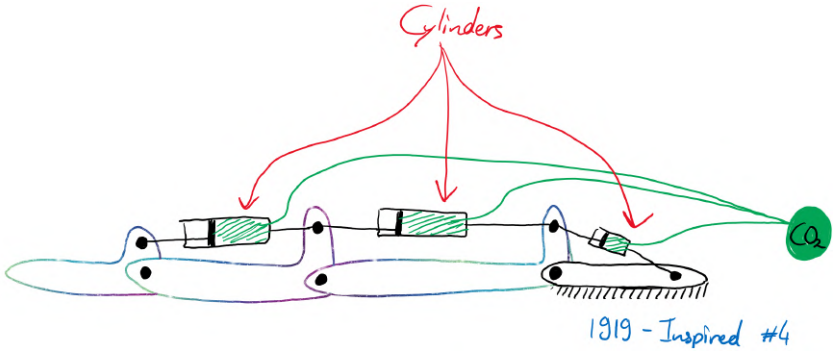


Figure 3.8: Simplified schematic drawing of concept 8. This concept is based upon the 1919 hand and features three conventional pneumatic cylinders that are operated by a single $CO_2$ supply.

This concept is again based upon the 1919 hand and is shown in figure 3.8. However, it features three simplified phalanges, instead of two bulky ones. Furthermore, the concept uses three conven-

tional pneumatic cylinders, one for each phalange, instead of the single one from the 1919 hand. Each of the pneumatic cylinders causes a link to bend with respect to the previous link. Therefore, extending all the pneumatic cylinders, causes the hand to close. Using three phalanges instead of two makes the finger more adaptive to the shape of the object and the addition of an extra pneumatic cylinder increases the forces that can be exerted on the object.

## 3.2. Concept selection

To see which of the eight aforementioned concepts shows the most promise, simplified force and moment balance calculations were performed to estimate and compare the performance of each of the design. The performance is based upon two factors: the number of grasping cycles on a single gas cartridge and the maximum force that it is able to exert at the tip of a finger. In order to be able to compare the concepts fairly, the dimension of the fingers and actuators were kept constant for all concepts. Therefore, the main difference in the calculations of the concepts is the number of actuators and the layout of the finger.

The MATLAB code that was used to make the performance estimations is shown in appendix B.1. The number of cycles was estimated by calculating the volume of a cylinder, which is the same in all designs, and then dividing the total amount of gas in a cartridge (12 milligrams) by the density of $CO_2$ times the amount of cylinders times the volume of a cylinder. The maximum force at the tip of a finger was estimated using simple force and moment balance equations based on the layout of the finger and the forces exerted by the pneumatic actuators, which was kept constant for all concepts. As the parameters were all estimated, the absolute values of the grasping cycles and tip forces are not representative. What is interesting, however, is when you compare them for each of the concepts, because this shows how well they compare with respect to each other. As the absolute values are not important, the grasping cycles and tip forces were normalized, in order to be able to compare them easily in the same graph.

Figure 3.9 shows a plot of the maximum tip force and the amount of grasping cycles for each of the concepts. Concept 3 was discarded beforehand because the friction in the belt transmission, and the complexity of the planetary gear mechanism already did not make it an attractive solution. This concept was created in order to show how the 1919 hand could be made to work. The values of concept 3 were, therefore, set to 0 for the comparison. The graph shows that concepts 1 and 8 perform the best when looking at the maximum tip force. Concepts 2 and 4, however, perform best when looking at the amount of grasping cycles. Since both of these factors are equally important, the normalized score of the maximum tip force and the amount of grasping cycles was combined into a single parameter, as shown in figure 3.10. The figure shows that concept 1 and concept 8 have the highest overall performance and, therefore, these concepts were chosen to continue with.

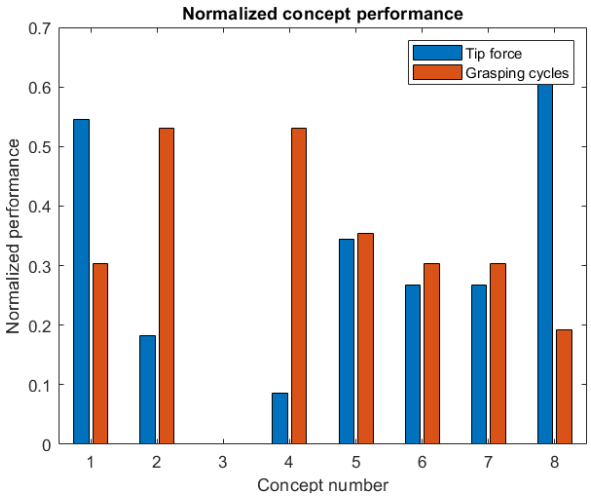


Figure 3.9: Bar graph of the normalized force at the tip of a finger and the normalized amount of grasping cycles with a single gas cartridge, plotted for each concept.

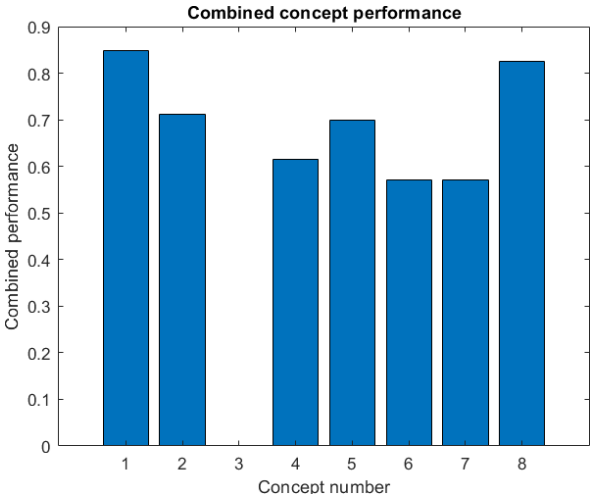


Figure 3.10: Bar graph of the combined normalized force at the tip of a finger and the normalized amount of grasping cycles with a single gas cartridge, plotted for each concept.

## 3.3. Concept combination

As both concepts 1 and 8 show promise for the design of a pneumatically powered hand prosthesis, I tried to combine the two together in order to get the best of both worlds. Furthermore, I also looked deeper into the design of the inspiration sources of both of the concepts: the Delft Cylinder Hand and the 1919 hand. After several design iterations, the final concept 9 that was created is as shown in figure 3.11. The finger consists of three links, corresponding to the metacarpal, proximal phalange, and a combination of the intermediate and distal phalange. The first link is fixed to the hand, and the other two are actuated by pneumatic cylinders. The last two links have an L shaped arm at the beginning, to which the pneumatic cylinder is attached. The L shaped arm makes sure that when the pneumatic cylinder is extended, it only slightly moves upwards, due to the rotation of the next link. If the L shaped arm would not be used, but rather a design such as in concept 8, then the link pneumatic cylinder would move slightly downwards, which would require that there is some spare room between the cylinder and link to prevent collision. The addition of the L shaped arm means that there is no spare room required and that the pneumatic cylinder can be placed against the link, saving space. Furthermore, this also means that the moment arm of the force exerted by the pneumatic cylinder only increases and does not get smaller, which means that the force exerted at the tip will stay higher. Tension spring are used to compress the pneumatic actuators when depressurized and return the hand to its opened position. The left side of the spring is attached to the same axis as the pneumatic cylinder, but the right side is attached to an axis that is further away from the pneumatic cylinder. This means that when the finger bends, the spring makes an angle with the pneumatic cylinder, which becomes larger the more the finger bends. As a result, the increase in spring force gets smaller the more the finger is bent. This is useful, as it means that less of the force exerted by the pneumatic cylinder goes to waste on overcoming the spring force, which increases when the fingers are bent, then if the spring would be aligned with the pneumatic cylinder.

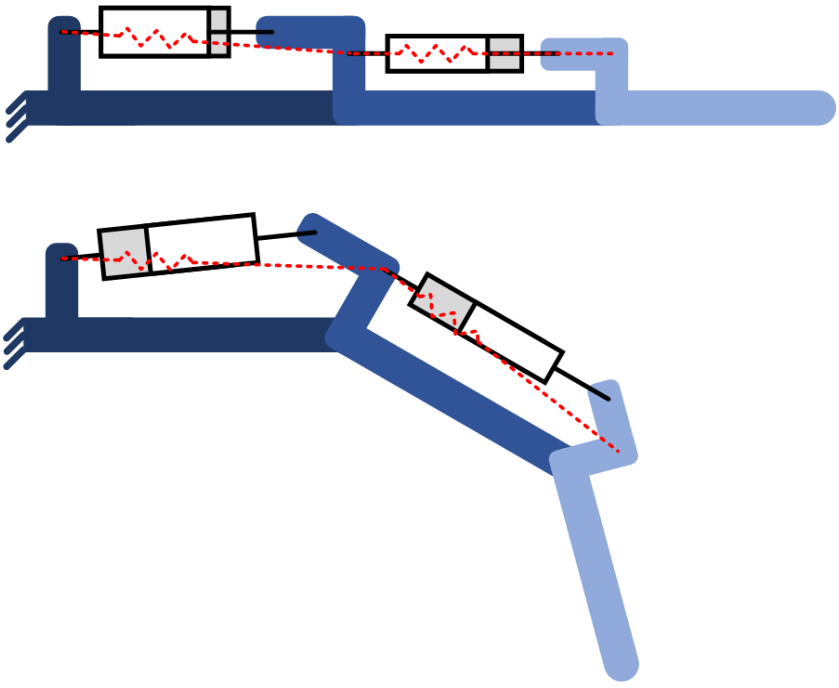

Figure 3.11: Schematic drawing of concept 9 of a finger of the hand prosthesis. The finger consists of three links; The metacarpal (dark blue), the proximal phalange (medium blue) and the intermediate and distal phalange are combined into one link (light blue). The finger is actuated with two pneumatic cylinders between the links and is returned to its open state through two return springs (red).

## 3.4. Dual-Mode actuation

As could be seen in figure 3.9, the concepts on which the combined concept 9 is based, both performed very well when looking at the maximum forces on the tip of the finger. The number of grasping cycles,

however, is relatively low compared to the other concepts. Therefore, I expected that concept 9 as detailed in section 3.3 would have the same kind of performance. In order to increase the efficiency of the hand concept, and thus the number of grasping cycles, I looked back at my literature study to see if there were techniques that I could apply. The technique that seemed promising for this concept is dual-mode actuation, as described in the advancement “Dual-Mode” in my literature paper in appendix A.

Dual-mode actuation basically splits up grasping in two phases: the prehension phase, where you move your hand to the object, but do not touch it yet, and the pinching phase, where you touch the object and apply a force. The mechanical characteristics of both phases are very different, as the prehension phase requires a large stroke, but almost no force, and the pinching phase requires a large force, but almost no stroke. Therefore, using the same actuator for both of the phases would be inefficient, and using different actuators for both of the phases could increase the efficiency significantly.

I initially came up with two different ways to implement dual-mode actuation in the concept shown in section 3.3. Concept *A* is shown in figure 3.12 and consists of pneumatic actuators with integrated dual-mode actuation, that would be used instead of the conventional pneumatic cylinders in the concept. The pneumatic actuator consists of a prehension cylinder, a locking mechanism and a pinching cylinder. The prehension cylinder has a large stroke, but a smaller diameter, as it does not require a large force, and the pinching cylinder has a low stroke, but a larger diameter, to be able to exert larger forces. The dual-mode actuator operates as follows; First the prehension cylinder is pressurized and extended. Next the locking mechanism is pressurized, which causes it to mechanically lock into the teeth on the prehension cylinder, preventing movement thereof. Finally, the pinching cylinder is pressurized, exerting a large force between the axes of the actuator. As stated in chapter 2, the control of the hand should be as easy as possible. Therefore, the control of this pneumatic actuator is done using only a single pressure regulator. As can be seen on the right side of figure 3.12, this pressure regulator controls the pressurization of the different phases of the dual-mode action, based upon the supply pressure.

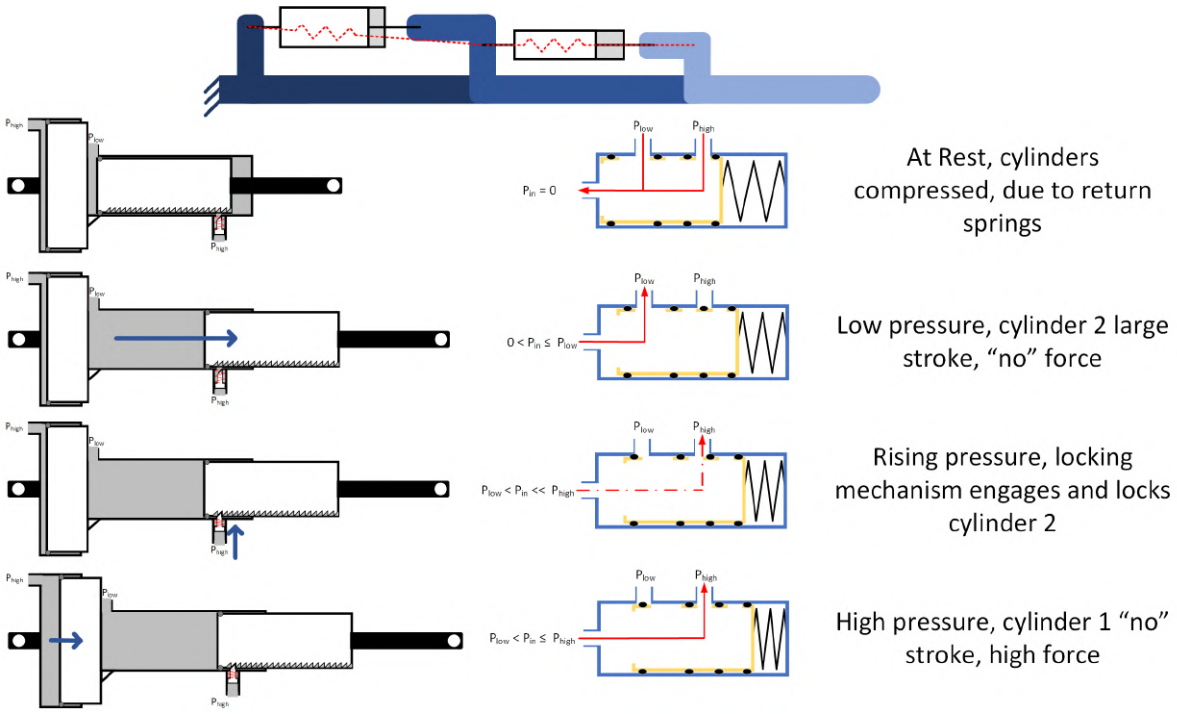


Figure 3.12: Concept *A* for a dual-mode actuator for the finger design concept. Each of the two cylinders is divided into two stages: one with a large stroke and low force, and one with a low stroke and large force. When the pressure regulator is pressurized, the large stroke cylinder is extended. Next the locking mechanism is activated, preventing movement of the large stroke cylinder. Finally, the large force cylinder is pressurized.

Concept *B* is shown in figure 3.13 and incorporates a pneumatic-to-hydraulic dual-mode transmission and the same pressure regulator as shown in the previous concept. The pinching phase is

performed by pneumatic cylinders with a large diameter, but a small stroke (the eight grey cylinders). The prehension phase is performed by hydraulic cylinders with a large stroke, but smaller diameter (the eight blue cylinders). The locking mechanism is added before the prehension cylinders to prevent flow and thus movement of the prehension cylinders once the pinching cylinders are exerting a force. Initially the idea was to also have the prehension cylinders work pneumatically, however then the locking mechanism would not work due to the compressibility of gas; When a force would be applied on the pneumatic prehension cylinders and the locking mechanism would be engaged, the cylinders would still be able to move backwards by compressing the gas within them. Therefore, the prehension cylinders work hydraulically, as water is nearly incompressible, meaning that once the locking mechanism is engaged, these cylinders cannot move backwards anymore. This did, however, require the pneumatic-to-hydraulic transmission cylinder, that is shown on the left, that allows the hydraulic prehension cylinders to be actuated using a pneumatic supply. Therefore, the concept works as follows; First the pneumatic-to-hydraulic transmission cylinder is pressurized, causing water to flow from this cylinder and the hydraulic prehension cylinders to extend, as water is nearly incompressible. Next, the locking mechanism is pressurized, which blocks the flow to/from the transmission cylinder, and thus prevents movement of the hydraulic prehension cylinders. Finally, the pneumatic pinching cylinders are pressurized, increasing the force exerted by the actuator on the fingers.

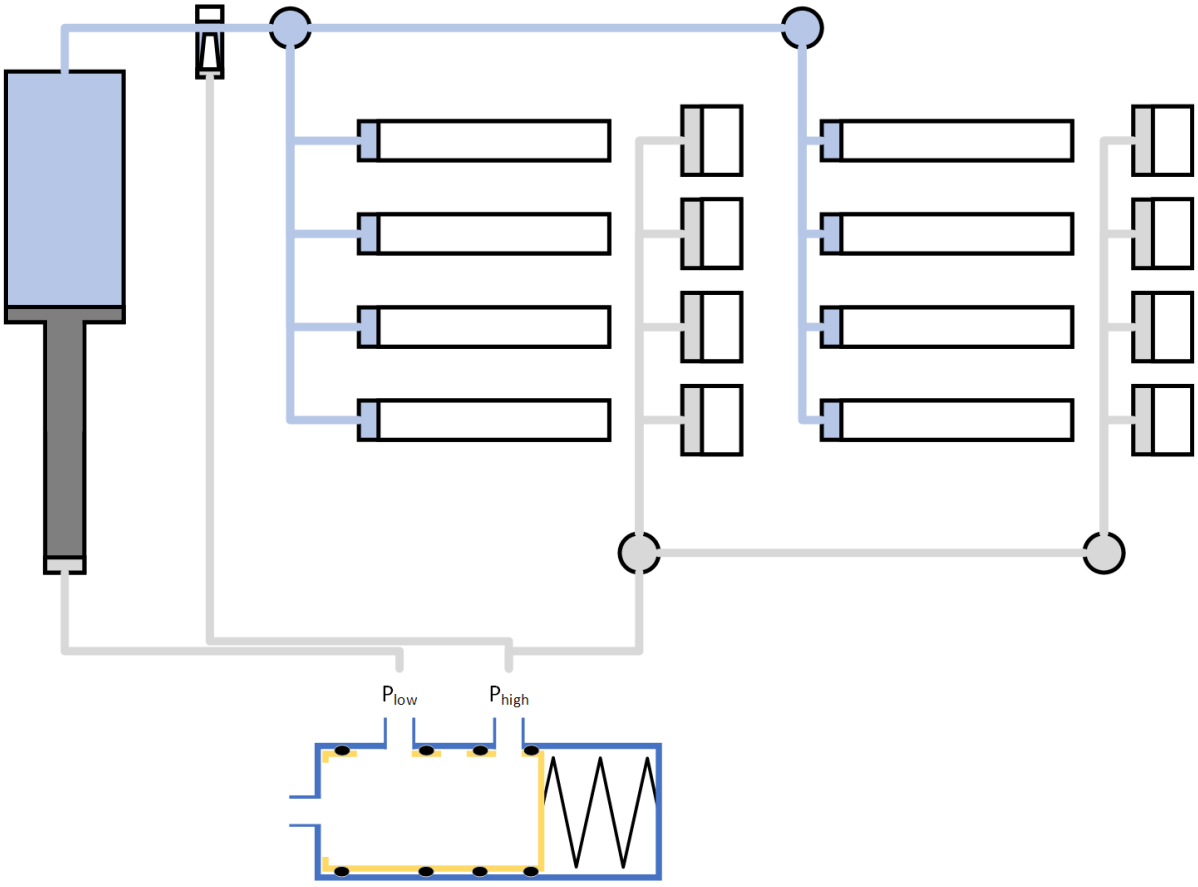


Figure 3.13: Concept *B* for a dual-mode actuation scheme for the finger design concept. Instead of a single cylinder, each finger joint now has a high force and a large stroke cylinder. The low-pressure output of the pressure regulator goes to a pneumatic-to-hydraulic transmission, used for the large stroke cylinders. The high-pressure output activates the locking mechanism, preventing flow from the large stroke cylinders, and is used for the high force cylinders.

Next, the concepts for the dual-mode actuation of the hand prosthesis concept were compared in order to see which one shows the most promise. Concept *B* as shown in figure 3.13, was deemed to be the most promising one, as it consists of several simple components instead of a more complicated integrated one and, furthermore, the near incompressibility of water gives the dual-mode operation of this concept a higher chance of success.

Through several iteration cycles the concept was improved even more, and the concept that was

eventually generated is concept *C* that is shown in figure 3.14. Instead of using separate cylinders for the prehension and pinching phase, the same hydraulic one is used for both. This is again possible due to the near incompressibility of water and means that less room is needed in the fingers for actuators. This does mean, however, that another pneumatic-to-hydraulic transmission cylinder is needed, now for the pinching phase. The advantage of this is that a high pressure transmission ratio can be incorporated, which means that an even higher force can be exerted using the same pneumatic supply pressure. The pneumatic-to-hydraulic transmission cylinder used for the pinching phase is shown in the top center of the figure. To conclude, this final concept works as follows; First the high stroke pneumatic-to-hydraulic transmission cylinder is pressurized, causing water to flow from this cylinder and the hydraulic cylinders to extend, as water is nearly incompressible. Next, the locking mechanism is pressurized, which blocks the flow to/from the high stroke transmission cylinder, preventing it to move back once the water is being pressurized. Finally, the high force pneumatic-to-hydraulic transmission cylinder is pressurized, causing the water pressure to increase and the hydraulic cylinders to exert a force.

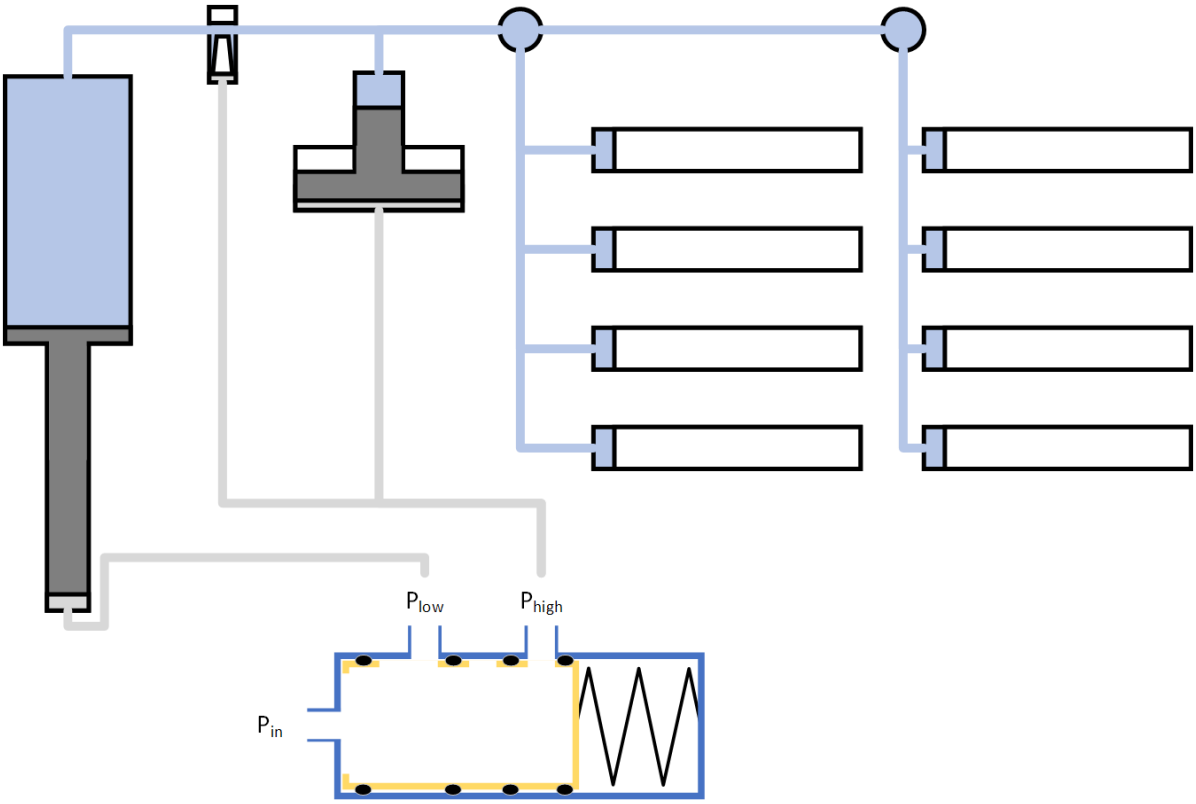


Figure 3.14: Concept *C* for a dual-mode actuation scheme for the finger design concept. Each finger joint has a single hydraulic cylinder. The low-pressure output of the pressure regulator goes to a pneumatic-to-hydraulic transmission with a low-pressure transmission ratio, used for the prehension phase of the cylinders. The high-pressure output activates the locking mechanism, preventing flow from the prehension phase transmission, and is used for another pneumatic-to-hydraulic transmission with a high pressure transmission ratio, used for the pinching phase of the cylinders.

# 4

# Design

This chapter will detail how the combination of concept 9 and C, shown previously in chapter 3 was turned into the final design for a pneumatically powered hand prosthesis. Section 4.1 will detail the analyses that were performed in order to find the dimensions and estimated performance of the hand. Next, section 4.2 will go in on the detailed design of the fingers of which the concept was shown in section 3.3. Hereafter, section 4.3 will describe the design of the transmission used for the dual-mode actuation, as described in section 3.4. Thereafter, section 4.4 will detail the design of the pressure regulator that is used to control the hand prosthesis. Next, section 4.5 will describe the design of the palm base of the hand, to which all other components are attached. Finally, section 4.6 will detail the complete overall design of the pneumatically powered hand prosthesis.

## 4.1. Force and dimension analysis.

To determine what the prosthetic hand, or more specifically the fingers and actuators must look like an analysis was performed using MATLAB. As stated in section 3.2 the important performance factors to design the fingers of the hand are the maximum force at the tip of a finger, and the number of grasping cycles. In order to calculate the force at the tip of the finger, the other forces on the finger also must be calculated. The first step to do this was to simplify the concept of the finger to the schematic drawing shown in 4.1, consisting of links EAB, FGBC and HICD, and with joints at points B and C. Here $\alpha$ is the angle of link FGBC with respect to link EAB, and $\beta$ is the angle of link HICD with respect to link FGBC.

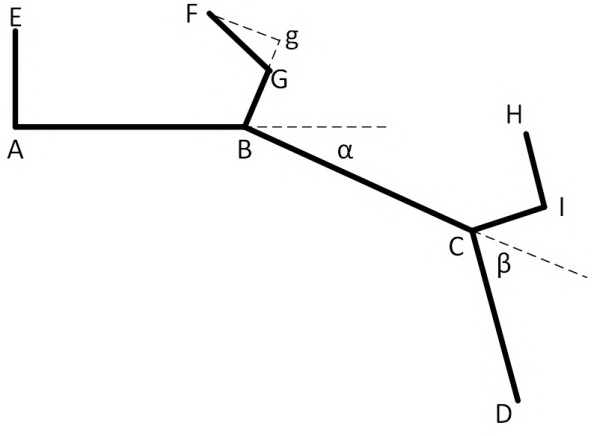


Figure 4.1: Schematic drawing of the finger prosthesis concept, consisting of three phalanges connected through joints at points B and C.

In order to calculate the forces on the finger, the equations to calculate them need to be composed. In order to do this free body diagrams were made for each of the links and, thereafter, the force and

moment balance equations were derived. The first free body diagram is that of link EAB and is shown in figure 4.2. This link is fixed at point A; therefore it has two reaction force components and a reaction moment in this point. In point E, a tension spring and a hydraulic cylinder are attached. Therefore, both exert a force on this point. As the exact orientation of these forces depends on the bending angle of the finger, both forces are split up into a horizontal and a vertical component. In point B links EAB and FGBC are connected through a joint, therefore there are two reaction force components in this point. The distance between points A and B is called $AB$ and the distance between points A and E is called $h_1$, as this dimension will also come back another link.

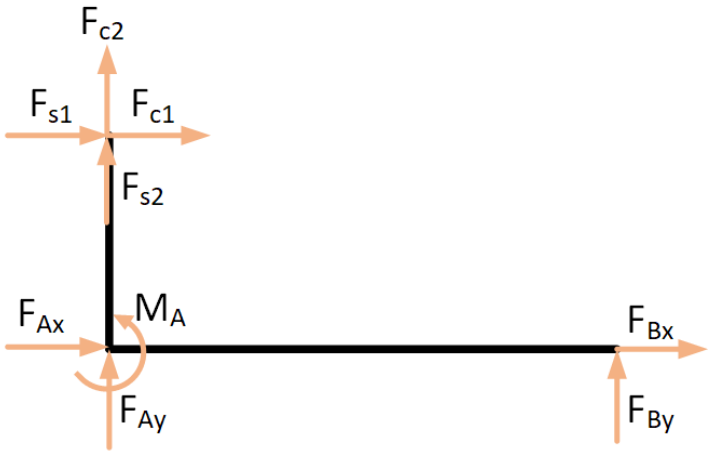


Figure 4.2: Free body diagram of the first finger phalange (AB) including forces and moments. $F_{c1}$ and $F_{c2}$ are the force components of the hydraulic cylinder, $F_{s1}$ and $F_{s2}$ are the force components of the tension spring, $F_{Ax}$, $F_{Ay}$ and $M_A$ are the reaction forces and moment in point A, and $F_{Bx}$ and $F_{By}$ are the reaction forces in point B.

Setting up the force balance equation in the horizontal direction resulted in equation 4.1, and in the vertical direction resulted in equation 4.2. Setting up the moment balance equation for this free body diagram resulted in equation 4.3.

$$F_{Ax} + F_{C1} + F_{S1} + F_{Bx} = 0 \tag{4.1}$$

$$F_{Ay} + F_{C2} + F_{S2} + F_{By} = 0 \tag{4.2}$$

$$M_A + AB * F_{By} = h_1 * (F_{C1} + F_{S1}) \tag{4.3}$$

The second free body diagram is that of link FGBC and is shown in figure 4.3. The hydraulic cylinders are attached in points F and G respectively, and the tension springs are connected in point G, therefore a horizontal and vertical component are added for each of these in the corresponding points. As stated before, point B is where this link is attached to link EAB through a joint, therefore the same reaction force components are added as in figure 4.2, although in opposite directions. In point C this link is attached to link HICD through a joint, therefore also here reaction force components are added. Finally, an external force that is the result of touching an object, is added halfway between points B and C. The distance between points B and C is called $BC$ and the distance between points B and G is called $h_2$, as this dimension will also come back another link. The horizontal ($Fg$) and vertical ($Bg$) distance between points B and F are both equal to $h_1$.

Setting up the force balance equation in the horizontal direction resulted in equation 4.4, and in the vertical direction resulted in equation 4.5. Setting up the moment balance equation for this free body diagram resulted in equation 4.6.

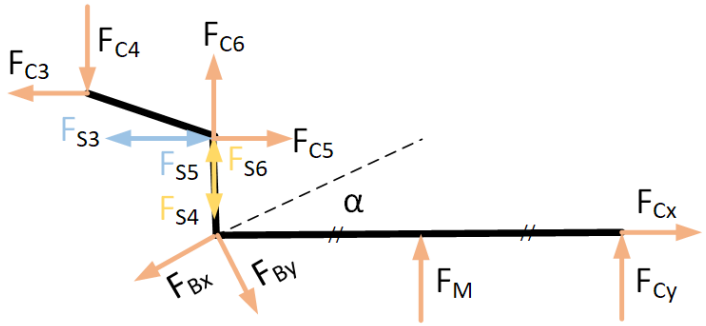


Figure 4.3: Free body diagram of the second finger phalange (BC) including forces and moments. This phalange is rotated by an angle $\alpha$ with respect to the first phalange (AB). $F_{c3}$, $F_{c4}$, $F_{c5}$ and $F_{c6}$ are the force components of the hydraulic cylinders, $F_{s3}$, $F_{s4}$, $F_{s5}$ and $F_{s6}$ are the force components of the tension springs, $F_{Bx}$ and $F_{By}$ are the reaction forces in point B, $F_{Cx}$ and $F_{Cy}$ are the reaction forces in point C, and $F_M$ is the contact force of this phalange with an object at the center of the phalange.

$$F_{C5} + F_{S5} + F_{By} * sin(\alpha) + F_{Cx} = F_{C3} + F_{S3} + F_{Bx} * cos(\alpha) \tag{4.4}$$

$$F_{C6} + F_{S6} + F_{Cy} + F_M = F_{C4} + F_{S4} + F_{Bx} * sin(\alpha) + F_{By} * cos(\alpha) \tag{4.5}$$

$$h_2 * (F_{C5} + F_{S5}) = h_2 * F_{S3} + h_1 * (F_{C3} + F_{C4}) + BC * F_{Cy} + \frac{1}{2} * BC * F_M \tag{4.6}$$

The third and final free body diagram is that of link HICD and is shown in figure 4.4. The hydraulic cylinder is attached in point H and the tension spring is connected in point I, therefore a horizontal and vertical component are added for each of these in the respective points. As stated before, point c is where this link is attached to link FGBC through a joint, therefore the same reaction force components are added as in figure 4.3, although in opposite directions. Finally, in point D the tip force, as a result of touching an object, is added. The distance between points H and I, and between points C and I are both equal to $h_2$. The distance between points C and D is called $CD$.

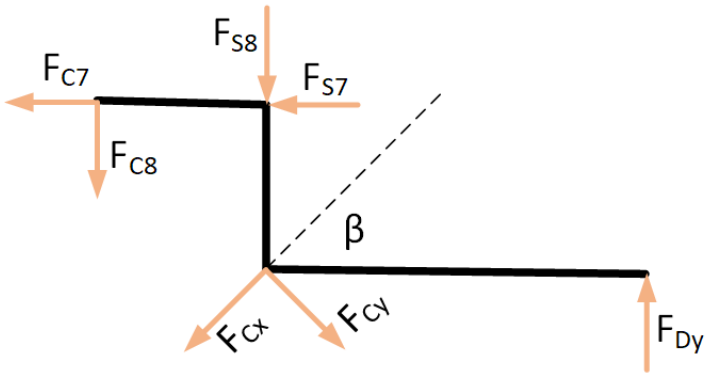


Figure 4.4: Free body diagram of the third finger phalange (CD) including forces and moments. This phalange is rotated by an angle $\beta$ with respect to the second phalange (BC). $F_{c7}$ and $F_{c8}$ are the force components of the hydraulic cylinder, $F_{s7}$ and $F_{s8}$ are the force components of the tension spring, $F_{Cx}$ and $F_{Cy}$ are the reaction forces in point C, and $F_{Dx}$ and $F_{By}$ is the contact force of this phalange with an object at the tip of the phalange.

Setting up the force balance equation in the horizontal direction resulted in equation 4.7, and in the vertical direction resulted in equation 4.8. Setting up the moment balance equation for this free body diagram resulted in equation 4.9.

$$F_{Cy} * sin(\beta) = F_{C7} + F_{S7} + F_{Cx} * cos(\beta) \tag{4.7}$$

$$F_{Dy} = F_{C8} + F_{S8} + F_{Cy} * cos(\beta) + F_{Cx} * sin(\beta) \tag{4.8}$$

$$CD * F_{Dy} + h_2 * (F_{C7} + F_{S7} + F_{C8}) = 0 \tag{4.9}$$

As could be seen in the previous figures there are a total of 25 unknown forces and moments in this system. So far 9 equations have been drawn up, so there are still 16 needed to solve this system. The rest of the equations will be determined both by the geometry of the system as by mechanical relationships. The first relationship has to do with the force exerted by the hydraulic cylinders. This force needs to be equal to the pressure inside the cylinder, $p$, times the area of the cylinder, which is equal to a quarter of $\pi$ times the diameter, $d$, squared. The force exerted by a cylinder was divided into a horizontal and a vertical component and its magnitude is therefore the square root of the sum of the squared force components. Combining these two, results in the equations 4.10 and 4.11.

$$4\sqrt{F_{C1}^2 + F_{C2}^2} = p * \pi * d_1^2 \tag{4.10}$$

$$4\sqrt{F_{C5}^2 + F_{C6}^2} = p * \pi * d_2^2 \tag{4.11}$$

A similar relationship can be found for the spring forces. This force needs to be equal to the extension of the spring, $\Delta$, times the spring constant, $k$. The force exerted by a spring was divided into a horizontal and a vertical component and its magnitude is therefore the square root of the sum of the squared force components. Combining these two, results in the equations 4.12 and 4.13.

$$\sqrt{F_{S1}^2 + F_{S2}^2} = k * \Delta EG \tag{4.12}$$

$$\sqrt{F_{S5}^2 + F_{S6}^2} = k * \Delta GI \tag{4.13}$$

The following relationships again have to do with the forces exerted by the hydraulic cylinders. As equilibrium of forces and moments is also valid for the hydraulic cylinders, the forces exerted on both ends of the cylinder must be equal in magnitude, but opposite in direction. Furthermore, the direction of the forces is determined by the coordinates of the axes to which the cylinder is connected, as the forces need to form a line through these points, since a cylinder can only exert a force along its length. Equations 4.14 and 4.15 make sure that the magnitudes satisfy these conditions for both cylinders respectively, and equations 4.16, 4.17, 4.18 and 4.19 make sure that the directions satisfy these conditions for both cylinders respectively.

$$F_{C1}^2 + F_{C2}^2 = F_{C3}^2 + F_{C4}^2 \tag{4.14}$$

$$F_{C5}^2 + F_{C6}^2 = F_{C7}^2 + F_{C8}^2 \tag{4.15}$$

$$\frac{F_{C2}}{F_{C1}} = \frac{\Delta y_{EF}}{\Delta x_{EF}} \tag{4.16}$$

$$\frac{F_{C3} * cos(\alpha) + F_{C4} * sin(\alpha)}{F_{C4} * cos(\alpha) - F_{C3} * sin(\alpha)} = \frac{\Delta x_{EF}}{\Delta y_{EF}} \tag{4.17}$$

$$\frac{F_{C6}}{F_{C5}} = \frac{\Delta x_{GH} * sin(\alpha) + \Delta y_{GH} * cos(\alpha)}{\Delta x_{GH} * cos(\alpha) - \Delta y_{GH} * sin(\alpha)} \tag{4.18}$$

$$\frac{F_{C7} * cos(\beta) + F_{C8} * sin(\beta)}{F_{C8} * cos(\beta) - F_{C7} * sin(\beta)} = \frac{\Delta x_{GH} * cos(\alpha) - \Delta y_{GH} * sin(\alpha)}{\Delta x_{GH} * sin(\alpha) + \Delta y_{GH} * cos(\alpha)} \tag{4.19}$$

Similar relationships can be found for the forces exerted by the tension springs. As equilibrium of forces and moments is also valid for the tension springs, the forces exerted on both ends of the spring must be equal in magnitude, but opposite in direction. Furthermore, the direction of the forces is determined by the coordinates of the axes to which the spring is connected, as the forces need to form a line through these points, since a spring can only exert a force along its length. Equations 4.20 and 4.21 make sure that the magnitudes satisfy these conditions for both springs respectively, and equations 4.22, 4.23, 4.24 and 4.25 make sure that the directions satisfy these conditions for both springs respectively.

$$F_{S1}^2 + F_{S2}^2 = F_{S3}^2 + F_{S4}^2 \tag{4.20}$$

$$F_{S5}^2 + F_{S6}^2 = F_{S7}^2 + F_{S8}^2 \tag{4.21}$$

$$\frac{F_{S2}}{F_{S1}} = \frac{\Delta y_{EG}}{\Delta x_{EG}} \tag{4.22}$$

$$\frac{F_{S3} * cos(\alpha) + F_{S4} * sin(\alpha)}{F_{S4} * cos(\alpha) - F_{S3} * sin(\alpha)} = \frac{\Delta x_{EG}}{\Delta y_{EG}} \tag{4.23}$$

$$\frac{F_{S6}}{F_{S5}} = \frac{\Delta x_{GI} * sin(\alpha) + \Delta y_{GI} * cos(\alpha)}{\Delta x_{GI} * cos(\alpha) - \Delta y_{GI} * sin(\alpha)} \tag{4.24}$$

$$\frac{F_{S7} * cos(\beta) + F_{S8} * sin(\beta)}{F_{S8} * cos(\beta) - F_{S7} * sin(\beta)} = \frac{\Delta x_{GI} * cos(\alpha) - \Delta y_{GI} * sin(\alpha)}{\Delta x_{GI} * sin(\alpha) + \Delta y_{GI} * cos(\alpha)} \tag{4.25}$$

The above systems of equations were solved using MATLAB in an iterative process; The dimensions of the finger and cylinders were based upon my own finger dimensions, but slightly adjusted each time to get a better performance. The pressure inside the cylinders was based upon the $CO_2$ supply pressure of 1.2 MPa and the dual-mode transmission, whose dimensions were also calculated using the same script. The spring constants were also adjusted iteratively but based upon real available springs. The system of equations was solved for all possible position of the finger meaning that $\alpha$ and $\beta$ both can range from 0 to 90 degrees. The code that was used to calculate the results of these calculations is shown in appendix B and consists of the following:

- The function in appendix B.4 was used to determine the coordinates of points A till I during the bending of the finger.
- The function in appendix B.7 contains the 9 force and moment balance equations.
- The function in appendix B.6 contains the 8 equations relating to the hydraulic cylinders.
- The function in appendix B.5 contains the 8 equations relating to the tension springs
- The function in appendix B.8 is used to solve the whole system of 25 equations.
- Finally, the code in appendix B.3 is the main program that uses all the aforementioned functions to calculate the performance of the system.

By running the aforementioned scripts and making iterative adjustments to optimize the performance of the pneumatic hand prosthesis, the parameters shown in table 4.1 were found, and these will be used for the further design of the pneumatically powered hand prosthesis.

Table 4.1: Parameters of the prosthetic hand design found using the MATLAB scripts. HS is used to indicate the high stroke transmission cylinder and HF to indicate the high force one. The cylinders in the bottom of the table are the hydraulic cylinders used in the fingers.

| | | | |
|---|---|---|---|
| $AB$ | 45 mm | Diameter of HF cylinder at CO2 | 25 mm |
| $BC$ | 40 mm | Diameter of HF cylinder at H2O | 14 mm |
| $CD$ | 30 mm | Stroke of HF cylinder | 1 mm |
| $h1$ | 10 mm | Max. pressure in hydraulic cylinder | 4.2 MPa |
| $h2$ | 8 mm | Diameter of pressure regulator | 8 mm |
| Spring constant $k$ | 0.2 N/mm | Stroke of pressure regulator | 12 mm |
| Diameter of HS cylinder at CO2 | 25 mm | Length of pressure regulator spring | 23.3 mm |
| Diameter of HS cylinder at H2O | 25 mm | Diameter of locking mechanism | 10 mm |
| Stroke of HS | 18 mm | Stroke locking mechanism | 8.2 mm |
| Diameter large of cylinder | 10 mm | Diameter of small cylinder | 7 mm |

Furthermore, the important performance factors, the amount for grasping cycles and the maximum force at the tip of a finger were calculated. Figure 4.5 shows the results of the forces at the middle link

and at the tip of the finger for different bending angles of the finger. As can be seen the force exerted by the middle link ranges from 0 to around 165 Newtons, and that by the tip of the finger ranges from 42 to a bit more than **60 Newtons**. Furthermore, the pneumatically powered hand prosthesis would be able to perform **456 grasping cycles** on a 12 milligram $CO_2$ cartridge. The same calculation was repeated for the same hand design, but without the dual-mode actuation, to see if this had indeed increased the efficiency of the hand. This was done using the script in appendix B.2 and resulted in a total of 42 grasping cycles on a 12 milligram $CO_2$ cartridge. The dual-mode actuation, therefore, indeed makes significant difference in the amount of grasping cycles as it increased the amount of possible cycles by more than a factor 10.

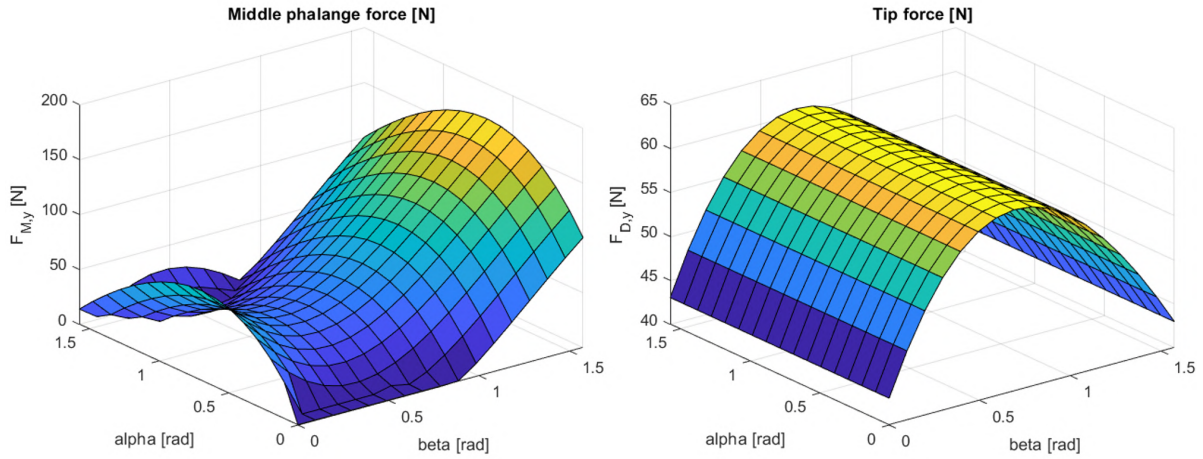


Figure 4.5: Results of the MATLAB simulation plotted for all bending angles. Left: maximum force exerted on an object by link FGBC ($F_M$). Right: maximum force exerted at the tip of the finger ($F_{Dy}$).

## 4.2. Fingers

Using the dimensions shown in table 4.1, a design for the fingers could be made. Here the diameters of the hydraulic cylinders and the locations of the joints are taken directly from the table. The overall design of a finger is shown in figure 4.6, and figure 4.7 shows the cross section of the finger, revealing the internal components.

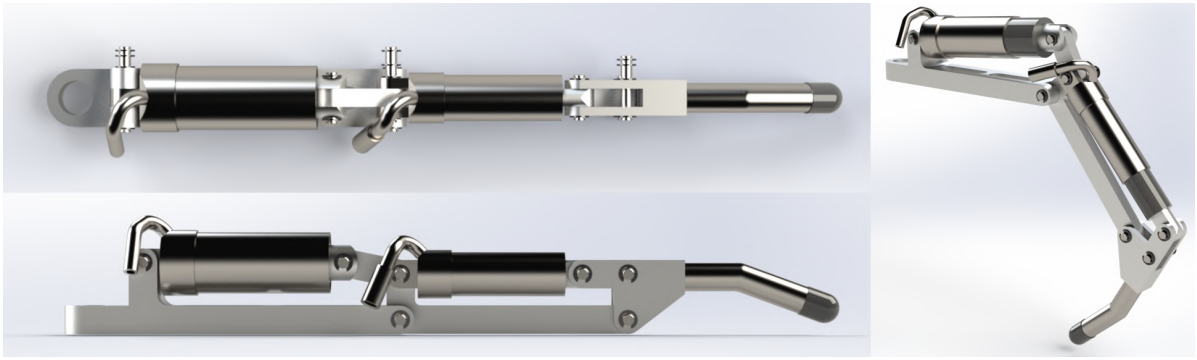

Figure 4.6: 3D design of the finger of the pneumatically powered hand prosthesis, excluding the tension springs. Top left: top view of the finger. Bottom left: side view of the finger. Right: overview of the finger in a bent position.

The finger consists of three aluminium links, whose thickness is based upon stress simulations in SOLIDWORKS, using the forces found in the MATLAB simulation from section 4.1. Here the thickness was iteratively adjusted until the maximum stress stayed well below the yield strength of aluminium. The links are connected through stainless steel axes of 2 mm in diameter, that are secured with 1.5 mm E-clips. As can be seen in figure 4.7, each of the axes passes through a plain bearing, that reduces friction when the finger is bent. Furthermore, the axes that pass through the joints to which the tension

springs must be attached stick out the side of the finger, as can be seen in the top of figure 4.6, in order to be able to attach the springs without them scraping against the cylinders. The E-clips on these protrusions keep the tension springs in place. The tension springs have a length of 34.8 mm and 31.75 mm respectively, an outer diameter of 3.05 mm, a wire diameter of 0.41 mm and a spring constant of 0.2 N/mm. In order to save weight and production time, the tip of the finger is made from a stainless-steel tube with an outer diameter of 5 mm and a wall thickness of 0.4 mm. One end of the tube is pressed inside the distal aluminium link and the other end is covered with a plastic cap.

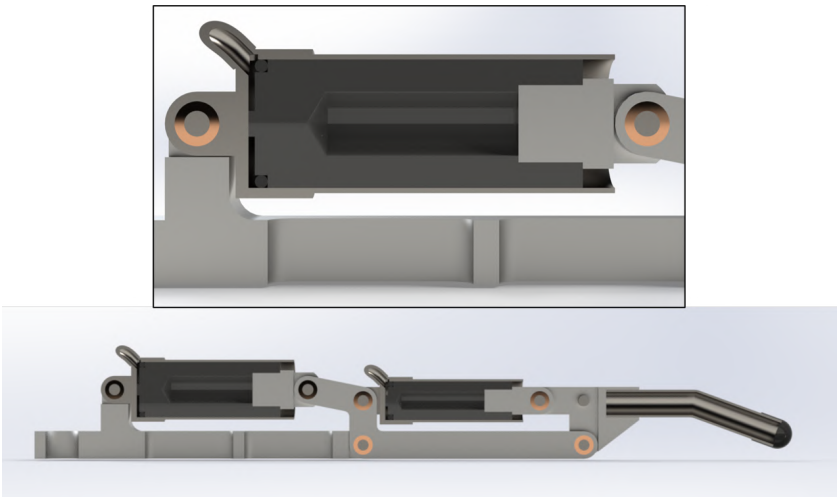

Figure 4.7: Cross section of the 3D model of the finger design, including an enlarged view of the proximal cylinder.

The shells of the hydraulic cylinders are made from stainless steel and have an internal diameter of respectively 10 mm and 7 mm, and a wall thickness of 0.4 mm. MATLAB was used to calculate the minimum wall thickness that was required, to make sure that it is strong enough, and this came down to 0.06 mm and 0.04 mm respectively. Therefore, the 0.4 mm is more than enough to withstand the pressure, but it also makes sure that the cylinders do not damage when they accidentally hit something. The respectively 10 mm and 7 mm in diameter pistons of the cylinders are made from PCTFE, which has a very low friction coefficient, and feature a floating o-ring that seals of the cylinder. The o-rings are respectively 8x1 mm and 5x1 mm in size. A floating o-ring has the advantage that it has a much lower friction coefficient, and it can be used in this design as it is a single acting cylinder, meaning that the hydraulic pressure pushes it one way, but it is returned through the tension spring forces. The piston is partially hollowed out, to save weight, and it is threaded on the right where an aluminium coupling is screwed in. This coupling is attached to the axis of one of the aluminium links. On the other end a stainless-steel cap is glued on the shell of the cylinder, and it is used to seal the end of the cylinder. This cap has a protrusion with a plain bearing inside which is attached to the axis of another aluminium link. Furthermore, the top of the cap is beveled and has a centered hole of 1.5 mm in diameter, to which a stainless-steel tube is attached. This tube is the hydraulic inlet of the cylinder and water flows through it to fill the cylinder.

## 4.3. Transmission

As with the fingers, the design of the dual-mode transmission cylinders is based upon the dimensions shown in table 4.1.

### 4.3.1. Stroke cylinder

The design of the high stroke pneumatic-to-hydraulic transmission cylinder, that is used for the prehension phase is shown in figure 4.8. The cylinder consists of a stainless-steel sleeve, with an inner diameter of 25 mm and a wall thickness of 0.4 mm, and two stainless steel caps that are glued on the sleeve. The cap on the left seals the hydraulic side of the cylinder and has a 4 mm in diameter centered hole, which is the inlet for the water. The cap on the right seals the pneumatic side of the cylinder. As with the hydraulic cylinders in the finger, the top of the cap is beveled and has a centered hole of 1.5 mm in diameter, which is the inlet for $CO_2$. Furthermore, this cap has a protrusion on the side with a

4 mm in diameter hole, which allows the cylinder to be attached to a base using an M4 screw. The 25 mm in diameter piston of the high stroke cylinder is again made of PCTFE, however, as this is a double acting cylinder, a floating o-ring cannot be used here. Therefore, a Turcon® Glyd Ring® sealing is used. This sealing is basically a normal o-ring with a polymer ring around it. The o-ring provides the pressure against the wall of the cylinder, which keeps it sealed, and the polymer ring makes sure that the friction coefficient stays low. The groove for the sealing has a width of 2.2 mm and a diameter of 20.1 mm, as prescribed by the manufacturer. The piston is 8.2 mm wide in total and has a stroke of 18 mm, as was calculated earlier with MATLAB.

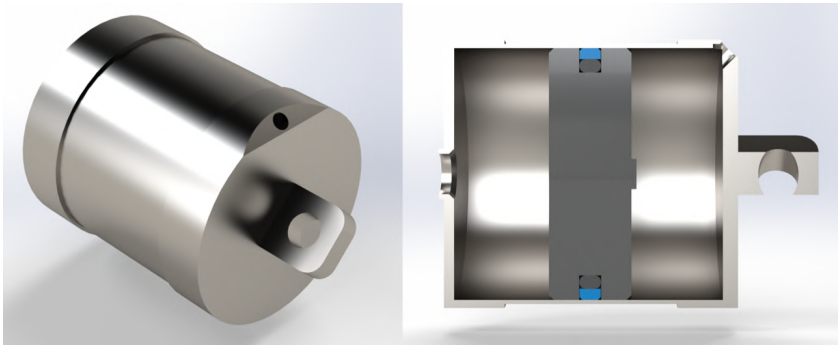

Figure 4.8: Overview of the design of the stroke cylinder of the transmission of the hand prosthesis. Left: external overview of the cylinder. Right: Cross section of the cylinder, showing the internal components.

### 4.3.2. Force cylinder

The design of the high force pneumatic-to-hydraulic transmission cylinder, that is used for the pinching phase is shown in figure 4.9. The cylinder consists of three stainless steel parts: the central T-shaped sleeve and two caps that are glued on. The T-shaped sleeve has a larger inner diameter of 25 mm and a smaller diameter of 14 mm, as was calculated with MATLAB. The wall thickness of the sleeve is 0.4 mm and the thickness of the side between the large and small wall is 1 mm. The sleeve has a hole in the top of 2 mm in diameter that lets air escape when the piston moves, as this would otherwise be compressed and counter the movement of the piston. The cap on the left seals the hydraulic side of the cylinder and has a 4 mm in diameter centered hole, which is the inlet for the water. The cap on the right seals the pneumatic side of the cylinder and is beveled with a centered hole of 1.5 mm in diameter, which is the inlet for $CO_2$. Furthermore, this cap has a protrusion on the side with a 4 mm in diameter hole, which allows the cylinder to be attached to a base using an M4 screw. The T-shaped piston of the high force cylinder is again made of PCTFE and has two Turcon® Glyd Ring® sealings. The groove for the large sealing has a width of 2.2 mm and a diameter of 20.1 mm, and for the small sealing a width of 2.2 mm and a diameter of 9.1 mm, as prescribed by the manufacturer. The large part of the piston has a width of 5.2 mm and a diameter of 25 mm, and the small part has a width of 6.2 mm and a diameter of 14 mm. Furthermore, the piston has a stroke of 1 mm, as was calculated earlier with MATLAB.

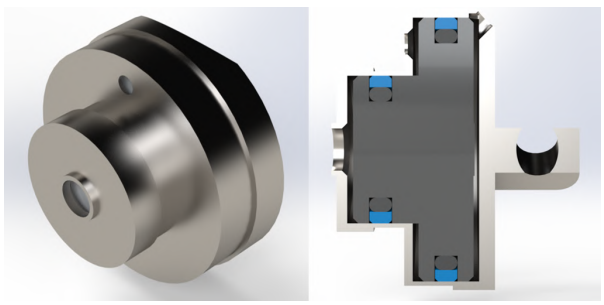

Figure 4.9: Overview of the design of the force cylinder of the transmission of the hand prosthesis. Left: external overview of the cylinder. Right: Cross section of the cylinder, showing the internal components.

### 4.3.3. Locking mechanism

Through many design iterations and after coming up with many different kinds of locking mechanisms, the locking mechanism that is schematically shown in figure 4.10 was conceived. It consists of a piston within a cylinder that has two inlets and two outlets. The locking mechanism is normally opened due to a compression spring that keeps the piston in place. As can be seen in the top figure, when the locking mechanism is not engaged, and thus kept open by the spring, water can flow freely from the hydraulic inlet to the hydraulic outlet. When the locking mechanism is engaged by pressurizing the pneumatic inlet, the piston slides to the right, thus sealing the hydraulic inlet and preventing the flow of water, as can be seen in the bottom figure. The pneumatic outlet on the right lets air escape when the piston moves to the right, as this would otherwise be compressed and hinder the movement of the piston.

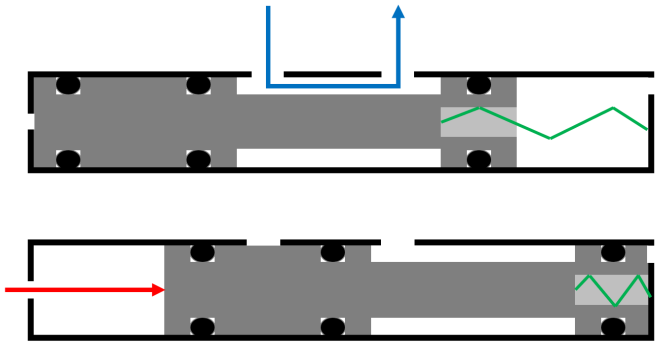

Figure 4.10: Schematic overview of the functioning of the locking mechanism of the transmission of the hand prosthesis. The top figure shows the locking mechanism in its opened state, where water (blue) can flow freely from the inlet to the outlet. The bottom figure show that when pneumatic pressure (red) is applied on the piston, it slides to the right, thus moving the locking mechanism to its closed state, where the flow of water is blocked.

Based on this schematic design, a model was made in SOLIDWORKS, which is shown in figure 4.11. The cylinder of the locking mechanism consists of a stainless steel sleeve with two stainless-steel caps that are glued on, and two connections that are glued on as well. The sleeve has an inner diameter of 10 mm and a wall thickness of 0.4 mm. Furthermore, it has two holes of 4 mm in diameter to which the connections are attached, which act as the hydraulic inlet and outlet. The cap on the left features a 2 mm in diameter hole, that lets air escape and has a protrusion of 2.5 mm in diameter and 5 mm long, that keeps the compression spring in place. The spring has an uncompressed length of 14 mm, an outer diameter of 3.05 mm, a wire diameter of 0.25 mm and a spring constant of 0.2 N/mm, as was calculated with MATLAB. The cap on the right seals the pneumatic side of the cylinder and is beveled with a centered hole of 1.5 mm in diameter, which is the inlet for $CO_2$. The 10 mm in diameter piston is again made of PCTFE and has three Turcon® Glyd Ring® sealings. The groove for the sealing has a width of 2.2 mm and a diameter of 5.1 mm. The thinner central part of the piston is 5.1 mm in diameter as well. Furthermore, the piston has a hole of 5.8 mm in length and 3.1 mm in diameter, that allows the spring to be placed inside. The piston has an overall length of 28.8 mm and a stroke of 8.2 mm, as was calculated with MATLAB. The shorter end of the slider is 4.2 mm in length, the longer end is 12.4 mm in length and the thinner central part is 12.2 mm in length.

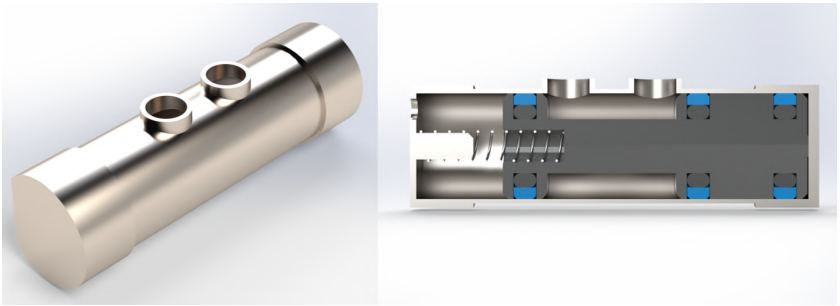

Figure 4.11: Overview of the design of the locking mechanism of the transmission of the hand prosthesis. Left: external overview of the locking mechanism. Right: Cross section of the locking mechanism, showing the internal components.

## 4.4. Pressure regulator

The pressure regulator is the part of this hand that was the most complicated to design. Through many design iterations and after coming up with many different ideas for it, the pressure regulator that is schematically shown in figure 4.12 was conceived. It consists of a piston within a cylinder that has one inlet and four outlets. The piston of the pressure regulator is kept in place by a pretensioned compression spring. When the pneumatic supply inlet on the left is pressurized with a low pressure, the $CO_2$ will flow through the piston and out the first pneumatic outlet, which leads to the stroke cylinder. When the pressure is increased and the forces of the spring and o-ring friction are overcome, the piston will slide to the right. It will first pass the pneumatic outlet that leads to the locking mechanism, which will thus be engaged, and when it slides further it will come to rest against the end of the cylinder and $CO_2$ will flow through the third pneumatic outlet, which leads to the force cylinder. The outlet on the right has two functions: it makes sure that the second and third pneumatic outlet stay/return to atmospheric pressure when they are not being pressurized and it prevents that the movement of the slider is hindered by the compression of gas in the cylinder.

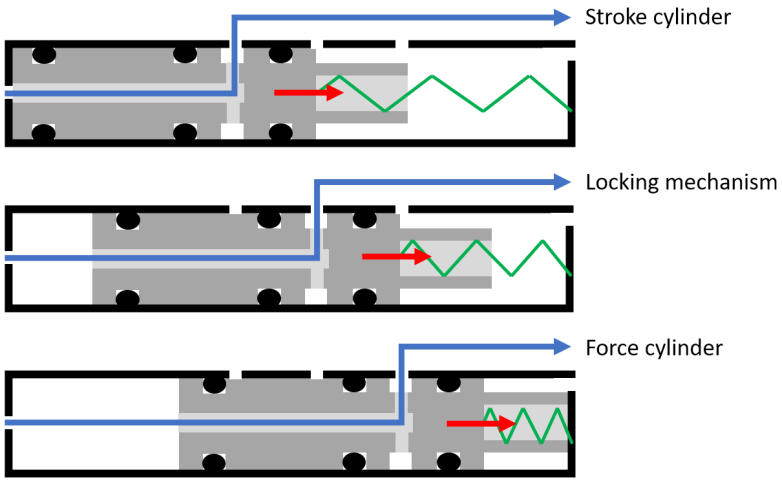


Figure 4.12: Schematic overview of the functioning of the pressure regulator of the hand prosthesis. The top figure shows the pressure regulator for low pressures, where the spring (green) is strong enough to prevent movement of the piston (red) as a result of the pneumatic pressure. Here the gas (blue) flows through the piston to the outlet that leads to the stroke cylinder. Furthermore, the hole in the cylinder end on the right keeps the outlets of the locking mechanism and force cylinder at atmospheric pressure. When the pneumatic pressure is increased, the force on the piston will overcome that of the spring, causing the piston to slide to the right. The piston will first slide past the outlet that leads to the locking mechanism, thus activating it, as can be seen in the middle figure. Next it will slide to the outlet that leads to the force cylinder and the piston will come to rest against the cylinder end, thus letting gas flow to the force cylinder, as can be seen in the bottom figure. When the pneumatic supply pressure is decreased, the piston will slide back and, thus, the outlets of the locking mechanism and the force cylinder will return to atmospheric pressure.

Based on this schematic design, a model was made in SOLIDWORKS, which is shown in figure 4.13. The cylinder of the pressure regulator consists of a stainless steel sleeve with two stainless-steel caps that are glued on. The sleeve has an inner diameter of 8 mm and a wall thickness of 0.4 mm. Furthermore, it has three 2 mm in diameter holes that act as the outlets to the transmission cylinders. The cap on the left is beveled with a centered hole of 2 mm in diameter, which is the inlet for the $CO_2$ supply. The cap on the right has a hole of 2 mm in diameter that lets gas escape. Furthermore, it has two protrusions of 2.5 mm in diameter and 4.5 mm in length, that keep the two compression springs that are used in place. Two springs are used to keep the piston aligned within the cylinder. As calculated with MATLAB, the springs needed to have a compressible length of at least 23.3 mm. However, springs are not fully compressible as the coils will stack against each other. The length of the fully compressed spring is called the block length. Therefore, the spring that was found to work has a length of 28.4 mm and a block length of 4.9 mm, which gives it a compressible length of 23.5 mm. This spring has an outer diameter of 3.05 mm and a coil diameter of 0.25 mm. Furthermore, it has a pretension of 11.5 mm, as was calculated with MATLAB. The springs have a spring constant of 0.1 N/mm which together gives them the required 0.2 N/mm. The 8 mm in diameter piston is again made of PCTFE and has three Turcon® Glyd Ring® sealings. The groove for the sealing has a width of 2.2 mm and a diameter of 3.1

mm. On the left side the slider has a central hole of 2 mm in diameter and 18 mm long, through which the $CO_2$ will flow. The piston has a total length of 26.9 mm. Between the second and third sealing there is a slit in the piston, which allows $co_2$ to flow from the inside of the piston to the pneumatic outlets in the cylinder. On the right side of the piston there are two 3.1 mm in diameter holes with a length of 4.9 mm, that allow the springs to sit in them.

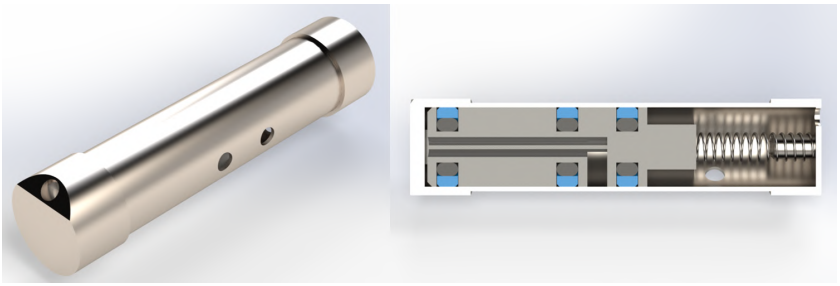

Figure 4.13: Overview of the design of the pressure regulator of the hand prosthesis. Left: external overview of the pressure regulator. Right: Cross section of the pressure regulator, showing the internal components.

## 4.5. Palm base

All the components that were designed need to be combined into a single hand, therefore they need to be attached to a common base. Furthermore, the hand does not have a thumb yet, which is an essential part of the hand. Therefore, a palm base including a thumb needed to be designed, which would integrate all the components and make the pneumatically powered hand prosthesis into a whole. The final design is shown in figure 4.14.

The palm itself is made of aluminium and consists of three parts, as this makes fabrication easier and cheaper. The parts are attached to each other using screws and the four fingers are attached using four M6 screws. The fingers are placed at different distances from the wrist, to mimic a real human hand, even though the same fingers are used. On top of the palm, four connectors are attached with screws that allow the cylinders of the locking mechanism and the pressure regulator to be attached with two connectors each. The stroke cylinder and the force cylinder are each attached with an M4 screw, with the protrusions in them that were made especially for it. The thumb is made of a stainless-steel tube with an outer diameter of 8 mm and a wall thickness of 1 mm. As with the fingertips, a plastic cap covers the tip of the thumb. The other side of the thumb is fixed into an aluminium part with a set screw, and this part is attached to the palm using a hinge, which allows the position of the thumb to be adjusted. At the back of the palm there is an M8 threaded hole with a depth of 10 mm, which allows the hand prosthesis to be attached to a wrist or arm.

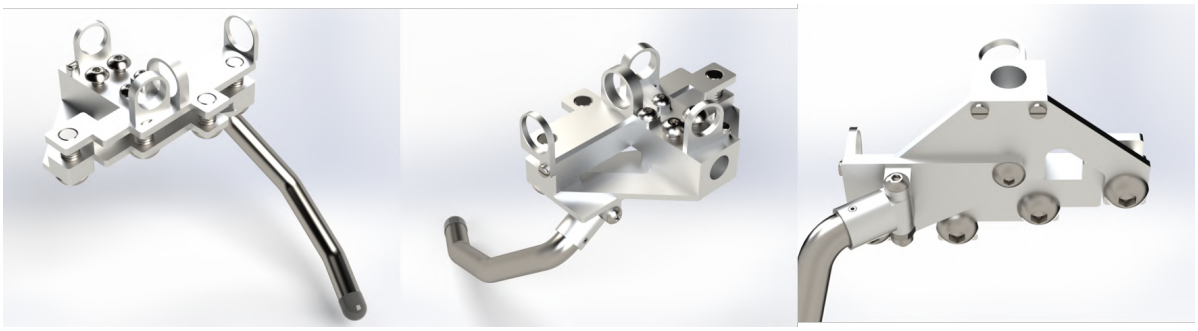

Figure 4.14: Three different views of the palm base, including the thumb, of the design of the hand prosthesis. Each of the four fingers is attached with one of the four M6 screws at the front of the palm. On top of the palm, the connectors for the transmission cylinders and pressure regulator are visible.

## 4.6. Complete hand design

Now that all the parts have been designed, they can be combined into a single pneumatically powered hand prosthesis. Figure 4.15 shows an overview of the complete design of the hand prosthesis including the fingers, transmission, pressure regulator, thumb, palm and connection elements. The outlets of the pressure regulator are connected to the transmission cylinder inlets using stainless steel tubes that are attached with glue. The only things missing in this design overview are the tension springs and the tubing.

Figure 4.15: Three different views of the complete design of the pneumatically powered hand prosthesis, excluding the tension springs on the fingers and the pneumatic tubing.

# 5

# Prototype

To see how well the design detailed in chapter 4 actually works and if its performance is similar to the MATLAB simulations, a prototype will be created that can be tested. This chapter will detail the design stages of the various prototypes and fabrication of the final prototype. Section 5.1 will detail the design of the first two prototypes, section 5.2 will describe the third prototype, section 5.3 will detail the design for the final prototype and, finally, section 5.4 will detail the fabrication and assembly of that prototype.

## 5.1. Prototype design V1 & V2

The first two versions for the prototypes are very similar to the design shown in chapter 4. However, changes are made to improve the functionality, difficulty of fabrication and ease of testing. Furthermore, it is not needed to build the whole pneumatically powered hand prosthesis in order to prove its functionality. The first version, therefore, consists only of the transmission, pressure regulator and a finger. In order to save a lot of production time, version two excludes the finger and will use an existing finger of the Delft Cylinder Hand which is similar and would be enough to prove the functioning of the prototype. The other main differences between the prototypes and the design in chapter 4 are:

- Standard Parker Legris fittings (3281 03 09) are used for connecting the tubing to the cylinders. This makes it easier to use standard tubes and to (dis)connect tubing whenever needed.
- Instead of gluing the caps on both ends of the cylinders, one end is glued, and the other end is screwed on. This means that the cylinders can be opened whenever needed and offers access to the pistons in case that this is needed.
- Standard sizes are used for the stainless-steel cylinder sleeves, which means that they can be bought instead of needing to be fabricated.
- Regular o-rings are used instead of the Turcon® Glyd Ring® sealings, as regular o-rings have been proven to work and are easy to mount on a piston, contrary to the polymer rings.
- The holes in the locking mechanism and pressure regulator along which o-rings slide are adapted to prevent the o-rings from being damaged by the hole edges.
- The protrusions in the locking mechanism and pressure regulator caps, that are used to keep the compression springs in place, are replaced with set screws, as the caps would be hard to fabricate with the protrusions.

Figure 5.1 shows the designs of these first two versions of the prototype. The difference between both versions is that the second version excludes the finger and uses aluminium for some parts instead of stainless-steel to save weight and allow easier fabrication. The following subsections will each describe the specific changes that were made in the second prototype for the designs of the components with respect to the original design from chapter 4.

Figure 5.1: Overview of the design of the first two versions of the prototype for the pneumatic hand prosthesis. Left: first version of the prototype, consisting of the transmission cylinders, pressure regulator, a finger and tube couplings. Right: second version of the prototype, consisting of the transmission cylinders, pressure regulator and tube couplings.

### 5.1.1. Stroke cylinder

The design for a prototype of the high stroke pneumatic-to-hydraulic transmission cylinder is shown in figure 5.2. Here the stainless-steel sleeve is made according to a commercial pipe size. The sleeve has an outer diameter of 28 mm and a wall thickness of 1.5 mm.

The right cap that seals the pneumatic side of the cylinder is still glued on, however, it is made thicker in order to allow a Parker Legris fitting with a 3 mm long M3 thread to be screwed into the beveled surface of the cap. Furthermore, it is made out of aluminium instead of stainless-steel.

The left cap is also made of aluminium and is divided into two parts in order to be able to open it. The outer part is glued to the cylinder sleeve and has an internal M30 thread.

The internal part has an external M30 thread, which allows it to be screwed into the outer part. This way the hydraulic part of the cylinder can be sealed, however, it is still possible to access the piston and to take it out if needed. The internal part, furthermore, has a centered M3 tapped hole in which another Parker Legris fitting can be screwed. Moreover, the internal part has two recesses that make it easier to clamp it and unscrew it.

Finally, the piston features an 21x2 mm o-ring set in a groove with a width of 2.7 mm and a diameter of 21.7 mm.

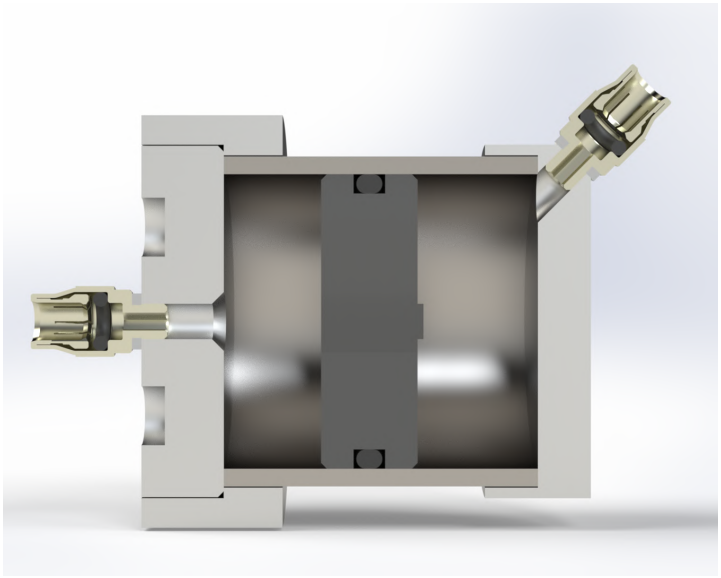

Figure 5.2: Cross section of the second prototype for the stroke cylinder of the transmission of the prosthetic hand.

### 5.1.2. Force cylinder

The design for a prototype of the high force pneumatic-to-hydraulic transmission cylinder is shown in figure 5.3. The right cap that seals the pneumatic side of the cylinder is now made of aluminium and thicker in order to allow a Parker Legris fitting with a 3 mm long M3 thread to be screwed into the beveled surface of the cap.

The outer aluminium part of the cylinder is glued on the right cap and has an internal M30 thread, that allows the left cap to be screwed into it.

The left cap that seals the hydraulic side of the cylinder is made T-shaped and out of aluminium. On the thicker side it has an external M30 thread, which allows it to be screwed into the outer aluminium part, and on the thinner side it has a centered M3 tapped hole in which another Parker Legris fitting can be screwed. Furthermore, this part features the 2 mm vent hole.

The thin side of the piston is now 12.9 mm long, in order to compensate for the thickness of the hydraulic end cap. The piston, furthermore, features an 21x2 mm o-ring set in a groove with a width of 2.7 mm and a diameter of 21.7 mm, and a 10x2 mm o-ring set in a groove with a width of 2.7 mm and a diameter of 10.7 mm

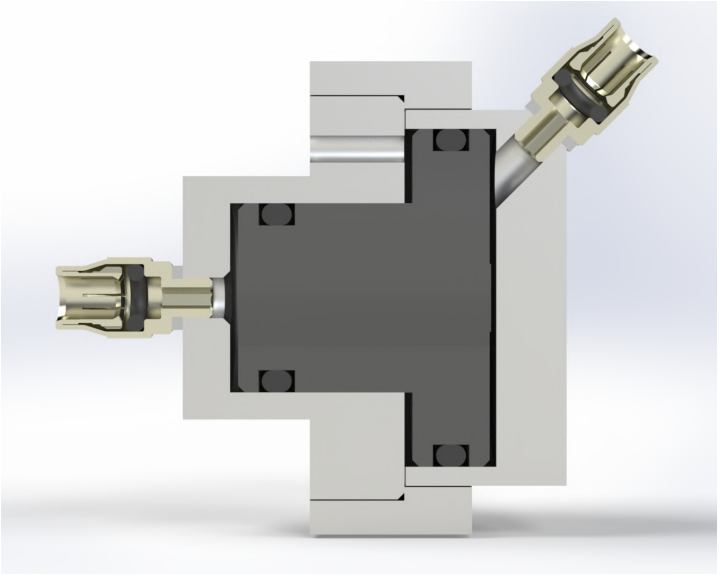

Figure 5.3: Cross section of the second prototype for the force cylinder of the transmission of the prosthetic hand.

### 5.1.3. Locking mechanism

The design for a prototype of the locking mechanism is shown in figure 5.4. Here the stainless-steel sleeve is made according to a commercial pipe size. The sleeve has an outer diameter of 12 mm and a wall thickness of 1 mm.

The right cap that seals the pneumatic side of the cylinder is now made of aluminium and thicker in order to allow a Parker Legris fitting with a 3 mm long M3 thread to be screwed into the beveled surface of the cap.

The connections, which act as the hydraulic inlet and outlet, have an internal M3 thread, which allows Parker Legris fittings to be screwed in. Furthermore, the drill hole on the right in the sleeve is internally chamfered to prevent damage to the o-rings.

The hydraulic end cap on the left is made of two aluminium parts. The outer part is glued on the stainless-steel sleeve and has an internal M14 thread.

The inner part has an external M14 thread, which allows it to be screwed into the outer part. This way the hydraulic part of the cylinder can be sealed, however, it is still possible to access the piston and to take it out if needed. The internal part, furthermore, has a centered M2.5 tapped hole in which the M2.5x10 mm set screw can be screwed, that is used to keep the compression spring in place. Moreover, the internal part features the 2 mm vent hole.

The sealings of the piston have been replaced for three 7x1.5 mm o-rings that are set in grooves that have a width of 2 mm and a diameter of 7.5 mm.

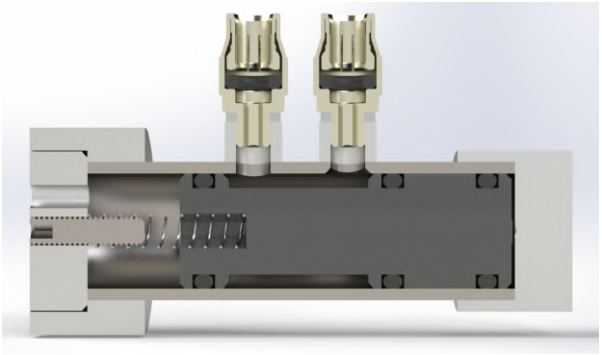

Figure 5.4: Cross section of the second prototype for the locking mechanism of the transmission of the prosthetic hand.

### 5.1.4. Pressure regulator

The design for a prototype of the pressure regulator is shown in figure 5.5. Here the stainless-steel sleeve is made according to a commercial pipe size. The sleeve has an outer diameter of 9 mm and a wall thickness of 0.5 mm.

The right cap that seals the pneumatic inlet side of the cylinder is now made of aluminium and thicker in order to allow a Parker Legris fitting with a 3 mm long M3 thread to be screwed into the beveled surface of the cap.

The three connections, which act as the outlets to the duel-mode transmission cylinders, have an internal M3 thread, which allows Parker Legris fittings to be screwed in. Each of the holes in the stainless-steel sleeve that leads to one of the aforementioned outlets has now been replaced by 5 holes with a diameter of 0.3 mm in a plus shaped pattern. The face of the o-ring that slides past the holes has a width of 0.38 mm and, therefore, choosing the holes smaller than this prevents the o-rings from being damaged.

The end cap on the left is made of two aluminium parts. The outer part is glued on the stainless-steel sleeve and has an internal M10 thread.

The inner part has an external M10 thread, which allows it to be screwed into the outer part. This way this part of the cylinder can be sealed, however, it is still possible to access the piston and to take it out if needed. The internal part, furthermore, has a two M2.5 tapped holes in which the M2.5x8 mm set screws can be screwed, that are used to keep the compression springs in place. Moreover, the internal part features the 2 mm vent hole.

The sealings of the piston have been replaced for three 5x1.5 mm o-rings that are set in grooves that have a width of 2 mm and a diameter of 5.5 mm.

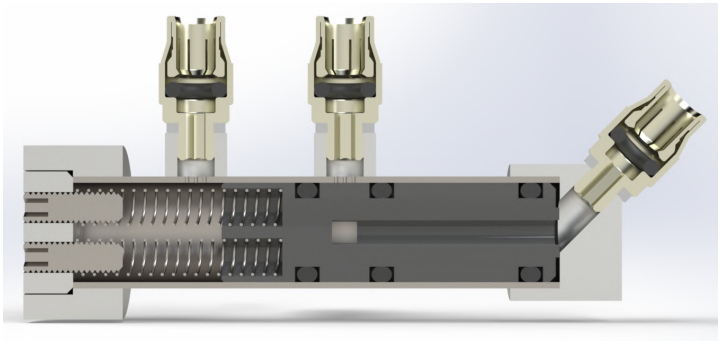

Figure 5.5: Cross section of the second prototype for the pressure regulator of the prosthetic hand.

## 5.2. Prototype design V3

Based upon the design of the second version of the prototype and many brainstorm sessions with other technicians, changes were made to the prototype in order to further improve the functionality, difficulty of fabrication and ease of testing. An overview of the design of the third version of the prototype is

shown in figure 5.6.

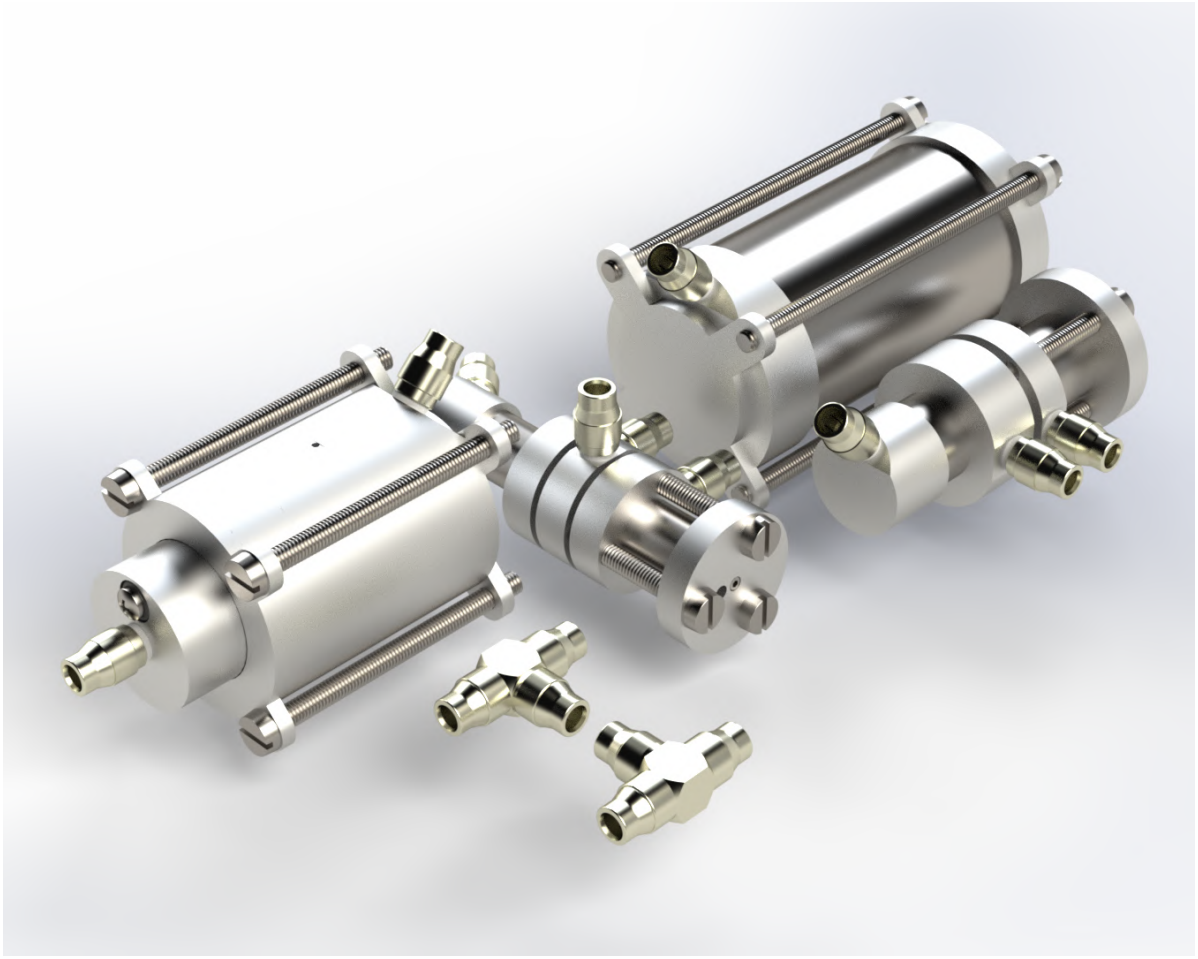

Figure 5.6: Overview of the third design for a prototype for the pneumatic hand prosthesis, consisting of the transmission cylinders, pressure regulator and tube couplings.

The main differences between the third version and second version of the prototype are:

- The length of the piston of the high stroke pneumatic-to-hydraulic transmission cylinder is increased in order to prevent blocking due to the piston tilting and getting stuck in the cylinder.
- The diameter of the pistons is decreased with 0.2 mm in order to leave a required clearance between the piston and the cylinder.
- The cylinder ends into which the pistons are inserted are internally chamfered under a 15-degree angle, which allows the o-rings to be gradually compressed when the pistons are inserted. This not only makes facilitates insertion, but it also prevents damage to the o-rings when inserted.
- Instead of sealing the cylinder ends using screwed in caps, the ends are plugged with a cap with an o-ring that is pressed inside the cylinder. This does not only make fabrication a lot easier and faster, but it also facilitates opening or closing the cylinders.
- The stroke of the high force pneumatic-to-hydraulic transmission cylinder is increased in order to prevent it from not working due to the elasticity of other parts in the system. This cylinder has a very short stroke but produces a high pressure, therefore, if another part in the system would deform due to the pressure, the stroke will be lost in compensating for this deformation instead of moving the fingers.
- Instead of using a chamfered hole for the hole along which an o-ring slides in the locking mechanism, the cylinder sleeve is cut and chamfered under a 15-degree angle at this location. A ring

with an outlet hole is placed around this cut to connect the two parts of the cylinder sleeve together. This solution prevents damage to the o-ring but still allows water to flow freely to the hydraulic outlet of the locking mechanism.

- The pressure regulator uses a single compression spring instead of two, as this is much easier to fabricate and does not suffer from alignment issues when compressed.
- Drain holes are added to the pneumatic-to-hydraulic transmission cylinders in order to facilitate the filling of the system with water.
- The end caps are kept in place using a cage construction using M3 screws. This keeps the cylinders together even under high pressure and is easy to (dis)assemble.

The following subsections will each describe the specific changes that were made in the third prototype for the designs of the components with respect to the second prototype from section 5.1.

### 5.2.1. Stroke cylinder

The design for the third prototype of the high stroke pneumatic-to-hydraulic transmission cylinder is shown in figure 5.7. The stainless-steel sleeve has a 15-degree chamfer on the left side, where the piston is inserted through.

The hydraulic end cap on the left now is designed like a plug. Therefore, it has a part with a smaller diameter of 24.8 mm that slides into the cylinder sleeve, with an o-ring to seal the cylinder. The o-ring is the same one as used in the piston and is a 21x2 mm o-ring set in a groove with a width of 2.7 mm and a diameter of 21.7 mm. Furthermore, a drain hole is added to the hydraulic end cap. Herefore, an M3 tapped hole is made into the end cap which allows water to flow through it when it is not sealed. At the end of this hole a 1.3 mm deep and 6.4 mm in diameter hole is made into which a 3x1.5 mm o-ring is placed. This o-ring together with the M3x8 mm screw seals the drain hole when it is not used.

The length of the piston was increased and is now 18.2 mm, and therefore two o-rings are used on the piston instead of a single one. Furthermore, the diameter of the piston was decreased to 24.8 mm to leave a clearance between it and the cylinder wall.

Two laser cut brackets, one at each end of the cylinder, are clamped together using four M3 screws and make sure that the hydraulic end cap plug remains in place even when the cylinder is pressurized.

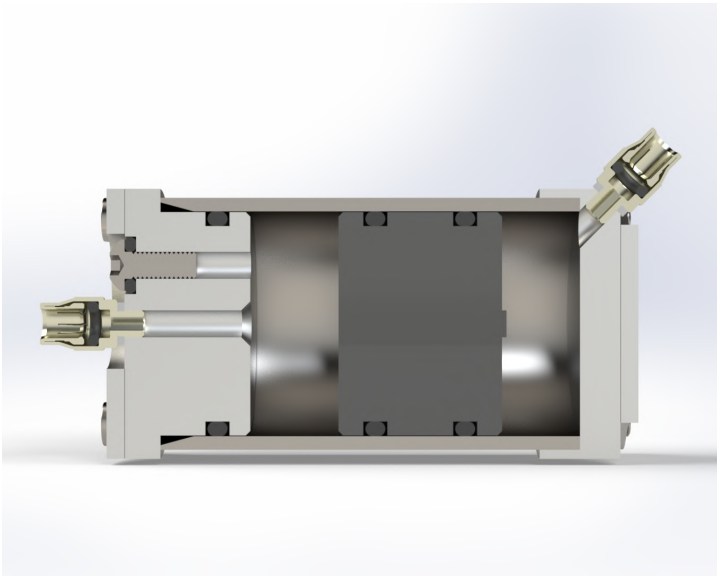

Figure 5.7: Cross section of the third prototype for the stroke cylinder of the transmission of the prosthetic hand.

### 5.2.2. Force cylinder

The design for the third prototype of the high force pneumatic-to-hydraulic transmission cylinder is shown in figure 5.8. The cylinder now consists of two aluminium parts: the pneumatic end cap and the

hydraulic end cap. The hydraulic end cap on the left now is designed like a plug. Therefore, it has a part with a smaller diameter of 24.8 mm that slides into the pneumatic end cap, with an o-ring to seal the cylinder. The o-ring is the same one as used in the piston and is a 21x2 mm o-ring set in a groove with a width of 2.7 mm and a diameter of 21.7 mm. Furthermore, the internal 14 mm in diameter hole of this cap has an internal chamfer of 15-degrees on the right side, where the piston is inserted through. Moreover, a drain hole is added to the hydraulic end cap. Herefore, an M2 tapped hole is made into the end cap which allows water to flow through it when it is not sealed. At the end of this hole a 1.3 mm deep and 5.4 mm in diameter hole is made into which a 2x1.5 mm o-ring is placed. This o-ring together with the M2x4 mm screw seals the drain hole when it is not used.

The pneumatic end cap has a 15-degree chamfer on the left side, where the piston is inserted through. Furthermore, it has a 1 mm in diameter vent hole on the top, that lets air flow when the piston moves, and prevents the movement of the piston from being hindered by the compression of air.

The length of the thin side of the piston was increased to 22.9 mm in order to compensate for the increased internal length of the hydraulic end cap. Furthermore, the large diameter of the piston was decreased to 24.8 mm and the small diameter to 13.8 mm, in order to leave a clearance between it and the cylinder wall.

Two laser cut brackets, one at each end of the cylinder, are clamped together using four M3 screws and make sure that the hydraulic end cap plug remains in place even when the cylinder is pressurized.

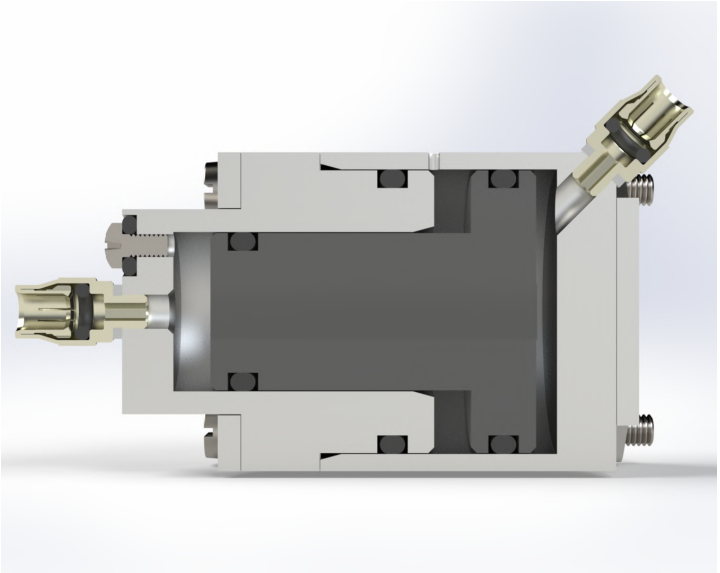

Figure 5.8: Cross section of the third prototype for the force cylinder of the transmission of the prosthetic hand.

### 5.2.3. Locking mechanism

The design for the third prototype of the locking mechanism is shown in figure 5.9. The stainless-steel cylinder sleeve is now divided into two pieces: one before the hydraulic outlet and one after the hydraulic outlet. Furthermore, the sleeve has 15-degree chamfers on the left side, where the piston is inserted through, and around the hydraulic outlet.

Two aluminium connection rings, both with M3 tapped holes for the Parker Legris fittings for the hydraulic inlet and outlet, are glued around the cylinder sleeve. The thinner one is placed around the left 3 mm in diameter hole in the cylinder sleeve and the thicker one connects both parts of the sleeve together to form the hydraulic outlet. Furthermore, the thinner ring has three M3 tapped holes in its side, spaced at 120 degrees angles, which will allow the pneumatic end cap to be screwed on.

The diameter of the pneumatic end cap has been increased, which allows three 3 mm in diameter holes to be drilled in, spaced at 120 degrees angles. Three M3x20 mm screws are placed through these holes, and they screw into the thinner connection ring. This makes sure that the pneumatic end cap is securely attached.

The diameter of the piston was decreased to 9.8 mm, in order to leave a clearance between it and the cylinder wall.

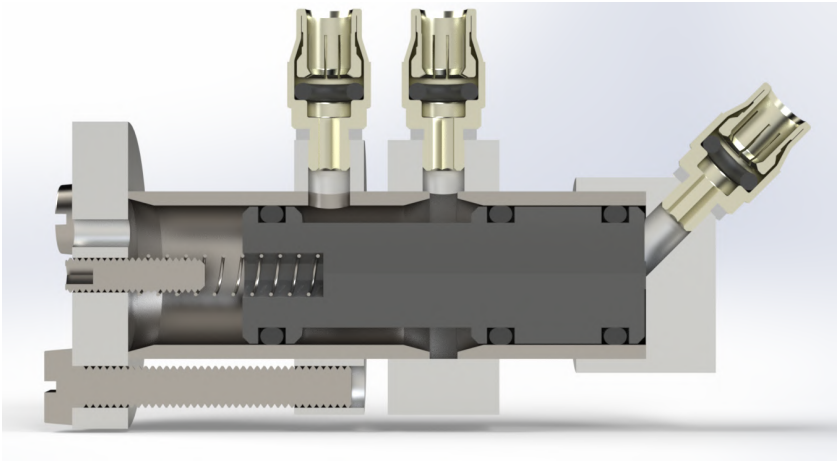

Figure 5.9: Cross section of the third prototype for locking mechanism of the transmission of the prosthetic hand.

### 5.2.4. Pressure regulator

The design for the third prototype of the pressure regulator is shown in figure 5.10. The five 0.3 mm in diameter holes that were drilled into the stainless-steel cylinder sleeve at a plus shape pattern are now replace by three 0.3 mm in diameter holes next to each other along the radius of the sleeve. Furthermore, the sleeve has a 15-degree chamfer on the left side, where the piston is inserted through.

Three aluminium connection rings, all with M3 tapped holes for the Parker Legris fittings for the pneumatic outlets, are glued around the cylinder sleeve. All are place around the 0.3 mm in diameter holes in the cylinder sleeve. Furthermore, the left ring has three M3 tapped holes in its side, spaced at 120 degrees angles, which will allow the left end cap to be screwed on.

The diameter of the left end cap has been increased, which allows three 3 mm in diameter holes to be drilled in, spaced at 120 degrees angles. Three M3x20 mm screws are placed through these holes, and they screw into the left connection ring. This makes sure that the left end cap is securely attached. Furthermore, instead of two M2.5 tapped holes, the left end cap now only has one M2 tapped hole in which an M2x12 mm set screw is placed, that keeps the compression spring in place. Instead of two parallel compression springs with spring constants of 0.1 N/mm, now a single compression spring with a spring constant of 0.2 N/mm is used.

The diameter of the piston was decreased to 7.8 mm, in order to leave a clearance between it and the cylinder wall. Furthermore, the two 3.1 mm in diameter holes for the springs to fit in were replaced by a single 3.1 mm in diameter hole, as only one spring is used now.

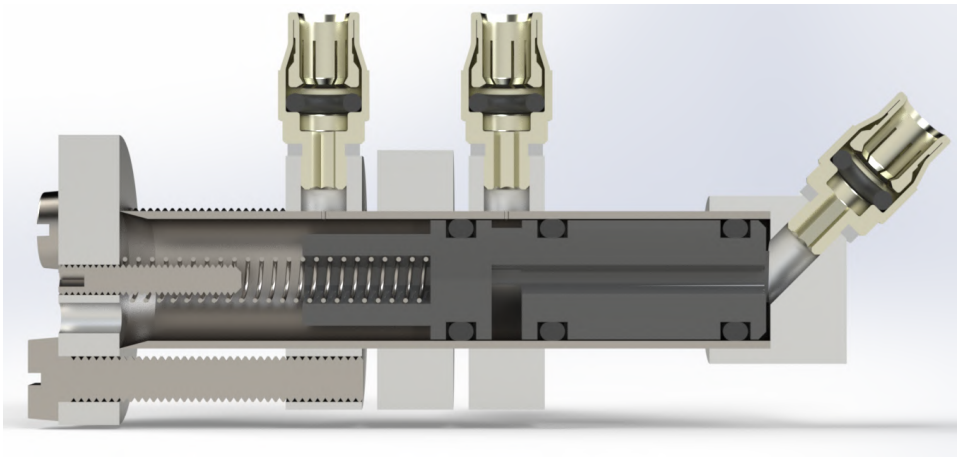

Figure 5.10: Cross section of the third prototype for the pressure regulator of the prosthetic hand.

## 5.3. Prototype design V4

Based upon the design of the third version of the prototype and many brainstorm sessions with other technicians, changes were made to the prototype in order to further improve the functionality, difficulty of fabrication and ease of testing. An overview of the design of the fourth and final version of the prototype is shown in figure 5.11.

Figure 5.11: Two different views of the fourth design for a prototype for the pneumatic hand prosthesis, consisting of the transmission cylinders and pressure regulator.

The main differences between the fourth version and third version of the prototype are:

- Instead of placing Parker Legris fittings on beveled edges on the caps of the cylinders, these are placed in the center of the caps. This makes them much easier to fabricate
- The o-rings in the pressure regulator were replaced with 4x2 mm o-rings, meaning that the holes along which they slide can be single 0.5 mm in diameter holes instead of three 0.3 mm in diameter holes.
- The pistons are made out of aluminium instead of PCTFE. This will make them much easier to fabricate and as the o-rings slide past the cylinder, and not the piston itself, it will not have an effect on the friction coefficient.
- The drilled holes in the pistons are now real drilled holes and not flat ended ones.
- The detachable caps of the locking mechanism and pressure regulator now have protrusions sticking into the cylinder sleeves, which helps them stay aligned.
- The gas channels in the pressure regulator piston were redesigned in order to be symmetric and thus not needing to be aligned.

The following subsections will each describe the specific changes that were made in the fourth prototype for the designs of the components with respect to the third prototype from section 5.2. The technical drawings with the dimensions of all the parts used in this prototype can be found in appendix C. Furthermore, appendix D shows the drawings for the brackets that are laser cut.

### 5.3.1. Stroke cylinder

The design for the fourth and final prototype of the high stroke pneumatic-to-hydraulic transmission cylinder is shown in figure 5.12. Here the piston is made of aluminium instead of PCTFE. Furthermore, the pneumatic end cap on the right now has a centrally tapped M3 hole, which allows a Parker Legris fitting with a 3 mm long M3 thread to be screwed in. To allow the fitting to pass through the right bracket that keeps the cylinder together, a 6 mm diameter hole is made in its center.

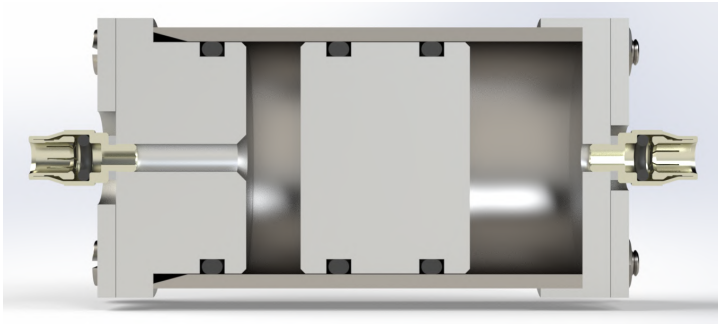

Figure 5.12: Cross section of the fourth prototype for the stroke cylinder of the transmission of the prosthetic hand.

### 5.3.2. Force cylinder

The design for the fourth and final prototype of the high force pneumatic-to-hydraulic transmission cylinder is shown in figure 5.13. Here the piston is made of aluminium instead of PCTFE. Furthermore, the end cap on the right now has a centrally tapped M3 hole, which allows a Parker Legris fitting with a 3 mm long M3 thread to be screwed in. To allow the fitting to pass through the right bracket that keeps the cylinder together, a 6 mm diameter hole is made in its center.

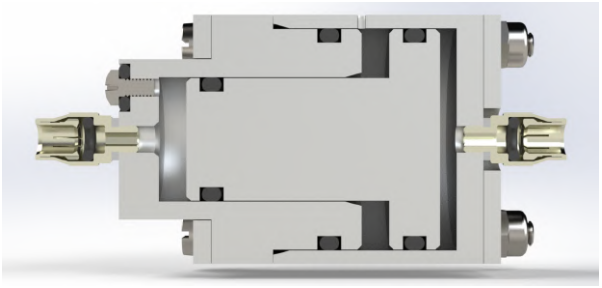

Figure 5.13: Cross section of the fourth prototype for the force cylinder of the transmission of the prosthetic hand.

### 5.3.3. Locking mechanism

The design for the fourth and final prototype of locking mechanism is shown in figure 5.14. Here the piston is made of aluminium instead of PCTFE and the hole for the spring to fit in is now drilled with a 3.2 mm drill bit to a depth of 5.8 mm. Furthermore, the end cap on the right now has a centrally tapped M3 hole, which allows a Parker Legris fitting with a 3 mm long M3 thread to be screwed in. The end cap on the left now has a 2 mm long protrusion with a diameter of 9.8 mm that sticks inside the cylinder sleeve and keeps it aligned. The centrally tapped M2.5 hole in this cap has been changed for a M2 hole, to allow an M2x12 set screw to be used.

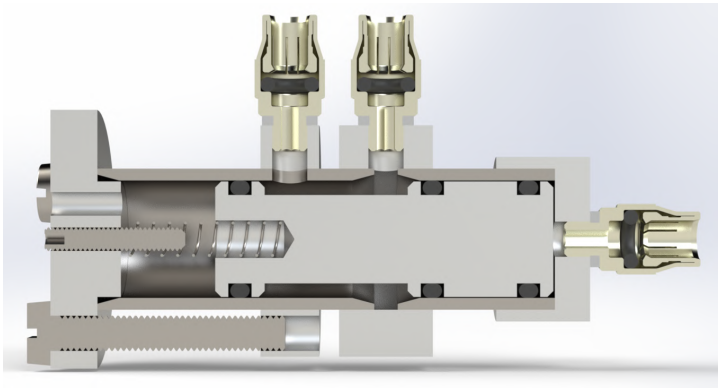

Figure 5.14: Cross section of the fourth prototype for the locking mechanism of the transmission of the prosthetic hand.

### 5.3.4. Pressure regulator

The design for the fourth and final prototype of pressure regulator is shown in figure 5.15. Here the piston is made of aluminium instead of PCTFE and the hole for the spring to fit in is now drilled in with a 3.8 mm drill bit to a depth of 8.4 mm. The three o-rings of the piston have been replaced by 4x2 mm o-rings placed in grooves with a width of 2.7 mm and a diameter of 4.7 mm. The central hole which allows gas to flow through the piston is drilled in with a 2 mm drill bit to a depth of 18 mm. At the end hereof, the diameter of the cylinder is reduced to 6 mm, and it is drilled through twice perpendicularly, using a 1.5 mm drill bit. This allows gas to flow from the central 2 mm canal, through the four 1.5 mm holes and into the groove with a width of 2 mm and a diameter of 6 mm. When this groove moves past one of the outlets, $CO_2$ will therefore flow from the supply inlet to this outlet.

The three side-by-side 0.3 mm in diameter holes in the stainless-steel cylinder sleeve have now been replaced by a single 0.5 mm in diameter hole. Furthermore, the end cap on the right now has a centrally tapped M3 hole, which allows a Parker Legris fitting with a 3 mm long M3 thread to be screwed in. Moreover, the end cap on the left now has a 2 mm long protrusion with a diameter of 7.8 mm that sticks inside the cylinder sleeve and keeps it aligned.

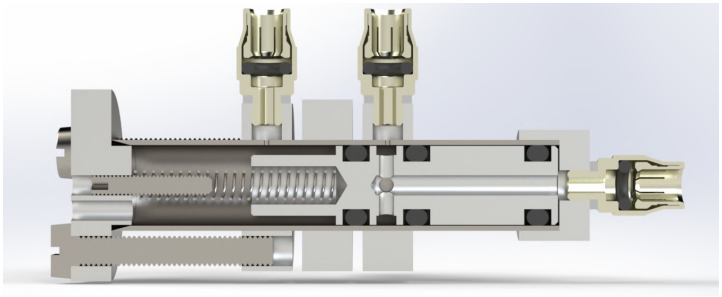

Figure 5.15: Cross section of the fourth prototype for the pressure regulator of the prosthetic hand.

## 5.4. Final Prototype

Using the technical drawings in appendices C and D, all the parts for the final prototype from section 5.3 were fabricated in the workshop of the 3mE faculty of the Delft University of Technology, with the help of Reinier van Antwerpen. Pictures of all the manufactured parts, with the names corresponding to those in the technical drawings, are available in appendix E. Furthermore, table 5.1 shows an overview of all the standard components that are used to make the prototype. The glue used to glue the components together is Loctite 638 and the o-rings are lubricated using Rocol Kilopoise. The picture in figure 5.16 shows an overview of the completely manufactured and assembled prototype, consisting of the high stroke cylinder, high force cylinder, locking mechanism and the pressure regulator.

Table 5.1: Inventory of the standard components used in the prototype for the pneumatically powered hand prosthesis.

| Category | Type | Size | Min. Qty |
|---|---|---|---|
| O-rings | | 10 x 2 mm | 1 |
| | | 21 x 2 mm | 5 |
| | | 4 x 2 mm | 3 |
| | | 2 x 1.5 mm | 1 |
| | | 3 x 1.5 mm | 1 |
| | | 7 x 1.5 mm | 3 |
| Legris | 3281 03 09 | M3 | 11 |
| | 3204 03 00 | M3 | 2 |
| Screws | | M3 x 40 mm | 4 |
| | | M2 x 4 mm | 1 |
| | | M3 x 60 mm | 4 |
| | | M3 x 8 mm | 1 |
| | | M3 x 20 mm | 6 |
| | Set screw | M2 x 12 mm | 2 |
| Nuts | | M3 | 4 |
| | Locknut | M3 | 4 |
| Springs | D10530 | | 1 |
| | D20530 | | 1 |
| | D10785 | | 1 |
| | D20785 | | 1 |
| | D10790 | | 1 |
| | D20790 | | 1 |

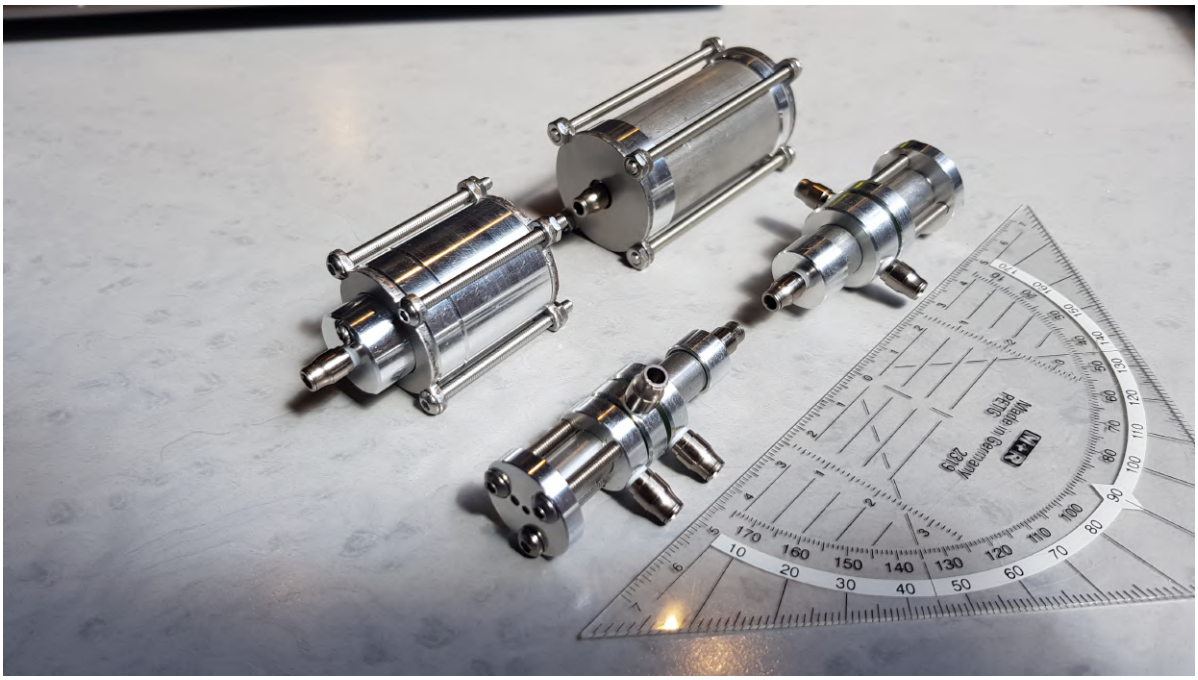

Figure 5.16: Picture of the fabricated and assembled prototype, consisting of the force cylinder (left), stroke cylinder (top), locking mechanism (right) and pressure regulator (bottom), next to a ruler showing the scale.

# 6

# Testing

The prototype designed and manufactured in chapter 5 needs to be tested, in order to measure its actual performance. This chapter will therefore detail the tests performed with the prototype, and the results thereof. Section 6.1 will detail the manual test that was performed, section 6.2 gives an overview of the setup used for testing, section 6.3 details the testing of the pneumatic side of the system and, finally, section 6.4 describes the testing of the fully functional prototype system.

## 6.1. Manual test

The first test that was performed with the prototype shown in section 5.4 was a manual one. Here the pistons of the high stroke cylinder, high force cylinder, locking mechanism and pressure regulator were manually moved using a small 1.5 mm hex key, that fits through the hole in the Parker Legris fittings. This was done to validate if the pistons were able to move at all, to estimate the friction caused by the compression of the o-rings, and to see if the return springs were strong enough to return the pistons to their initial position.

The pistons were indeed able to slide around when manual pressure was applied using the hex key. The amount of force needed to get them to move, however, was much more than expected. For the high stroke cylinder, I even needed almost all the force in my arms to get it to move. This indicates that the friction created by the o-rings is much higher than expected and even too much for this application. Furthermore, although the compression spring of the pressure regulator was able to successfully return the piston to its initial position, due to the significant pretension, the compression spring of the locking mechanism did not move the piston at all.

The cylinders of the prototype were, therefore, opened and the pistons were removed in order to see what could cause the excessive friction. Inspection of the components and consultation with Jan van Frankenhuyzen, led to the following observations:

1. The compression of the o-rings, as prescribed by the manufacturer, is too much for this application and would be more suited for industrial applications. In the prototype, o-rings are compressed up to 18% of their thickness, but for this kind of application a compression of 10% would suffice.

2. The lubricant used for the o-rings in the prototype should have been Rocol Kilopoise, as mentioned in section 5.4. However, as it turns out a syringe containing the wrong kind of lubricant was supplied by the workshop and used in the prototype. This lubricant is much tackier and viscous than Rocol Kilopoise and, therefore, also contributes to the increased o-ring friction.

To overcome these problems, and hopefully reduce the amount of o-ring friction, the following two changes were made to the prototype:

1. The grooves in the pistons for the o-rings were made deeper, to limit the compression of the o-rings to 10% of their thickness. The MATLAB script in appendix B.9 was used to calculate the exact groove depth for each of the o-rings. The diameter of the grooves in the piston of the high stroke cylinder for the 21x2 mm o-rings were, therefore, reduced from 21.7 mm to 21.4 mm. The diameter of the grooves in the piston of the high force cylinder were reduced from 21.7 mm to

21.4 mm for the 21x2 mm o-ring, and from 10.7 mm to 10.4 mm for the 10x2 mm o-ring. The diameter of the grooves in the piston of the locking mechanism for the 7x1.5 mm o-rings were reduced from 7.5 mm to 7.3 mm. Finally, the diameter of the grooves in the piston of the pressure regulator for the 4x2 mm o-rings were reduced from 4.7 mm to 4.4 mm.

2. All components that were covered with the wrong kind of lubricant were cleaned using turpentine. Next, the correct lubricant, Rocol Kilopoise, was applied to all the o-rings before assembling the prototype again.

After applying these changes, the prototype was reassembled, and the same manual test as described earlier was repeated. This showed that the friction in the pistons of the high stroke cylinder, high force cylinder and pressure regulator had decreased significantly. These were now able to move with a fraction of the force that was needed before. The locking mechanism, however, still showed a significant amount of resistance; Not because of the o-ring friction -this was also significantly lower than before- but because of the resistance of the o-ring when it exits the first half of the cylinder sleeve and enters the second one. Here the o-ring needs to be compressed again to enter the sleeve and this takes a force that although it is possible to do it by hand, the return spring that belongs to the locking mechanism is not strong enough to return the piston to its original position. This compression spring was therefore replaced by a stronger, pretensioned spring, i.e. the same spring as used in the pressure regulator, in order to hopefully be strong enough to overcome this resistance.

## 6.2. Overview setup

Figure 6.1 shows a schematic overview of the setup that is used for testing the prototype of the pneumatically powered hand prosthesis. A pneumatic supply is used to pressurize the pressure regulator. The controls the distribution of $CO_2$ to the rest of the system, and its outlets are connected to the pneumatic inlets of the high stroke cylinder, high force cylinder and the locking mechanism. The hydraulic outlet of the high stroke cylinder is connected to the hydraulic inlet of the locking mechanism. The hydraulic outlets of the locking mechanism and high force cylinder both lead to one end of a Parker Legris T-coupling. The hydraulic outlet of this T-coupling is connected to the inlets of the hydraulic cylinder(s) of the finger(s).

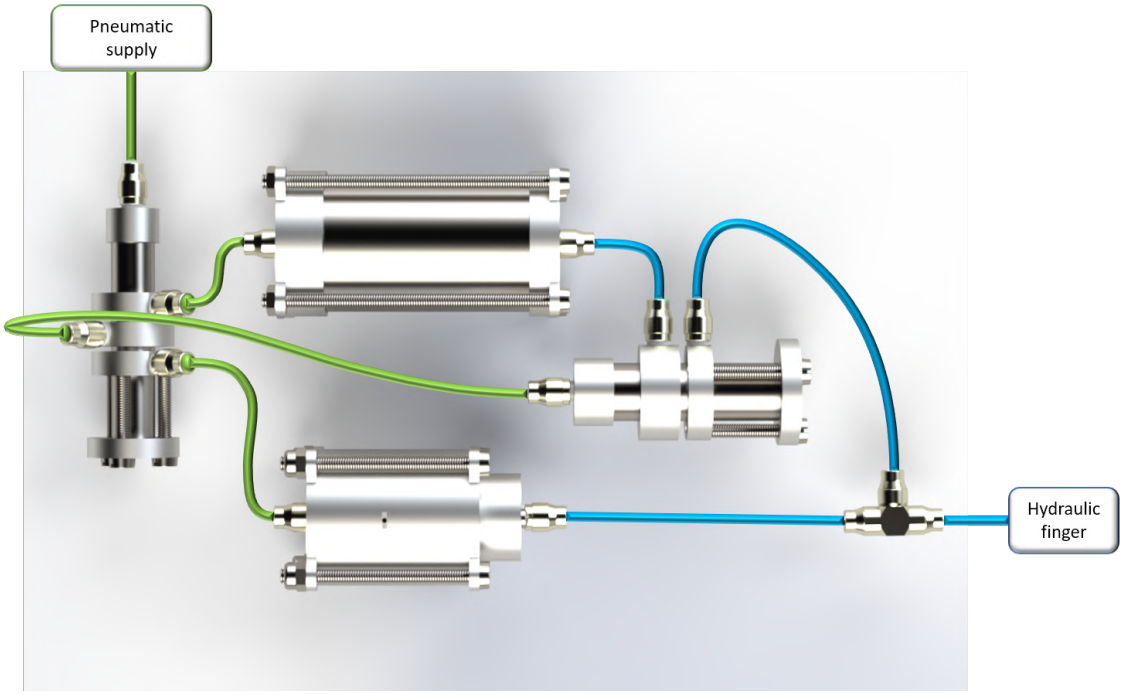


Figure 6.1: The connection scheme of the prototype. Green is used to indicate pneumatic tubing, and blue to indicate hydraulic tubing. A pneumatic supply is connected to the inlet of the pressure regulator, which controls the transmission. The outlets of the transmission are connected to a T-coupling that joins them and leads to the inlet of the hydraulic finger.

Figure 6.2 shows the hand prosthesis of which the finger(s) will be used to test the prototype. This hand is the second version of the Delft Cylinder Hand; however, adjustments have been made for various other projects. The middle two finger are, however, still unchanged and are those that will be used for testing. Contrary to my design for the fingers, this hand only has a single hydraulic cylinder per finger. Therefore, the movement of all phalanges is coupled to the extension of this cylinder.

Figure 6.2: The hydraulic hand prosthesis of which one finger was used for testing the prototype. Top picture: overview of the hand that was used, consisting of four fingers. Bottom picture: side view of the hand, showing the construction of a finger.

## 6.3. Pneumatic test

After having performed manual tests on the components of the prototype, tests were performed using a pneumatic supply in order to validate the correct functioning of the pneumatic side of the system before testing the complete hybrid system. This way problems with the pneumatic side of the system can be detected more easily than when the whole setup is connected. The setup that is used in these tests is shown in figure 6.3. Here a 410g $CO_2$ SodaStream canister is used as the pneumatic supply and a custom flow regulating valve is used to control the supply flow. A Festo MA-23-16-R1/8 manometer, with a range of 0 to 16 bar, is used to measure the supply pressure.

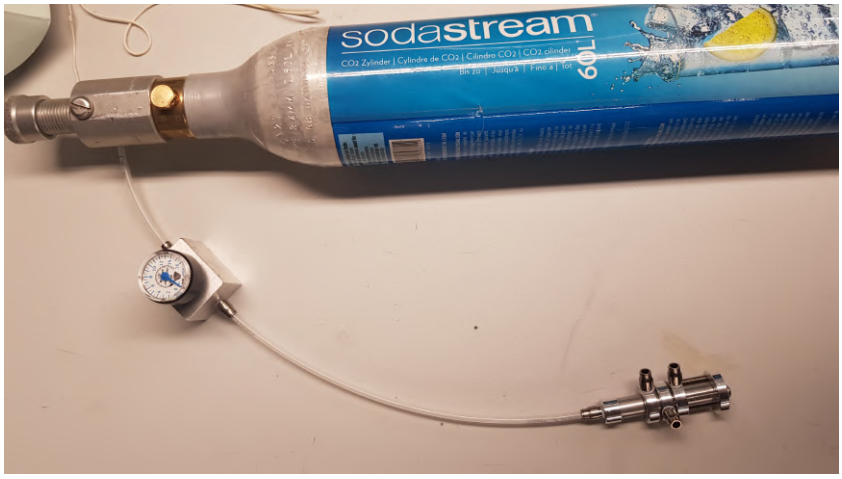


Figure 6.3: Setup used to for pneumatic testing, in this case the pressure regulator is attached. A $CO_2$ supply consisting of a SodaStream canister with a flow regulating valve, is connected to a manometer, which in turn is connected to the pneumatic inlet of the component that will be pressurized.

### 6.3.1. Individual components

The first thing that was done was to pressurize each of the four components individually, to see their response to being pressurized and to validate if this is in line with the expected behavior.

The first component to be tested was the pressure regulator. Figures 6.4, 6.5 and 6.6 show the pressure regulator under an increasing supply flow. The figures show that the pressure regulator indeed performs as intended, i.e. the supply flow leads to the first, second and third outlet respectively under an increasing inlet pressure. Furthermore, the compression spring proved to be strong enough to return the piston to its original position once the regulator was depressurized.

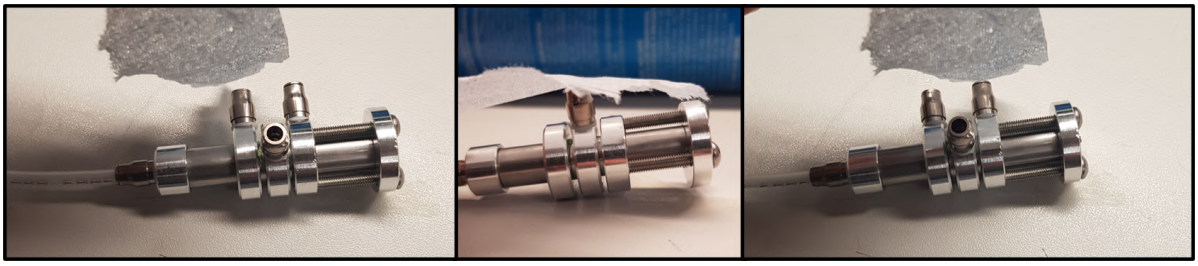

Figure 6.4: Response of the pressure regulator to a low pneumatic inlet flow. Here it can be seen that the $CO_2$ flows from the inlet to the first outlet, i.e. the outlet leading to the high stroke cylinder.

Figure 6.5: Response of the pressure regulator to a moderate pneumatic inlet flow. Here it can be seen that the $CO_2$ flows from the inlet to the second outlet, i.e. the outlet leading to the locking mechanism.

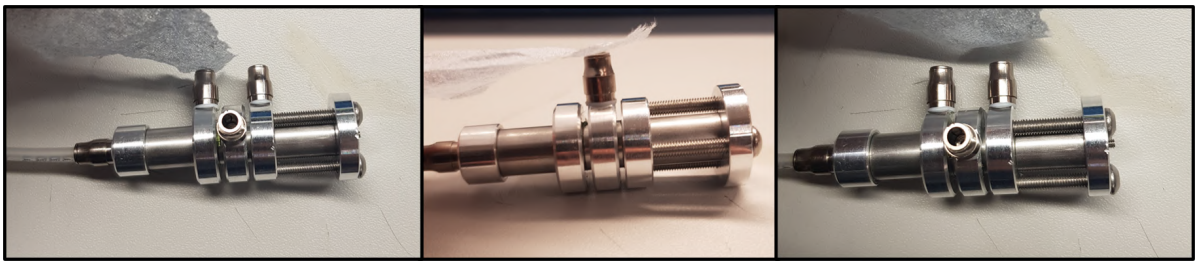

Figure 6.6: Response of the pressure regulator to a high pneumatic inlet flow. Here it can be seen that the $CO_2$ flows from the inlet to the third outlet, i.e. the outlet leading to the high force cylinder.

The next component to be tested was the locking mechanism. Figure 6.7 shows the locking mechanism before and after being pressurized at the pneumatic inlet (left coupling). Air was blown in at the hydraulic inlet (bottom coupling) to see if the locking mechanism indeed engaged and sealed the hydraulic outlet (top coupling). As can be seen in the figure, the locking mechanism works as intended, i.e. when depressurized the locking mechanism allows flow from the hydraulic inlet to the hydraulic outlet, but when the locking mechanism is pressurized it seals off the hydraulic outlet and prevents flow from the hydraulic inlet to the hydraulic outlet. The return spring, however, is not strong enough to return the piston of the locking mechanism to its original position after depressurization, even after being replaced with the stronger spring. The piston therefore has to be pushed back to its original position manually using a 1.5 mm hex key that fits through the air venting hole in the end cap on the right.

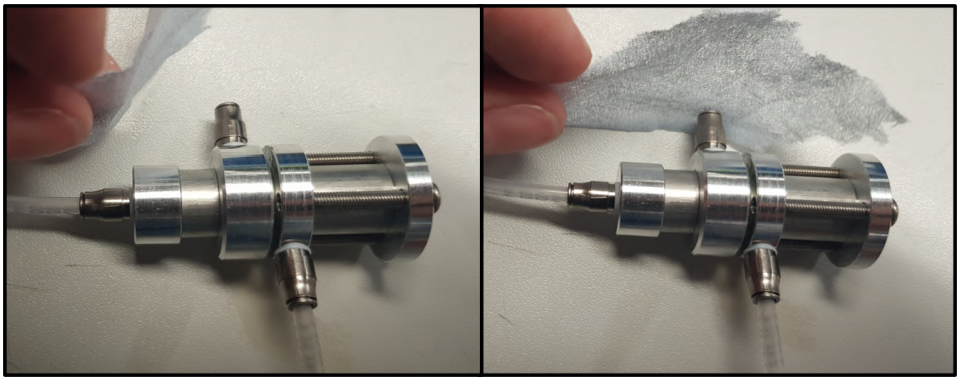

Figure 6.7: Response of the locking mechanism to pressurization. Left: the locking mechanism before being pneumatically pressurized, with air flowing through the cylinder. Right: the locking mechanism after being pneumatically pressurized, with the air flow being blocked.

Finally, the high stroke and high force cylinders were tested. Here the inlet pressure was gradually increased, which resulted in the pistons of the respective cylinders gradually sliding from the pneumatic inlet side to the hydraulic outlet side. Very little inlet pressure was needed to get the pistons moving and their behavior is therefore in line with the design.

### 6.3.2. Connected system

After having tested each of the components individually, the high stroke cylinder, locking mechanism and high force cylinder were connected to the pressure regulator, to see how the connected system behaves when pressurized and to validate if this is in line with the expected behavior. 1.5 mm hex keys were inserted into the ends of the high stroke cylinder, locking mechanism and high force cylinder and placed against the internal pistons, in order to reveal the movement of these pistons. A piece of white tape was place around the hex key at the place where it entered the components, to be able to see how much the hex key was moved. Figure 6.8 shows the prototype during gradual pressurization of the pressure regulator.

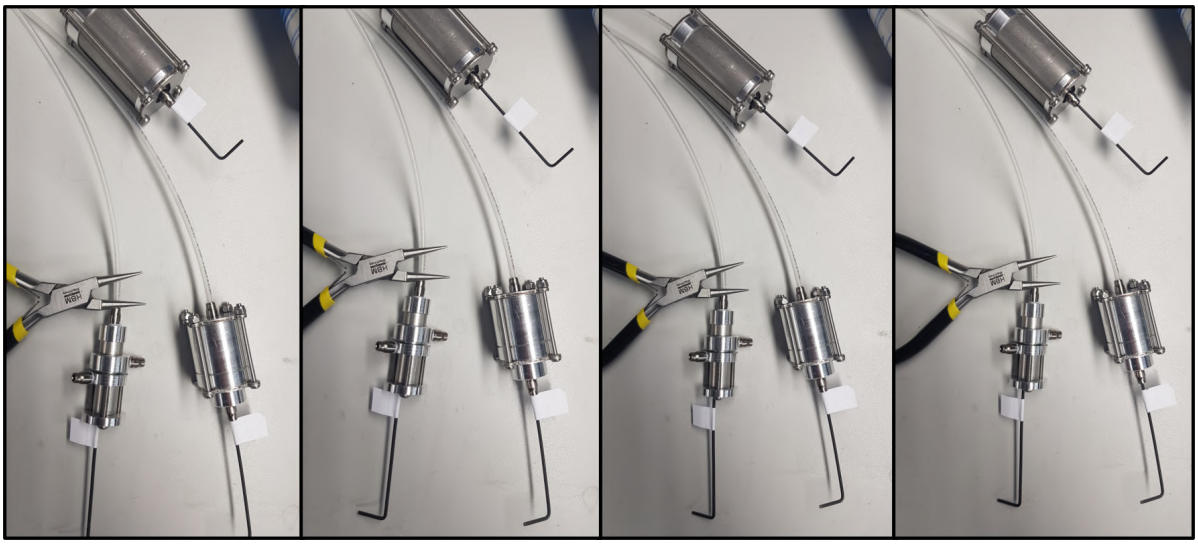

Figure 6.8: Gradual pneumatic pressurization of the pressure regulator, connected to the rest of the prototype. Hex keys with white tape are used to reveal piston movement.

The pressure was increased until something moved, then a picture was taken and then the pressure was increased further. The test and figure showed the following behavior in order of appearance and each corresponding to one of the pictures in figure 6.8:

1. When the pressure regulator is depressurized, all other components are at their initial position.

2. When the pressure regulator is pressurized with a low pressure, the high stroke cylinder starts extending until it is fully extended.
3. Further increasing the pressure of the supply to the pressure regulator causes the locking mechanism to engage.
4. Finally, increasing the pressure even further causes the high force cylinder to start extending until it is fully extended.

This behavior and the order in which components are activated is exactly as was designed. Therefore, the pneumatic distribution by means of the pressure regulator seems to be successful and further testing should show whether it also works when attaching the hydraulic part of the system.

The strokes of the pistons of the high stroke cylinder, locking mechanism and high force cylinder were measured in order to see if the stroke corresponded to the theoretically designed one. This was done by measuring the distance that the piece of white tape on the hex key had travelled during extension. Figure 6.9 shows the measured stroke for each of the prototype components.


Figure 6.9: Measurement of the stroke of the pistons of the prototype components when pressurized and fully extended. Left: the high stroke cylinder. Center: the locking mechanism. Right: the high force cylinder.

As designed in section 5.3, the stroke of the high stroke cylinder should be 18 mm, the stroke of the locking mechanism 8.2 mm and the stroke of the high force cylinder should be 5 mm.

The stroke of the high stroke cylinder was measured to be 18.0 mm and therefore is exactly as designed.

The stroke of the locking mechanism is 8.0 mm and is therefore 0.2 mm less than was designed. This is due to the usage of the stronger, pretensioned spring, which has a larger block height. This means that the piston will stop moving not because it has hit the end cap, but 0.2 mm earlier because it is blocked by the compressed spring. As shown in the tests this does, however, not have a negative effect on the functioning of the locking mechanism and is, therefore, not a problem.

The stroke of the high force cylinder is 4.7 mm and is therefore 0.3 mm less than was designed. This is due to the protrusion of the M2x4 mm screw for the drain hole. The length of this screw is perfect when it keeps the o-ring in place, but when it is tightened in order to compress the o-ring and seal the drain hole, the screw protrudes slightly into the cylinder, blocking the piston 0.3 mm before it is fully extended. Later on, a washer will be added to this screw which overcomes this problem.

For a final pneumatic test, the hydraulic side of the system was attached, however, without filling it with water. Here the high stroke cylinder is connected to the locking mechanism and the locking mechanism and high force cylinder are both attached to a T-coupling, which in turn is connected to one of the fingers of the Delft Cylinder Hand. Figure 6.10 shows an overview of this setup.

Pressurizing the pressure regulator showed that the system still works as intended with the high stroke cylinder being activated first, followed by the locking mechanism and, finally, the high force cylinder. The finger, however, did not move at all. This shows that this dual-mode actuation scheme indeed needs to be a hybrid between pneumatic and hydraulic actuation, as the compressibility of the air in this test resulted in the finger not moving at all, even though the components worked as intended.

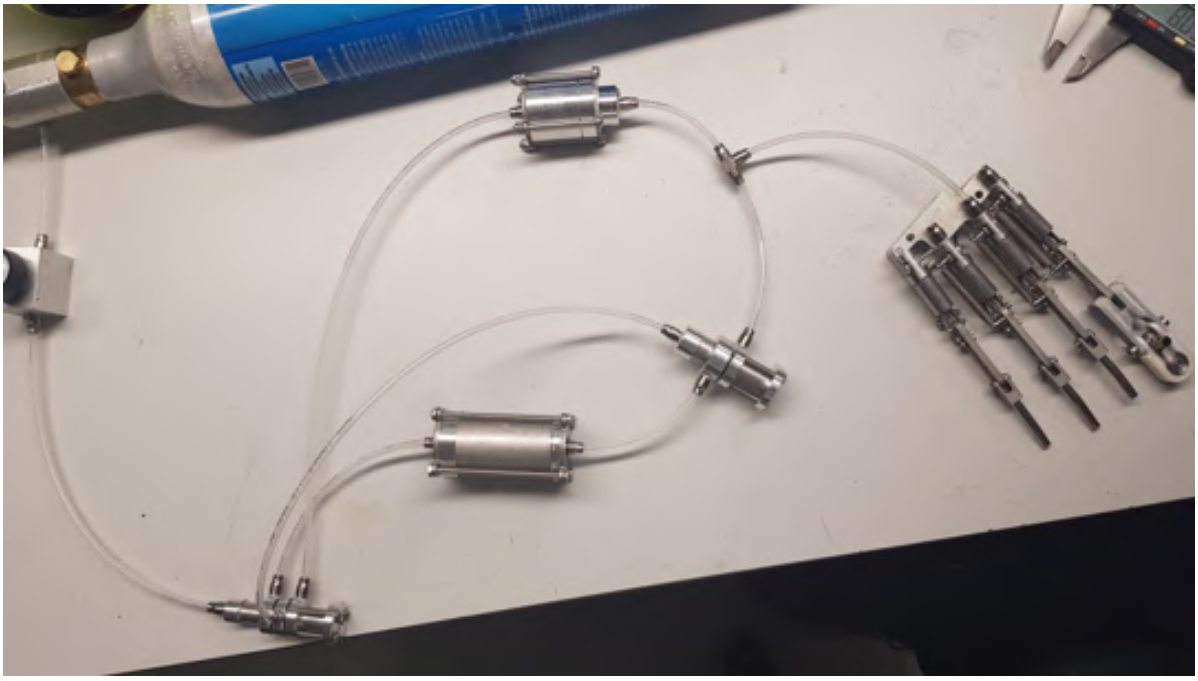

Figure 6.10: Complete setup of the prototype without the hydraulic side being filled with water.

## 6.4. Hybrid test

After having performed tests on the prototype, using only the pneumatic side of the system, tests were performed using the full hybrid system consisting of both the pneumatic and the hydraulic side. In order to do this the components of hydraulic side of the system were filled with water. This was done by submerging the entire component underwater and forcing water through the hydraulic side, thus blowing out any air. The pneumatic inlets were connected to a tube that lead out of the water, to prevent this side from filling with water too. Before filling, the drain holes of the high stroke and high force cylinders were opened to let air escape and once the cylinders were filled with water, these holes were sealed using the screw and o-ring.

### 6.4.1. Individual components

The first thing that was done was again to test each of the parts of the system individually, to see their response to being pressurized and to validate if this is in line with the expected behavior. The first part to be tested was the high stroke cylinder and locking mechanism. The pneumatic inlet of the high stroke cylinder was directly connected to the pneumatic supply and the hydraulic outlet was connected to the hydraulic inlet of the locking mechanism. The hydraulic outlet of the locking mechanism was connected to a WIKA manometer with a range of 0 to 16 bar, used to measure the output pressure. Figure 6.11 shows an overview of this setup and the readings of the input and output manometers for three different pressure levels.

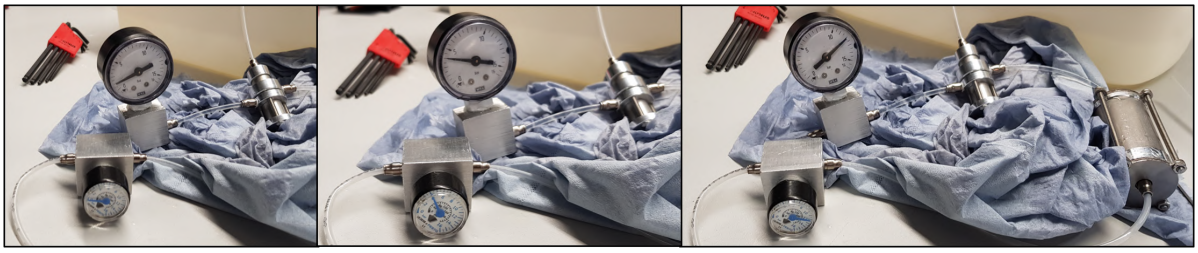

Figure 6.11: Gradual pressurization of the high stroke cylinder for three increasing pneumatic pressure levels. The readings of the pneumatic input pressure (Festo manometer) and hydraulic output pressure (WIKA manometer) are shown.

The pressure level measurements obtained with this test setup are shown in figure 6.12. Here the pressure of the hydraulic outlet is plotted against the pressure of the pneumatic supply. The MATLAB code shown in appendix B.10 was used to create this plot. This plot also shows the theoretical pressure, which is the line of equal pressure, as this cylinder does not have a transmission ratio.

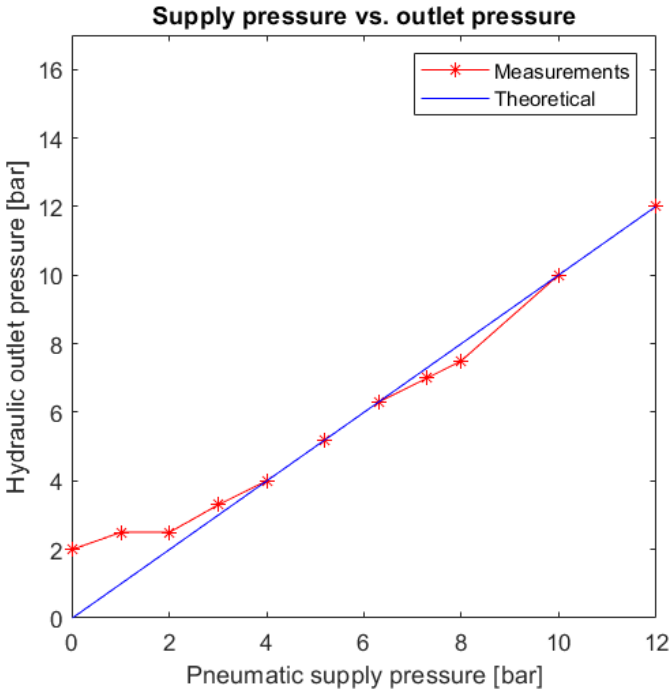


Figure 6.12: Plot of the hydraulic output pressure against the pneumatic inlet pressure of the high stroke cylinder.

The figure shows that for pressures higher than 2 bar, the prototype is very close to the theoretical model. For pressure lower than 2 bar, however, the measured pressure is higher than the theoretical pressure. This could in part be due to friction in the cylinder but could also be a results of inaccuracies of the WIKA output manometer. I noticed that when no supply is connected, the manometer already gave a reading higher than 0, even though nothing was connected. When the supply pressure was increased gently, the pressure first stayed at that level until it started increasing, as if there was some minimum level of pressure before the manometer starts working. Therefore, it seems that the output manometer is less accurate for pressure lower than 2 bar.

Next the same experiment was performed, but then for the high force cylinder. Here the pneumatic supply was directly connected to the inlet of the high force cylinder and the hydraulic outlet was connected to the WIKA manometer. Figure 6.13 shows an overview of the setup and the manometers for two different pressure levels.

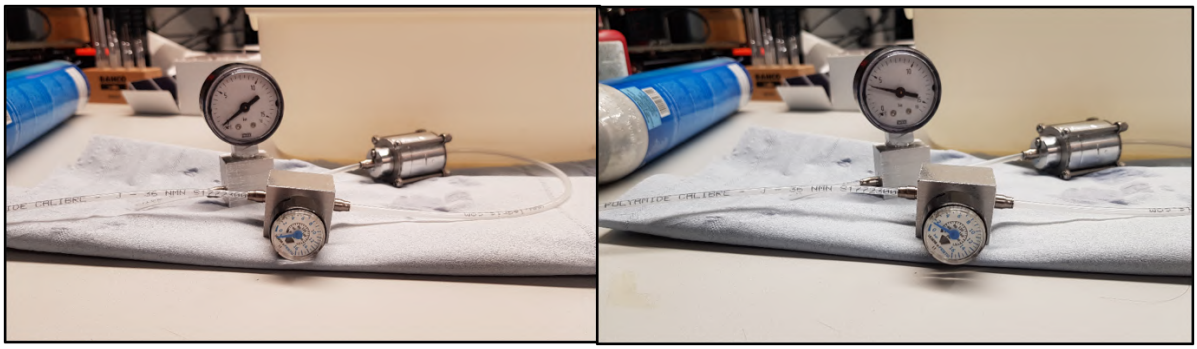

Figure 6.13: Gradual pressurization of the high force cylinder for two increasing pressure levels. The readings of the pneumatic input pressure (Festo manometer) and hydraulic output pressure (WIKA manometer) are shown.

The measurements obtained with this setup were much lower than expected, and even lower than that of the high stroke cylinder, even though this cylinder does have a transmission ration. Careful inspection showed that water was leaking out of the drainage hole in the cylinder. Apparently, the head of the M2x4 mm screw was not wide enough to seal and keep the o-ring in place. An M2 washer was therefore placed between the head of the screw and the o-ring to create a better seal. This, however, resulted in leakage between the washer and the screw at higher pressure levels. The washer was therefore glued to the head of the screw using the same Loctite 638 as was used for assembling the prototype. This did have the wanted effect as the cylinder does not leak under any pressure in the desired range of up to 12 bar. To be sure that the same does not happen in the high stroke cylinder, an M3 washer was also glued to the M3x8 mm screw thereof.

### 6.4.2. Connected system

Now that the parts of the prototype have been tested separately and seem to work as intended after some improvements, the separate parts can be connected in order to test the full hybrid system with both the pneumatic and the hydraulic side. To fill the complete hydraulic side of the system, each of the components was submerged in a bucket filled with water. The pneumatic side of the system was connected to tubes that stuck out of the water to prevent this side from filling with water. Each of the components and hydraulic tubes was blow through with water to ensure that no air remained within them. Finally, all the submerged components and tubes were connected to each other, while still submerged, in order to seal of the hydraulic system without any air present. Figure 6.14 shows the system being connected while submerged in water on the left and the right side shows the sealed hydraulic side of the system.

Figure 6.14: Left: hydraulic side of the prototype submerged in water, in order to fill it with water and seal it without air entering the system. Right: The filled and sealed off hydraulic side of the prototype.

The Festo manometer was again used to measure the pressure of the pneumatic supply at the inlet of the prototype, and the WIKA manometer was place before the hydraulic Delft Cylinder Hand in order to measure the hydraulic output pressure of the prototype. Figure 6.15 shows a picture taken of the setup of the complete and connected prototype.

Many tests and test cycles were preformed using this setup to see exactly how it performed and how the behavior of the complete system is. There were, however, two main tests: an unloaded test, where the finger could move freely, and a loaded test, where a heavy object was placed on the finger to prevent its movement.

#### Unloaded

The unloaded test showed many interesting results such as:

- The hydraulic pressure required to close the finger is about 4.5 bar.
- The unloaded finger does not close gradually, but rather it goes from completely opened to completely closed when the hydraulic outlet pressure reaches a level around 4.5 bar.

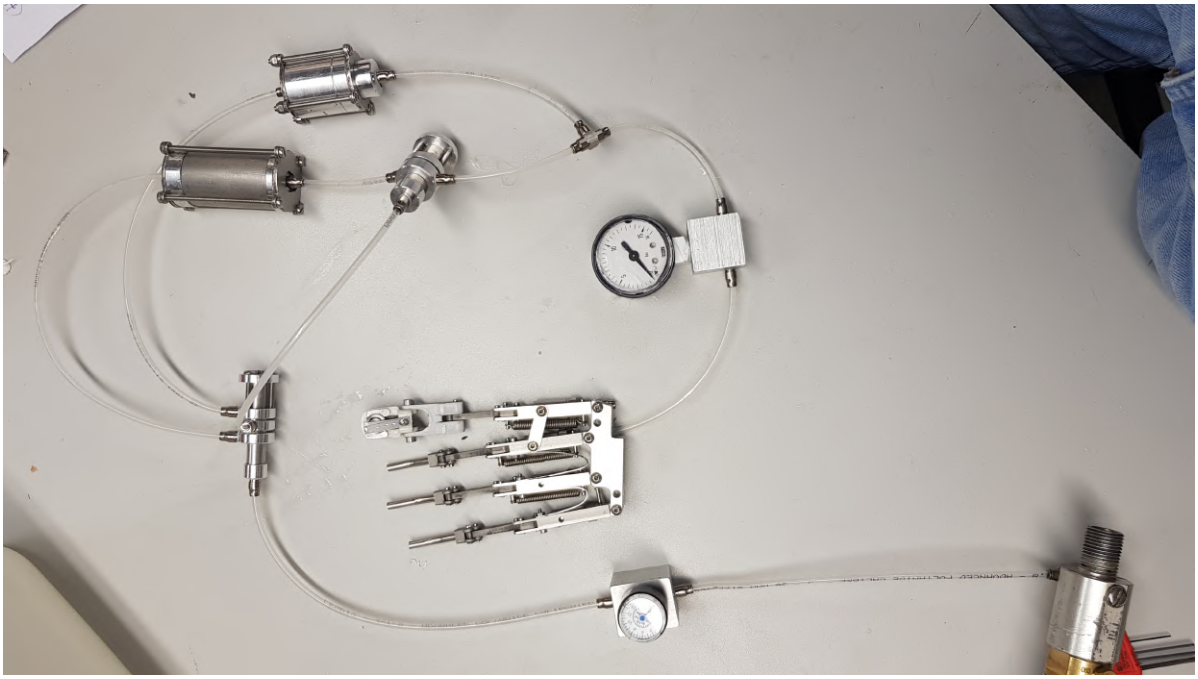

Figure 6.15: Picture taken of the complete prototype setup, including two manometers for measurements.

- The point where the finger closes and where the locking mechanism engages, and the high force cylinder starts moving appear to coincide. This is coincidental as different kinds of tests showed that both require a similar pressure level, and it is not a result of one affecting the other. Although this is coincidental it is not very practical, as in the design the idea was to first close the hand and then apply a force, and not have both at the same time.
- Tiny amounts of air enter the hydraulic side of the system through the finger when it moves. This means that the sealing of this produced Delft Cylinder Hand is insufficient. Air bubbles become apparent in the hydraulic tubing after around 10-15 operating cycles.
- When the finger is closed and the finger is manually opened while the system is still pressurized, the hydraulic outlet pressure sharply rises.
- When the system is depressurized, the finger, pressure regulator, high stroke cylinder and high force cylinder all return to their initial position without needing help. The locking mechanism also slides back, however, as stated before it is not able to move to its initial position completely.

**Loaded**

The loaded test was performed by placing heavy objects on top of the Delft Cylinder Hand, in order to block the movement of the finger. Figure 6.16 shows an example, where a heavy roll of 3D printing filament is placed on top of the finger. A block of metal was tried before this; however, the hand was strong enough to launch this block of the table and close the finger.

Both of the manometers were put alongside each other and recorded with a camera. This allowed data points to be gathered after completing the experiment, without having to stop to record a measurement during the actuation of the hand using the prototype. The test had to be cut short, however, as the output manometer already reached its limit when the pneumatic input pressure was at only 3.5 bar out of 12 bar. Using the full 1.2 MPa (12 bar) could damage the manometer and the supply pressure was therefore not increased above the 3.5 bar even though the prototype could have gone on much further. The results of this test are plotted in figure 6.17 using the MATLAB script shown in appendix B.11. The figure clearly shows the distinction between the two phases of the dual-mode actuation; Below a supply pressure of 2 bar the hydraulic output pressure slowly increases linearly, due to the high stroke cylinder. Around 2.3 bar the locking mechanism is engaged, block flow to the high stroke cylinder, and the high force cylinder starts extending. The rapid jump in pressure can be explained by the fact that when

Figure 6.16: Picture of the loaded test where a heavy object, in this case a big roll of 3D printer filament is placed on top of the finger.

the pressure regulator activates the output to the high force cylinder, the pressure at this output jumps from atmospheric pressure to a high level of pressure that was needed to move the pressure regulator to this outlet. Hereafter, the pressure starts gradually increasing again corresponding to the increase in supply pressure. This results in the steeper linear increase in the hydraulic output pressure that starts around a supply pressure of 2.5 bar. For each of the two phases a regression line is calculated and plotted which shows the distinction between the prehension (blue) and the pinching (green) phase.

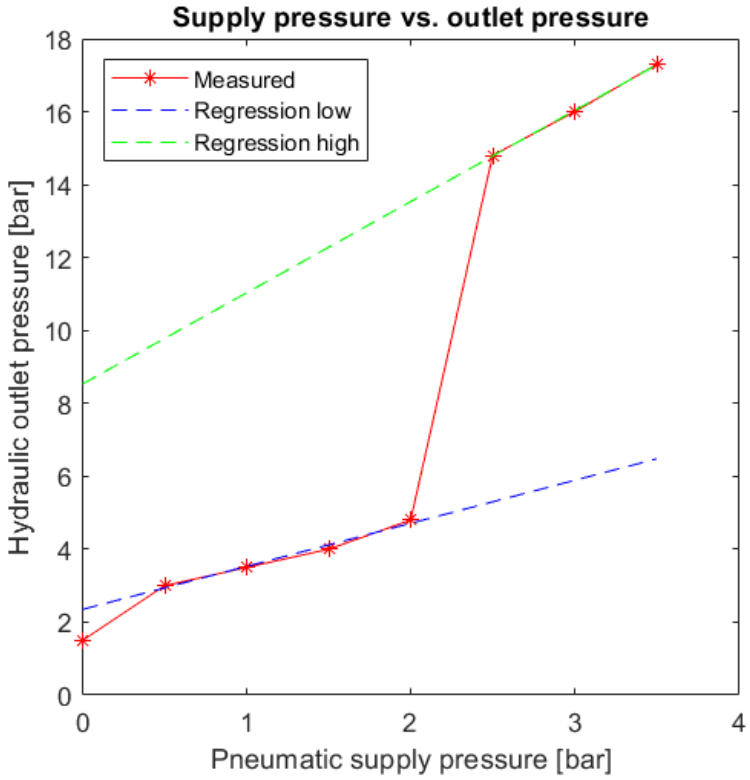


Figure 6.17: Plot of the measurements of the hydraulic output pressure against the pneumatic inlet pressure of the full prototype. Regression lines are calculated and added for both of the dual-mode actuation phases.

As the experiment had to be cut off to prevent damage to the manometer, the experiment was

repeated without the WIKA manometer, to be able to use the full range of supply pressure. When increasing the pressure, the weight on top of the hand had to be increased as the increasing strength of the finger was lifting the objects. Gradually increasing the supply pressure once again started with showing the same behavior as shown in figure 6.17. Hereafter, however, the force of the finger kept increasing linearly until the supply pressure reached 12 bar. This could be seen as the weight that needed to be added with each step in pressure was equal for equal steps in pressure. Although there were unfortunately no manometers available in the lab that went above 16 bar, and due to the Corona virus there was no possibility to obtain it elsewhere, the maximum pressure could be estimated using the finding that the force kept increasing linearly even above a supply pressure of 3.5 bar. In order to do this the regression line that was calculated and shown in figure 6.17 was used and this results in an estimated maximum pressure of 39 bar or 3.9 MPa.

# 7

# Discussion

This chapter will discuss the observations that were made throughout this whole graduation project. Section 7.1 will discuss the prototype that was made for the pneumatically powered hand prosthesis, and the observations from testing it. Next, section 7.2 will reflect back on the requirements that were set in chapter 2. Finally, section 7.3 will give recommendations for future research on this pneumatically powered hand prosthesis.

## 7.1. Prototype

The prototype that was design and built in chapter 5 and tested in chapter 6 showed many promising aspects but also showed some unexpected behavior. This section will therefore first give an overview of the promising aspects of the prototype and afterwards an overview of the points that will need some more attention.

### 7.1.1. Promising aspects

The pressure regulator is able to activate components sequentially for dual-mode actuation. As shown in the tests the pressure regulator first pressurizes the high stroke cylinder, followed by the locking mechanism and, finally, the high force cylinder. This allows the dual-mode actuation to work as intended and the grasping to be split up in the prehension and pinching phase, resulting in both a lower gas consumption and a larger grip strength.

The measurements of the full system indeed show the dual-mode actuation characteristics, where the prototype starts with a large stroke and low force and later with a large force and low stroke, meaning that the dual-mode actuation was implemented successfully.

The tests show that a high output pressure can be obtained. Even though, the maximum pressure could not be measured, due to the lack of a manometer with a larger measuring range, the tests indicate that a high output pressure can be achieved using this prototype.

The majority of system automatically returns to initial position when depressurized. The pressure regulator, high stroke cylinder, high force cylinder and finger all automatically return back to their initial position when the system is depressurized. This is as designed and advantageous as it means that at the end of each grasping cycle the hand can reset itself for a new cycle, without needing any help. The locking mechanism also moves back partially, however, it is not able to move back completely.

After hundreds of operating cycles have been performed with the prototype during the testing, no signs of wear or fatigue are visible. Furthermore, the prototype also did not block or fail in any other way. This is a good indication as it could mean that the design is able to have a long life cycle before needing any repairs or maintenance.

After all the leakage problems had been fixed, the prototype did not show any leakage even after being pressurized at high levels for extended periods of time. Leakages introduce air into the system, which deteriorates its performance. Therefore, the lack of leakages shows promise for a reliable system.

The components that make up the prototype are relatively easy to assemble. This not only reduces the time it takes to build the prototype, but it also means that it is easy to replace a part in case there is

wear or a failure. This reduces both the price and duration of maintenance, which makes it attractive to a potential user.

The prototype is a modular system, which means it consists of separate components that can easily be connected through tubes. This makes the prototype as a whole easy to assemble and also means that in case something is wrong with one of the components, it can be disconnected and replaced by another one. Furthermore, this allows each of the components to be tested separately, which can be favorable in case there would be problems with the prosthesis, and it is not known where the problem lies.

### 7.1.2. Points of attention

The o-ring friction was a lot higher than expected. Increasing the depth of the o-ring grooves reduced the friction significantly, as the o-ring are compressed less, however, the friction is still higher than anticipated. Although the system works, the friction means that higher pressure levels are necessary to actuate the system and decrease its performance slightly.

The resistance in the locking mechanism is still too high. The expansion and re-compression of the o-ring while moving between the two halves of the cylinder sleeve requires too much force to be performed by the return spring. A much stronger spring could be used to return the locking mechanism to its initial state, however, that would reduce its functioning. The solution should therefore lie in reducing the resistance in the mechanism.

The switch between the two dual-mode phases happens too early. At this moment the switch happens at around the same time as that the finger closes. The intention is that the high stroke cylinder close the finger and that the high force cylinder applies a force after the finger is already closed. Right now, both happen at the same time and this reduces the functionality of the dual-mode actuation. It would therefore be favorable if the switch between the prehension and the pinching phase happens at a later stage, after the finger is closed. This could, however, be in part due to the usage of a different finger design, which has a single cylinder that is smaller than in my design. This means that to close the finger a higher pressure is needed, which means that the finger closes at a later moment, thus coinciding with the dual-mode phase switch.

The pressure measurements were done using simple manometers. These manometers seemed to be slightly less accurate for very low pressure and only had a range of up to 16 bar. This meant that the full range of the output pressure of the prototype could not be measured and had to be estimated based upon unmeasured tests and regression lines.

The usage of another kind of finger with the prototype means that the results, like for example pinching strength, are different when using this finger than if the one that I designed would have been used.

The prototype was simplified with respect to the full design that was made in chapter 4. This made many parts of the fabrication, assembly and testing easier, but it also means that the performance could be slightly different from the designed one.

The prototype is just part of the full hand prosthesis. The results obtained with it are therefore useful to indicate its performance, however, the whole design should be made in order to find out the real performance of the design made in chapter 4. Unfortunately, this duration of this project was not long enough to do so, especially with the Corona virus outbreak.

## 7.2. Requirements

To see how the design made in chapter 4 performs with respect to the requirements set in chapter 2, this section will examine each of the requirements and evaluate how the design (or prototype) preform with respect to it.

> **Req. 1: Mass.** *The total mass of the prosthetic hand (excluding control and supply) should not exceed 250 grams.*

The total weight of the design made in chapter 4 is 235 grams, according to the SOLIDWORKS model. Therefore, this requirement appears to be fulfilled. The whole hand was not built, however; therefore it cannot be said with certainty that the actual weight stays below 250 grams. The prototype that was built was heavily simplified and as a result weighs much more than the one in the initial design. It could

therefore be that when redesigning the whole hand prosthesis, it could exceed the 250 grams, however the current SOLIDWORKS design shows promise as it is below that.

**Req. 2: Grip strength.** *The maximum grip force at the tip of a finger should be at least 60 N.*

The MATLAB simulations indicate that a tip force of just over 60 N could be achieved, so in theory this requirement should be met. Tests performed with the prototype, however, estimate a maximum output pressure of 3.9 MPa, which is lower than the calculated 4.2 MPa with MATLAB. Therefore, an estimation for the grip strength would be 60N * (3.9 MPa / 4.2 MPa) = 56 N. This is slightly below the requirement, and it seems therefore that the prototype does not meet the requirement, although it gets very close. Fabrication of the full design made in chapter 4 should show exactly what the grip strength is of the actual design.

**Req. 3: Size.** *The prosthetic hand should fit completely inside the contours of an adult male human hand.*

The design of the whole hand fits inside the contours of a human hand, so this requirement is met. The prototype, however, is much bulkier due to the simplifications that were made. It should, therefore, be examined if the design of the full hand prosthesis can be produced and function with the compact design made in chapter 4.

**Req. 4: Motion.** *The prosthetic hand should be able to grasp differently shaped and sized common office objects, using different kinds of grip.*

The full hand prosthesis was not completely made, so the exact range of motion is unknown. But the SOLIDWORKS model and similar Delft Cylinder Hand indicate that this requirement can be met without further adjustments.

**Req. 5: Grip speed.** *The prosthetic hand should be able to switch from the completely opened to completely closed position in less than one second.*

Depending on the speed of increase in the supply pressure the prototype acts very quickly. The finger closes in a fraction of a second. When the prototype is depressurized the finger returns to its initial position just as fast. The switch from the completely opened to completely closed position, therefore, takes much less than one second, and meets the requirement.

**Req. 6: Gas.** *The gas used for the pneumatic actuation of the prosthesis is carbon dioxide, $CO_2$.*

$CO_2$ was used for powering the hand and also the prototype.

**Req. 7: $CO_2$ pressure.** *The pressure of the $CO_2$ supplied to the prosthetic hand should be 1.2 MPa.*

In the design a supply pressure of 1.2 MPa is used indeed.

**Req. 8: Usage time.** *The prosthetic hand should be able perform at least 400 cycles with a single $CO_2$ cartridge.*

The simulations made with MATLAB indicate a total of over 400 cycles on a single cartridge, and therefore this requirement should be met. The amount of gas used by the prototype could not be measured, however, and therefore the actual gas consumption is unknown. Further tests should, therefore, reveal what the exact usage time of the hand prosthesis is.

**Req. 9: Loudness.** *The loudness of the sound produced by the prosthetic hand should stay below 45 dB at a distance of one meter.*

The prototype itself and the finger barely make any sound at all, and their sound is not noticeable in quiet office. Thus, the requirement is met. The gas supply that was used for testing, however, produces much sound and does not stay below 45 dB. So, although this gas supply is not part of the design, it should be taken into account that this will be the louder part of the system.

> **Req. 10: Cosmetic.** *The prosthetic hand should consist of four fingers and a thumb, connected to a hand palm. Furthermore, the prosthetic hand should be similar both in dimensions and movement to a real human hand.*

The design of the hand prosthesis indeed consists of four finger and a thumb, connected to a palm, with similar movement and dimensions as a real hand.

> **Req. 11: Integration.** *All parts of the prosthetic hand system, except the control unit and the $CO_2$ supply, should be incorporated within the hand itself.*

In the design all the components are integrated. However, only a partial prototype was built, therefore, the whole hand should be fabricated to see if the whole hand will function with all parts integrated.

> **Req. 12: Environment.** *The hand prosthesis should be water and dust proof (IP67/68) and non-reactive to common chemicals and substances.*

The prototype is water and dust proof and the exterior materials are resistant to most chemicals, therefore this requirement is met. When the whole hand prosthesis is built, this requirement should be checked again to see if it is also valid for the hand as a whole.

> **Req. 13: Durability.** *The hand prosthesis should last at least 100,000 cycles without needing maintenance or repairs.*

No durability test was performed, so this is something that should still be tested. The prototype does not show any signs of wear or fatigue after hundreds of test cycles, so this shows promise for meeting the requirement.

> **Req. 14: Control.** *The operation of the hand prosthesis should be as simple as possible, preferably by a single valve.*

The design of the pressure regulator allows the whole hand to be controlled using a single $CO_2$ supply and, therefore, could be controlled using a single valve.

## 7.3. Recommendations

Based upon the findings of the tests performed in chapter 6 and on general observations made during this project, a number of recommendations can be made for further research on this topic:

- In further design the higher o-ring friction should be compensated. The MATLAB simulation now used a lower level of friction and, therefore, problems arose during testing. Redesign using the knowledge that the friction is higher than anticipated could improve the function of the system as a whole.
- Currently the resistance in the locking mechanism is too high to be overcome by a return spring. This means that the mechanism can be used to lock the dual-mode actuation, however, it does not return to its initial, unlocked position when depressurized. As stated before, this is due to the expansion and re-compression of the o-ring while travelling between the two halves of the cylinder sleeve. The locking mechanism should therefore be altered or redesigned in order to decrease the resistance and to make sure it functions both ways.
- At the moment the switch between the dual-mode actuation phases and the closing of the finger happen at around the same pressure level. As stated earlier this is unwanted behavior, and therefore it should be tried to either have the finger close earlier or have the switch between the phases happen later. This could lead to significant improvements in the performance of the system and are therefore definitely worth the research.
- When continuing testing with the current prototype, other measurement devices should be used. The current manometers appeared to be slightly inaccurate for low pressure levels and their range was insufficient for the current design. It should therefore be tried to test the prototype with measurement devices that have a larger range and that are recently calibrated, so that it is sure that their readings are accurate. Unfortunately, I was not able to do this due to restrictions in time and the fact that the Corona crisis made access to instruments and facilities much more difficult than normally.

- The current prototype was heavily adjusted and simplified to make production and assembly easier, as time was running out, especially due to the Corona crisis. It should be tried to create a more compact prototype to see if the weight and size can be reduced, whilst maintaining the performance.
- The prototype was only part of the full hybrid hand prosthesis and, therefore, does not show all the aspects and performance of the whole hand. Producing one of my fingers or the whole hand prosthesis and testing them, can show exactly how the full design performs and which aspects should still be improved. Furthermore, the full design made in chapter 4 can be adjusted or partially redesigned based upon the findings with the prototype.
- The prototype is currently still far from being commercially viable. Several improvements are still needed before the whole prosthetic hand can be built and tested. Those tests should indicate whether the improved performance of this design, and its main selling points indeed lead to a commercially viable product or if more adjustments are needed.

# 8

# Conclusion

This thesis presents the design a pneumatically powered hand prosthesis, that combines a high grip strength, a high opening/closing speed and lightweight into a single device, whilst maintaining a reasonable usage time.

- ■ The combination of pneumatic actuation with a hydraulic transmission gives the hybrid actuated hand a relatively high pinch force of an estimated 56 N.
- ■ With a grip speed of much less than a second, the hybrid actuated hand is fast enough to be intuitively operated by a user.
- ■ With a mass of only 235 grams, the hybrid actuated hand weighs less than most of its competitors and is comfortable in use.
- ■ The dual-mode actuation significantly increases the efficiency of the hybrid actuated hand and gives it a usage time of 400 cycles per cartridge.

For future research the following recommendations are given:

- □ The locking mechanism should be adjusted or redesigned in order to overcome the resistance that currently hinders its return stroke.
- □ The pressure regulator should be adjusted in order to improve the timing of the switch between dual-mode phases.
- □ The full hand prosthesis should be constructed and thoroughly tested in order to prove its commercial viability.

# Bibliography


[1] M. Borchardt, K. Hartmann, R. Leymann, and S. Schlesinger. *Ersatzglieder Und Arbeitshilfen: Für Kriegsbeschädigte Und Unfallverletzte*. Springer, Berlin, Heidelberg, 1919.

[2] R. F. Chandler, C. E. Clauser, J. T. McMconville, H. M. Reynolds, and J. W. Young. Investigation of inertial properties of the human hand. Technical Report DOT HS-801 430, U.S. Department of Transportation, 1975.

[3] D. C. Doedens. Optimal co2 pressure for a pneumatic system. Master thesis, TU Delft, 2015.

[4] H. W. Kay and M. Rakic. Specifications for electromechanical hands. In *Proceedings of the 4th International Symposium on the External Control of Human Extremities*, pages 137–155, 1972.

[5] J. W. Limehouse and T. A. Farnsworth. A preliminary study of 40+ upper extremity patients using the animated control system. In *Myoelectric Controls/Powered Prosthetics Symposium*, page 196, Fredericton, NB, Canada, 2005.

[6] B. Peerdeman, G. Smit, S. Stramigioli, D. Plettenburg, and Sarthak Misra. Evaluation of pneumatic cylinder actuators for hand prostheses. In *The Fourth IEEE RAS/EMBS International Conference on Biomedical Robotics and Biomechatronics*, pages 1104–1109, Roma, Italy, 2012.

[7] D. H. Plettenburg. *Pneumatically Powered Prostheses: An Inventory*. Delft University of Technology, Delft, Netherlands, 2002.

[8] J. L. Pons, E. Rocon, R. Ceres, D. Reynaerts, B. Saro, S. Levin, and W. Van Moorleghem. The manus-hand dextrous robotics upper limb prosthesis: Mechanical and manipulation aspects. *Autonomous Robots*, 16:143–163, 2004. doi: 10.1023/B:AURO.0000016862.38337.f1.

[9] G. Smit. Delft cylinder hand: Natural grasping, 2013. URL `https://www.bitegroup.nl/category/prosthetic-devices/delft-cylinder-hand/`. [Accessed: 15- Jul- 2020].

[10] R. F. Weir. Design of artificial arms and hands for prosthetic applications. In M. Kutz, editor, *Standard Handbook of Biomedical Engineering and Design*, chapter 32, pages 32.1–32.59. McGraw-Hill, New York, 1 edition, 2004.

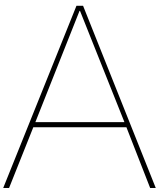

# Literature review

# Advances in Pneumatically Powered Hand Prostheses since 2000

Ad Hoek†

***Abstract*—A common type of prostheses is the upper extremity prosthesis, of which (partial) hand prostheses are the most common. Different forms of actuation have been used for hand prostheses throughout time, one of which is pneumatics. The use of pneumatic actuation for hand prostheses spiked during the thalidomide disaster, however, it never became very popular due to drawbacks such as unmanageable control, bulkiness of gas storage and difficulty of refilling the gas storage. Since the turn of the century many efforts have been made to improve pneumatically powered hand prostheses. The aim of this paper is, therefore, to see if the advances in pneumatically powered hand prostheses have been sufficient for a comeback of pneumatic power, and if they make it an attractive actuation method for future prostheses. Through a literature study, advances were found in the areas of actuation, control, energy, ergonomics and fabrication, leading not only to improvements in both the performance and appearance of the prosthesis, but also the affordability. Although the hand prostheses presented in this paper are not yet ready for commercialisation, the current designs show numerous promising aspects and further development could result in successful commercial pneumatic hand prostheses. As a result of the recent advancements, pneumatics has now become an attractive actuation method for hand prostheses, as the major drawbacks from the past have been overcome, whilst more and more advantages are becoming apparent.**

***Index Terms*—Prosthetics, hand prostheses, pneumatic actuators, biomechanical engineering.**

## I. Introduction

IT is estimated that at least 100 million of people worldwide are in need of a prosthesis or orthosis [1]. However, only about 20% of them has access to one. Furthermore, it is estimated that of the people that do have access to prostheses or orthoses more than 26.3% reject them [2]. An even larger amount of people state that the prostheses are inconvenient to use or state that there is a real need for improvement [3]. There are, however, also many people that are very content with their prosthesis and that even depend on them for living. It is therefore clear that there is a big need for prostheses and that there is still a lot of room for improvement, both in usage as in access, as prostheses are an important and sometimes even essential part of the life of the user.

Throughout time there have been many different prostheses. These can either be passive, i.e. without movement or requiring an external force to move, or they can be actuated to allow them to move without external forces. A common type of prosthesis is the upper extremity prosthesis. Prostheses for upper extremities are usually actuated, as the movement of hands and arms are essential for almost all daily activities. Actuated prostheses can be mainly divided into three categories, based on their actuation method; Body powered prostheses, pneumatically powered prostheses and electrically powered prostheses.

Body powered prostheses have been around the longest. These prostheses commonly consist of a hook that can be opened or closed using a cable that is attached to the body of the user, using a harness. Their relative simplicity makes them lightweight, as they do not require energy supplies or advanced transmissions, and furthermore also durable, as they do not consist of many moving parts that are prone to wear and fatigue. On the downside, however, these prostheses are awkward to control, as they are controlled by moving other body parts, and they require the user to be able to exert enough force to actuate the prosthesis, as the force by the user and the force exerted by the prosthesis are directly coupled.

Pneumatically powered upper extremity prostheses have been around since 1877. In contrast to the body powered prostheses, the input from the user and the output of the prostheses have been decoupled; The input of the user, such as an electrical signal from the muscles or brain, is used to control a pneumatic supply, that in turn is used to power the prosthesis. The advantage of this is that the user does not need to use a large range of motion or much force to control a prosthesis that does have a large range of motion and large forces. Their popularity spiked during the thalidomide disaster [4], however, in the first century of their existence, pneumatically powered prostheses never really became successful, due to their unmanageable control, the bulkiness of the gas storage and the difficulty of refilling the gas storage [5].

With the advances in electronics and the decrease of rechargeable battery sizes, electrically powered prostheses gained in popularity. As with pneumatically powered prostheses, the input of the user and the output of the prostheses are not directly linked. Here the input of the user is used to electronically control the actuators, that are powered by batteries. Currently electrically powered prostheses are the most popular choice for an upper extremity prosthesis, as these prostheses offer a large range of motion and do not require harnessing.

The popularity of electrically controlled prostheses, does not mean that they are necessarily better than pneumatically powered prostheses. As stated in the article of Plettenburg [6], pneumatic power has several advantages over electrical power, such as high operating speeds, increased reliability and low component weight, which could make pneumatically powered prostheses a favorable choice for an upper extremity prosthesis, if the downsides of pneumatic actuation were to be overcome.

In 2002 an overview of the efforts made by researchers to

† Master Student Mechanical Engineering at the Delft University of Technology. Student ID: 4445058. Contact: a.l.hoek@student.tudelft.nl

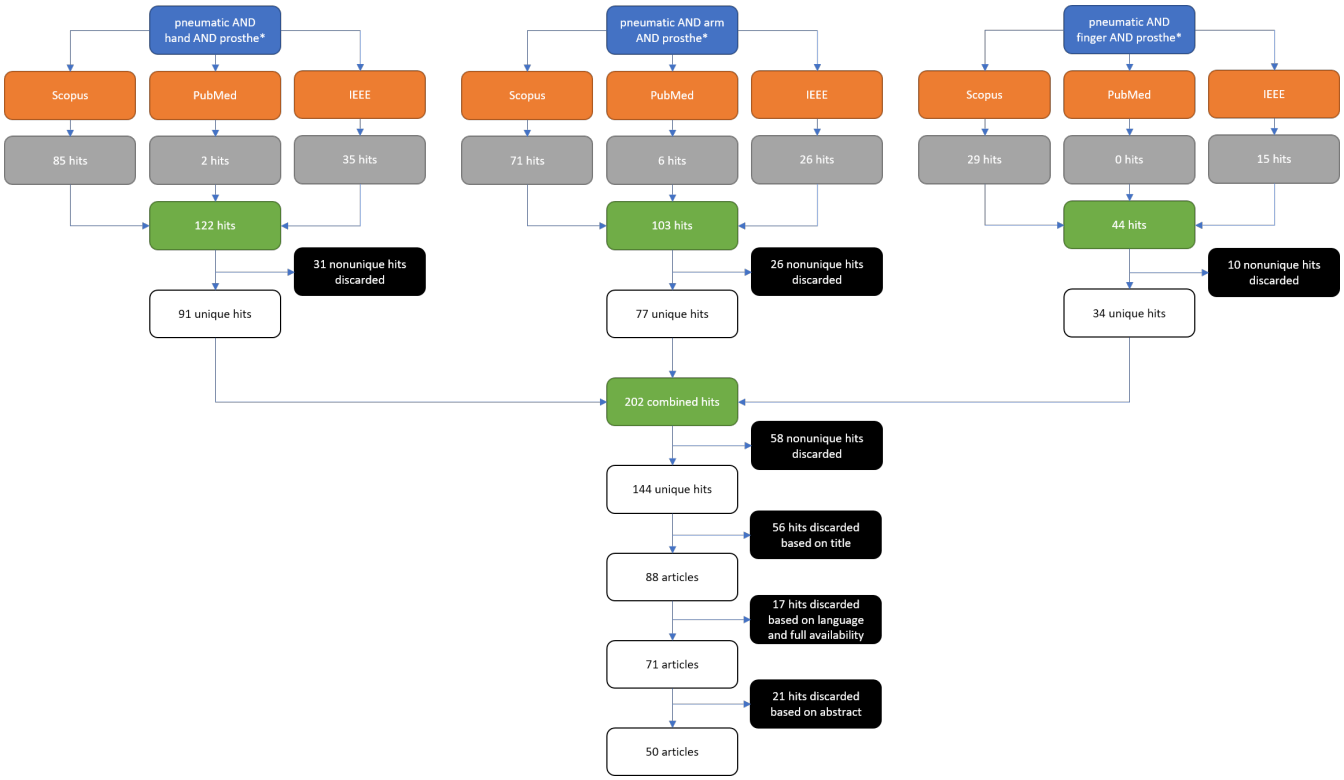


Fig. 1. Selection tree summarizing the literature searching process in online publication databases.

develop pneumatically powered hand prostheses was published by Plettenburg [5]. Since then many efforts have been made to overcome the aforementioned weaknesses of pneumatic prostheses. Therefore the aim of this paper is to see if the advances in pneumatically powered hand prostheses have been sufficient for a comeback of pneumatic power, and if they make it an attractive actuation method for future prostheses. In order to do this, this paper will give an overview of the advances in pneumatically powered hand prostheses that have taken place since the start of this millennium.

## II. Methods

To create an overview of the advances in pneumatically powered hand prostheses, relevant literature was sought in online databases and the repositories of the Delft University of Technology. Subsection II-A will detail the searching methodology and selection of research articles and subsection II-B will detail that of patents.

### A. Research articles

The search for relevant research articles was started by searching in the online databases: Scopus, PubMed and IEEE. Web of Science was also consulted afterwards, however, this was left out as its results were already included in the first three databases. The first search term that was used was: “pneumatic AND hand AND prosthe*”. However, a hand prosthesis can also be part of a full arm prosthesis, therefore, the search was extended with the search term: “pneumatic AND arm AND prosthe*”. Furthermore, advances in pneumatically powered hand prostheses could also include the most important part of them, namely the fingers. Therefore, the search was further extended with the search term: “pneumatic AND finger AND prosthe*”. In these search terms the “AND” means that all the three words need to be present in the article. Furthermore, “prosthe*” indicates that the word has to start with “prosthe” but can end in any way.

Figure 1 shows the hits belonging to the search terms and databases, and the selection of the found articles. Articles were discarded based on nonuniqueness, the relevance of their title, the language in which they were written (English), the availability of the full text article and, finally, on the information found in their abstract. This resulted in a total of 50 selected research articles.

Next relevant research articles and papers were sought in the two TU Delft repositories: the research repository, consisting of research articles, and the education repository, consisting of master theses and dissertations. These repositories use different search term operators than the Scopus, PubMed and IEEE databases; When a search term consists of multiple terms that all need to be present in the article, the “AND” operator is not added between words, rather the system automatically searches for articles that include all the terms. Furthermore, the “*” operator at the end of a word is not recognized by the TU Delft repositories. Therefore, the aforementioned three search terms were adapted to be able to find results in the TU Delft repositories. The only search term that yielded promising results was “pneumatic hand prosthesis”. Figure 2 shows the hits belonging to this search term. The results were discarded

based on the relevance of their title, the availability of the full text article and, finally, on the information found in their abstract. This resulted in a total of 18 selected research articles and papers.

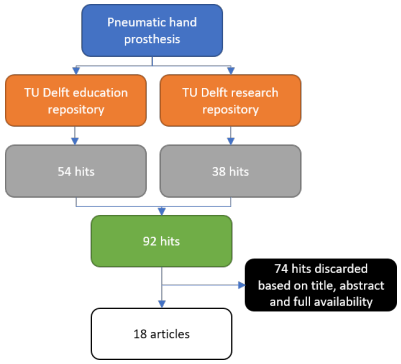


Fig. 2. Selection tree summarizing the literature searching process in the TU Delft repositories.

### B. Patents

To find relevant patents, the online patent database, Espacenet Worldwide, was used. The search term used to find relevant patents was: "pneumatic AND hand AND prosthe*". As can be seen in figure 3, this resulted in 2254 hits. Therefore, the following filters were added: the publication country was restricted to WO (Worldwide), EP (Europe), US (United States) or NL (The Netherlands), and the publication language was restricted to English. This resulted in 1479 filtered hits.

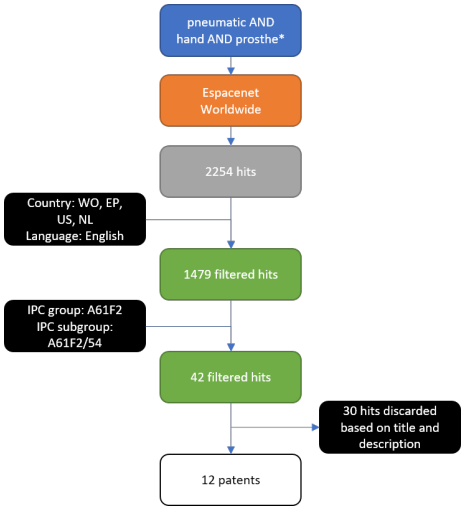


Fig. 3. Selection tree summarizing the patent searching process in the Espacenet Worldwide database.

The amount of results was still too much, therefore, the exact classification of patents for prosthetic hands was sought in the International Patent Classification (IPC), to make sure that only relevant hand prosthesis patents were found:

| | |
|---|---|
| A | Human necessities |
| A61 | Medical or veterinary science; Hygiene |
| A61F | Filters implantable into blood vessels; Prostheses; Devices providing patency to, or preventing collapsing of, tubular structures of the body, e.g. stents; Orthopaedic, nursing or contraceptive devices; Fomentation; Treatment or protection of eyes or ears; Bandages, dressings or absorbent pads; First-aid kits |
| A61F2/00 | Filters implantable into blood vessels; Prostheses, i.e. artificial substitutes or replacements for parts of the body; Appliances for connecting them with the body; Devices providing patency to, or preventing collapsing of, tubular structures of the body, e.g. stents |
| A61F2/50 | Prostheses not implantable in the body |
| A61F2/54 | Artificial arms or hands or parts thereof |

Filtering the previously found results, based on the IPC group A61F2 and IPC subgroup A61F2/54, resulted in a total of 42 filtered results. Finally, the results were discarded based on the relevance of their title and the information found in the description of the patent. This resulted in a total of 12 selected patents.

## III. Results

All the articles and patents that were selected in section II were categorized based upon the technological advancements discussed within them. Literature discussing the same advancements were grouped together and all the advancements were then grouped in five main areas of advancements, namely: Actuation, Control, Energy, Fabrication and Ergonomics. Figure 4 shows a schematic overview of the categorization of the selected literature.

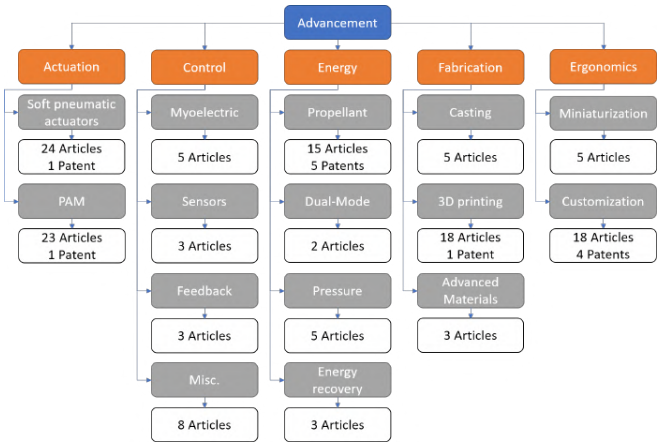


Fig. 4. Schematic overview of the categorization of the found articles and patents.

The following five subsections will each discuss one of the five main areas of advancements, and each sub-subsection will discuss one of the specific advancements, with examples from the literature.

### A. Actuation

*1) Soft pneumatic actuators:* Most conventional prosthetic hands consist of "hard" metal/plastic parts connected through

joints [7]. However, more and more research is being done on soft prosthetics, i.e. prosthetic hands made of “soft” elastic materials, such as silicone, with integrated pneumatic actuation through internal bladders. These actuators are generally called soft pneumatic actuators. The geometry and material composition of the actuator determines its deformation upon pressurization: bend, twist, extend, contract or combinations. A soft prosthetic hand can therefore be made that moves like a human hand when pressurized.

An advantage of soft prosthetics is that the hand is compliant, which allows it to grasp a much wider range of objects than rigid prostheses and also makes it safer to use in the presence of humans. Furthermore, this makes it easier to control, as the prosthesis itself forms to the object that is being grasped. Another advantage is that the prosthesis can be entirely 3D printed, molded or a combination of both. This not only makes the fabrication of the prosthesis easier and cheaper, but it also allows the prosthesis to become more cosmetically appealing as it can be modelled after a real human hand. A disadvantage, however, is that the soft materials of the prosthesis can withstand much lower pressures than stronger, more rigid materials. This means that the supply pressure is lower, which in turn decreases the grasping forces of the hand. Furthermore, the soft materials increase the chance of a rupture in the hand due to over-pressurization or fatigue, and the hand is more easily damaged by external objects [8]–[32].

Fras and Althoefer [25] designed a soft prosthetic hand that is modelled after a 3D scan of a human hand. Each finger is actuated by a soft pneumatic actuator, of which a schematic drawing is shown in figure 5. Contrary to the other fingers, the thumb has two actuators, making it capable of both apposition and opposition.

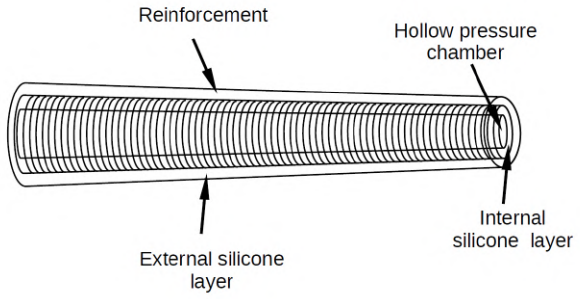


Fig. 5. Design of a soft pneumatic actuator in [25]. The actuator consists of a helically wound thread reinforcement sandwiched between two tapered silicone tubes. The end with the smaller diameter is sealed, creating a hollow internal pressure chamber.

When the hollow internal chamber is pressurized the forces on the silicone layers cause the actuator to expand by stretching the silicone. The helically wound thread, however, prevents the actuator from expanding radially and therefore, the actuator only expands in the axial direction. Thus, increasing the pressure inside the actuator, causes the actuator to elongate.

A 3D printed mold, based of 3D scans of a human hand, is used to mold the exoskeleton structure around the soft pneumatic actuators. This is shown in figure 6.

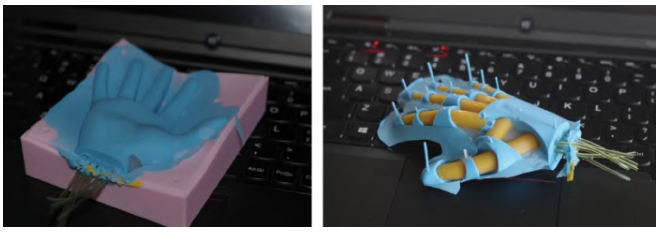

Fig. 6. Molding of the exoskeleton of a prosthetic hand (blue) around the soft pneumatic actuators (yellow) in [25], using a 3D printed mold.

The exoskeleton is made of a stiffer silicone than the actuators. This allows it to still have a degree of flexibility, allowing bending of the exoskeleton, but also more rigidity than the actuators. The semi-open structure of the exoskeleton prevents expansion of the actuator in the closed parts, but allows it in the open parts. Upon pressurization of an actuator this therefore results in the bending of the finger, as shown in figure 7.

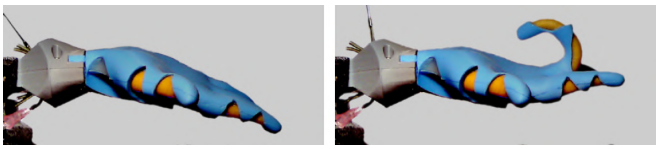

Fig. 7. Pressurization of a single soft pneumatic actuator of the soft prosthetic hand of Fras and Althoefer [25], resulting in the bending of the pressurized finger.

The soft prosthetic hand is operated using six solenoid valves, one for each actuator, and these are controlled by a Raspberry PI module. In the current experiment the hand is controlled by the human using a simple joystick, however, efforts are being made to control the hand by means of electromyography (EMG). When using a supply pressure of 100 kPa, the hand is able to exert a maximum force of around 0.9 N at the tip of a finger.

Although the soft prosthetic hand of Fras and Althoefer is in an early stage of development, it shows promising aspects for further development of pneumatic hand prostheses. The flexibility of the hand and its cosmetic resemblance to a human hand make it a very attractive prosthesis. Furthermore, its simple and cheap fabrication could make it available to a much broader group of users than currently available hand prostheses. Moreover, although the weight of the prosthesis is not mentioned in their work, the used materials and hollow design suggest that the hand prosthesis could be relatively lightweight compared to conventional hand prostheses. The grip force, however, is at least an order of magnitude lower than that of commercially available electrically powered hand prostheses [33]. Although the soft prosthetic hand proved to be able to pick up several every day objects, the grip force is something that needs to be addressed before this design can be turned into a commercially viable prosthesis. Furthermore,

the control of the prosthesis should be further developed in order to make it easier for the user to control it. As stated before, EMG control is currently being developed for the soft prosthetic hand and this could prove to be a very attractive solution.

*2) PAM:* Pneumatic Artificial Muscles (PAMs) are pneumatic actuators that mimic human muscles, i.e. they contract when they are activated (pressurized). PAMs originally were developed under the name McKibben Artificial Muscles in the 1950s, however, their usage in hand prostheses did not become popular until the 2000s. A PAM consists of a tube/balloon made of elastic material, which is covered by a braided fiber mesh. The fibers that make up the mesh have a high tensile strength and thus can not elongate, and therefore they can only change direction. The braid pattern of the mesh therefore determines how the PAM deforms when pressurized. Increasing the pressure inside the tube causes it to expand. However, the pattern in which the fibers are braided to form the mesh, causes the PAM to expand in radial direction, but contract in axial direction. Figure 8 shows a PAM in both neutral and pressurized state, alongside a schematic drawing of the PAM.

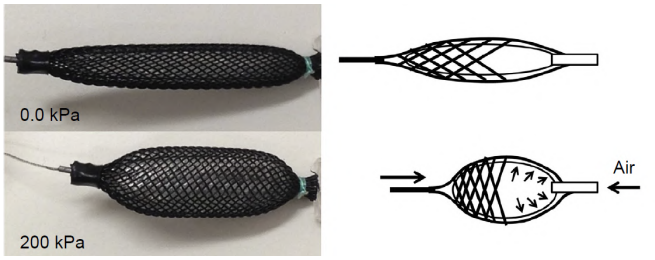


Fig. 8. Pressurization of a PAM in [40]. The increased pressure causes the elastic balloon to expand, however, the mesh geometry restrains expansion and causes the PAM to expand radially and contract axially.

A big advantage of PAMs is that they are compliant, which means they can adapt to the situation, are less sensitive to alignment issues and they are safer to use in proximity of a human. The simple design also makes them easy to manufacture and low in cost. It is often stated that another advantage of PAMs over other pneumatic actuators is that they have a relatively high power-to-volume/weight ratio, which is true when they are compared to standard components, such as industrial cylinders. Plettenburg [34] shows, however, that careful design of pneumatic cylinders results in a much higher power-to-volume/weight ratio than that of PAMs. A disadvantage of PAMs is that the stroke is on average 30% of its total length, which is relatively low compared to other pneumatic actuators. Furthermore, the deformation of a PAM is nonlinear which increases the difficulty of control. Moreover, they can only provide a unidirectional tension, which means that for most use cases an antagonistic pair is needed, similar to muscles in the human body [6], [35]–[57]. Figure 9 shows a schematic overview of such an antagonistic pair, that works to bend a finger. The overview shows the three different states of the system and the corresponding pressure differences.

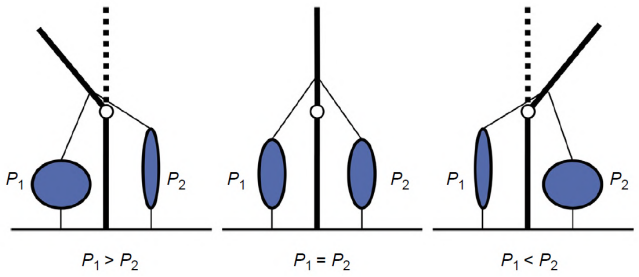


Fig. 9. Antagonistic PAM movement in [40]. Pressure differences between the PAMs cause the system to bend in the direction of the higher pressure.

Honda, Miyazaki and Nishikawa [39] designed a pneumatically powered robotic hand, consisting of 16 joints, 25 PAMs and 17 degrees of freedom. Ide and Nishikawa [40] further developed the controller of this hand.

The thumb and little finger of the prosthesis use three PAMs to mimic human movement and the other fingers use four. Here some movements are coupled to a single PAM, e.g. the bending of the distal and medial phalange of the little finger is coupled. Figure 10 shows the complete robotic hand without its cosmetic cover. On the left side the PAMs in the wrist are visible and on the right side the PAMs in the fingers are visible.

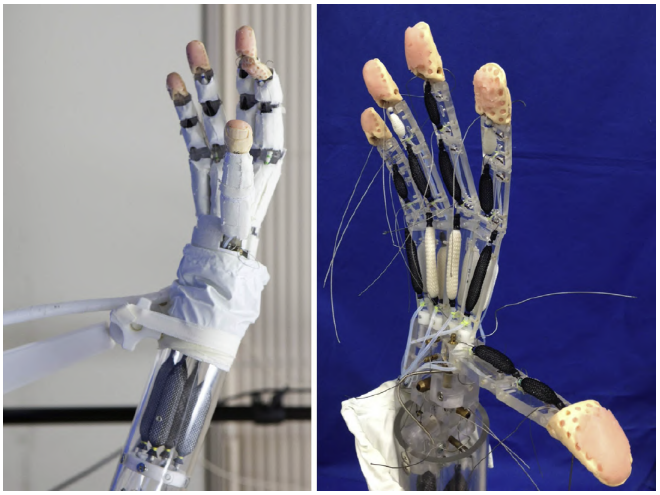

Fig. 10. Robotic hand from [40], with and without covering, showing the PAMs used to actuate the phalanges of the fingers.

The robotic hand is still in a very early stage of development, therefore not much is reported on its performance in the reports of both Honda, Miyazaki and Nishikawa [39], and Ide and Nishikawa [40]. They do show, however, that the fingers have a step response of approximately 0.5 s for opening or closing, which is relatively fast for a hand prosthesis and therefore seems promising. The control method used by Honda, Miyazaki and Nishikawa [39], however, leads to a steady-state error in the bending angles of the joints in the range of 1 to 5 degrees. As stated by the authors this will need to be addressed in a following design, for example by using angle sensors. Ide and Nishikawa [40] used another approach for the control of the hand, which among other things led to the

elimination of the steady state error. This, however, increased the operating cycle of the hand by an order of magnitude. The usage of PAMs in a hand prostheses seemed promising due to their high power-to-volume ratio, however, the aforementioned design does not yet show or state specifications that support this statement. When the robotic hand is further developed it would be interesting to see performance specifications such as the grip force and the mass of the entire hand, to be able to compare it to other designs of robotic/prosthetic hands in order to judge if PAMs are indeed a promising direction of hand prosthesis actuation.

### B. Control

*1) Myoelectric:* In myoelectric control, electromyography (EMG) is used to control a prosthesis. EMG is a form of medical electrodiagnosis where the electrical potential of the muscles is measured using needle electrodes that are inserted into the skin or patch electrodes that stick to the skin. When these muscles are activated, their electrical potential changes, which can be seen in an electromyograph. Thus, EMG can be used to monitor muscle activity. Most muscles that control the human hand are located in the forearm. Therefore, when a hand is amputated, most of these muscles remain partially intact. The brain can still activate these muscles and thus, by monitoring the muscle activity using EMG, the user's intention of hand movement can be derived and performed by the prosthesis.

An advantage of myoelectric control over conventional control methods is that it provides a direct link between the user's brain and prosthesis. However, this link only works one way; The brain can send signals to the prosthesis (feed forward), but the prosthesis can not send direct signals to the brain (feedback). This means that the user can actuate the prosthesis in the same way he would actuate a human hand, however, he does not get any feedback, which complicates the control of the hand. Another advantage of myoelectric control is that it allows for complex movements without complex control algorithms or effort from the user, as the actuation of the prosthesis is directly coupled to the muscle activity of the user, which is controlled by the brain already. A disadvantage, however, of myoelectric control is that the accuracy of EMG is currently still relatively low, even though it is getting better and better. Adipose tissue, such as fat, affects measurements, therefore, myoelectric control does not work equally well for all users. Furthermore, activity from muscles that are located deeper within the body, is harder to measure and the signal is heavily influenced by the activity of surrounding muscles. At this point it is therefore not yet feasible to single out activity from individual muscles, and therefore control is now based upon the activity of larger muscle groups [8], [9], [15], [21], [58].

Feng et al. [21] designed a myoelectrically controlled soft robotic hand. The EMG electrodes are connected to the right arm of the user as shown in figure 11.

The electrodes are placed on the mayor muscle groups controlling the hand movement, and consist of three channels and a reference. To control a prosthesis using the EMG signal, an experiment was done in order to create a mathematical model that accurately determines the type of hand movement based on the three EMG channels. In the experiment subjects were asked to perform the fine hand gestures, as shown in figure 12, and their EMG signal was recorded.

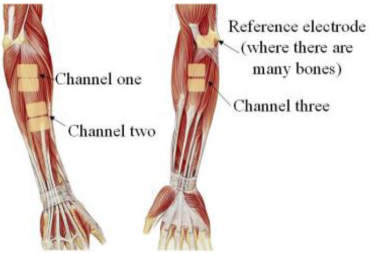


Fig. 11. Muscle anatomy of the right human forearm and the electrode positions for EMG measurement in [21]. The three electrode channels are used to measure muscle group activity with respect to the reference electrode.


Fig. 12. The ten types of fine gestures used in the experiment of Feng et al. [21] to try to find patterns in the corresponding EMG measurements.

Based on the data of all subjects, a model for the translation from EMG to prosthesis movement was derived, with an accuracy of 93.2%. Using this model and the test setup shown in figure 13, the user is able to control the hand prosthesis, based on the movement of their real hand.

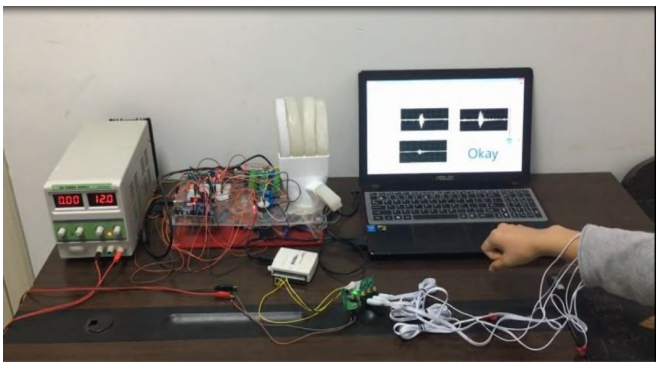


Fig. 13. Test setup used by Feng et al. [21] to test the myoelectric control of a hand prosthesis, using the derived EMG-to-movement translation model.

*2) Sensors:* Tjahyono et al. [35] developed a novel strain sensor. The sensor is made form natural rubber (NR) coated with a layer of the conducting polymer polypyrrole (PPy). This combination is used as NR has the mechanical properties needed for a large strain sensor and PPy has the conducting capabilities to detect and measure strain. When strain is applied to the NR/PPy sensor, its electrical conductivity decreases. This relationship can be used to derive the applied strain from the measured electrical conductivity.

When compared to a laser distance sensor the absolute measurement error of the strain sensor is less than 1.5 mm, with an average of 0.7 mm, which is acceptable for usage in a hand prosthesis. Furthermore, experiments with the novel strain sensor and a hand prosthesis proved that it could be used to smoothly move the hand to desired setpoints.

An advantage of this sensor over conventional strain sensors is that its compliance not only allows it to measure large strains but also allows the sensor to adapt to the motion of prosthesis, which allows for a wider range of motion. Furthermore, the sensor is compact and lightweight, which makes it ideal for usage in a prosthetic hand. A disadvantage, however, is that the compliant materials of the sensor are more prone to damage from contact with more rigid or sharp, parts or objects. Moreover, the accuracy of the strain sensor is affected by the effects of elastic hysteresis of the materials, i.e. the relation between stress and strain is different for loading and unloading of the sensor.

Kadota et al. [45] developed a balloon sensor to measure external forces. This sensor is shown in figure 14.

Fig. 14. Balloon sensor developed by Kadota et al. [45]. It consists of a rubber tube, closed on one end and connected to a differential pressure sensor through a tube on the other end.

When an external force is applied to the sensor, the tube is compressed and the pressure inside it increases, which is measured by the differential pressure sensor. Thus, by monitoring the pressure inside the tube the external forces can be determined. Experiments show that the pressure measured with the sensor increases linearly with the applied force.

An advantage of this sensor is that the balloon and sensor can be placed at a distance from each other. This means that the compact and lightweight balloon can be placed at the extremities of the prosthesis, where weight and size play an important role, and the heavier sensor can be placed at the base of the prosthesis. A disadvantage, however, is that the longer the tube between the balloon and sensor is, the bigger the error in the pressure reading becomes due to fluid mechanics.

Scharff [30] details the design of several 3D printed soft pneumatic pressure sensors. One of the designs is the double bellow pressure sensor, shown in figure 15.

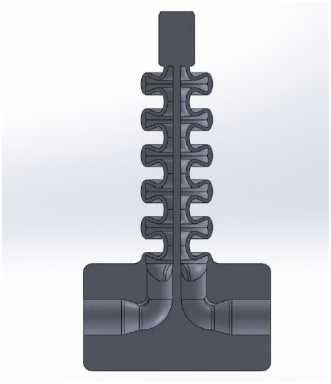

Fig. 15. Double bellow pressure sensor developed by Scharff [30]. This design features a column of bellows, that are divided in two chambers along the length of the column. In this way a separate air chamber is formed for respectively the left and right side of the sensor.

When the bellow column is bent to the left or right the pressure on one side increases, while the pressure on the other side decreases. The pressure difference between the two sides is, therefore, a measure for the bending angle of the column. Using a mathematical model the bending angle can, therefore, be calculated from the pressure difference.

The double bellow pressure sensor is still in the concept stage of development and, consequently, no data is available yet on the performance of this sensor.

An advantage of these soft 3D printed sensors is that their compliance allows them to be used with adaptive hand prostheses, such as soft pneumatic hands. Furthermore, fabrication of the sensors is simple and cheap, as they consist of a single 3D printed part. Besides, the design of the sensor can be easily adapted for the specific use case. A disadvantage, however, is that the soft material of the sensor is more prone to tearing and fatigue, and 3D printing introduces minor faults in the material, which increases the chance of tearing even further.

*3) Feedback:* Feedback for the control of prostheses is not something new; Old body-powered prostheses already had a form of feedback through the operation forces. However, feedback in prostheses is something that has been neglected throughout time, especially with the switch to electronic prostheses. Researchers are, however, starting to realize more and more the importance of feedback in controlling a prosthesis.

An advantage of feedback is that the user has more awareness of the forces that the prosthetic hand is applying on an object, which not only allows for more precise control of the prosthesis but also makes sure that the applied force is not too large or small for the task at hand. This results in a much more intuitive control for the user and an overall better acceptance of the prosthetic hand by users. A disadvantage is, however, that the wrong amount of feedback or the wrong

kind of feedback can lead to over-stimulation of the user, which in turn negates the intended effect of the feedback [11], [24], [55].

Huaroto et al. [11] developed a soft pneumatic actuator (SPA) meant for giving feedback to the user of a prosthetic hand in the form of tactile and kinesthetic forces on the residual limb. The design of this SPA is shown in figure 16.

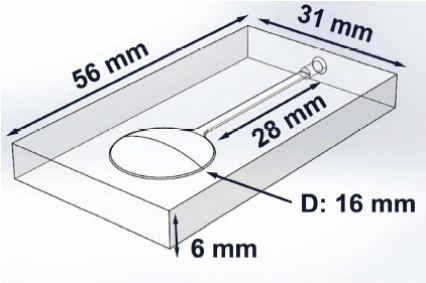


Fig. 16. SPA design of Huaroto et al. [11]. The design of the SPA consists of a silicone rubber liner, with an internal chamber. This chamber is shaped like a plano-convex lens, where one side is flat and the other has a circular curvature. A small tube allows the chamber to be pressurized.

When the SPA's chamber is pressurized, the liner expands as shown in figure 17, with a total displacement of 2.8 mm. This displacement results in a force between the liner and the residual limb. By controlling the magnitude and frequency of this force, feedback is given to the user of the hand prosthesis.

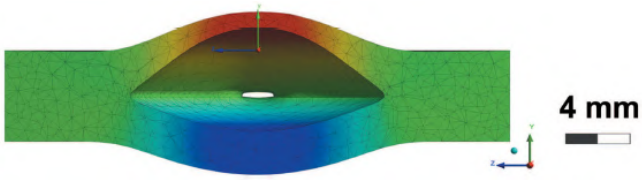


Fig. 17. Pneumatic expansion of the SPA of Huaroto et al. [11] when pressurized. Positive displacement is shown in red and negative displacement in blue.

While only weighing 8 grams, the SPA is able to produce a force up to 12.5 N with a frequency of 70 Hz, using a pneumatic pressure of 60 kPa. Compared to other tactile and kinesthetic devices, the SPA is much simpler and smaller. Furthermore, Huaroto et al. [11] showed that the usage of the SPA resulted in a significant improvement of the perception of a prosthesis user and shows high potential for future prosthesis designs.

As shown in the dissertation of Witteveen [59], this kind of tactile feedback helps users in controlling their prosthesis, eventhough the tactile nature of this feedback means that it is relatively slow, thus limiting the increase of performance with this feedback.

*4) Miscellaneous:* There have been many other advances in the field of control for pneumatically actuated hand prosthesis, such as the improvement of control algorithms [40], [41] and the electrical control schemes [17], modelling of the full prosthesis [53], and pneumatic transmissions [12].

Vorob'ev, Mikheev and Morgunenko [60] developed a way to control a hand prosthesis using one's foot. Here tactile sensors are placed within an insole and the hand prosthesis can be controlled by applying forces to these sensors with one's foot. Seven sensors are placed within the insole:

- The five sensors underneath the toes are used to control finger movement.
- The sensor underneath the heel is used to fix wrist position and is switched off during walking.
- The sensor underneath the ball of the foot is used to control grip strength.

Figure 18 shows the insole with sensors and the test setup used to control the pneumatically actuated prosthetic hand.

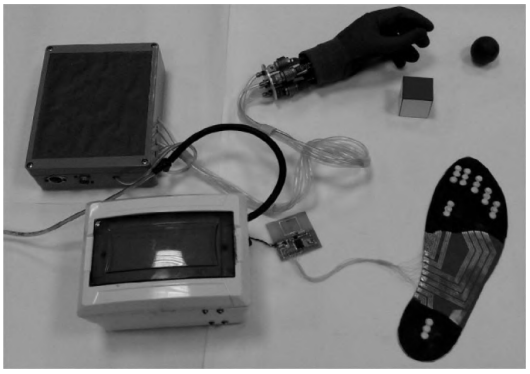

Fig. 18. Setup used to test the control of a prosthetic hand with the foot controller of Vorob'ev, Mikheev and Morgunenko [60]. The tactile sensors are visible on the insole.

An advantage of this form of control is that one can control the prosthetic hand using other limbs in a discreet way. Furthermore, this form of control allows all the fingers to be controlled independently and also allows control over the magnitude of the grip force. A disadvantage, however, is that one will need a lot of practice to use this form of control. Besides, this controller cannot be used when the foot is used normally, such as during walking.

No specifications on the performance of this controller are reported, which could either mean that not enough data is available yet, as it is still in an early stage of development, or that the performance of this controller is much worse than expected. Either way it would be interesting to see how well this kind of controller performs, to see whether it is an attractive option for a future prosthesis design.

### C. Energy

*1) Propellant:* Different kinds of propellants have been used for pneumatically powered hand prosthesis throughout the years. The first prostheses used air, as this is available everywhere and could be compressed using a bellow and muscle power. However, the energy density of this supply is very low and, therefore, the hand could not be used long before it needed new compressed air. Therefore, the switch

was made to compressed carbon dioxide ($CO_2$), which has a higher energy density, which means that it can last longer until a refill is needed. Using a portable cartridge to store highly pressurized $CO_2$ resulted in even longer usage without a refill [5]. Nowadays, $CO_2$ cartridges are commonly available as they are used for a wide variety of applications, and they are also recyclable, which means that they are perfect for usage in a hand prosthesis that uses around one cartridge a day. Furthermore, $CO_2$ is a relatively safe gas and also cheap, as it is a byproduct of many processes. The downside, however, is that the emission of $CO_2$ is frowned upon from an environmental standpoint, but the amount of $CO_2$ emitted by the hand prosthesis is relatively low.

In recent research the usage of a liquid mono-propellant, i.e. hydrogen peroxide ($H_2O_2$), has been investigated. The advantage that $H_2O_2$ has over $CO_2$ is that its energy density is an order of magnitude higher, which means that the hand prosthesis can be used longer, with less propellant. Opposite to $CO_2$, $H_2O_2$ needs a catalyst to be converted to pressurized gas in the form of $H_2$ and $O_2$. An advantage is that these gasses are environmentally friendly, in contrast to $CO_2$ [6], [23], [47], [56], [61]–[76].

Fite et al. [63] designed a complete pneumatically powered arm prosthesis, that uses $H_2O_2$ as propellant. Figure 19, shows an overview of the actuation system of the prosthesis.

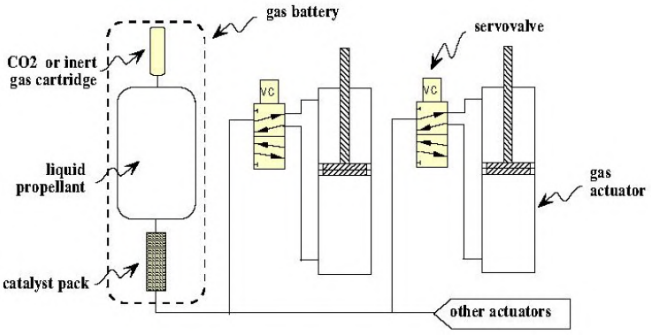


Fig. 19. Schematic overview of gas supply and actuator configuration in [63]. $H_2O_2$ is stored in a fuel cartridge and a catalyst is used to break the molecular bonds and, thus, convert the liquid propellant into pressurized gas that is used to actuate the prosthesis. A small $CO_2$ cartridge is used to pressurize the liquid propellant, which forces it to go through the catalyst pack when needed.

Figure 20 shows a computer-aided design (CAD) model of the full prosthetic arm, including the fuel cartridge.

The full arm prosthesis weighs 2.0 kg in total, including the fuel cartridge with a weight of 450 g when full. Although no performance specifications are reported, Fite et al. [63] show that the arm is able to grasp a wide range of differently shaped objects. This prosthesis has a very large range of motion which seems attractive, however, this also significantly increases the difficulty of controlling it and its weight, as many actuators and valves are needed to operate it. For future designs it would be interesting to see whether this range of motion is needed, or that a simpler and lighter prosthesis, with a decreased range of motion, is sufficient for the user.

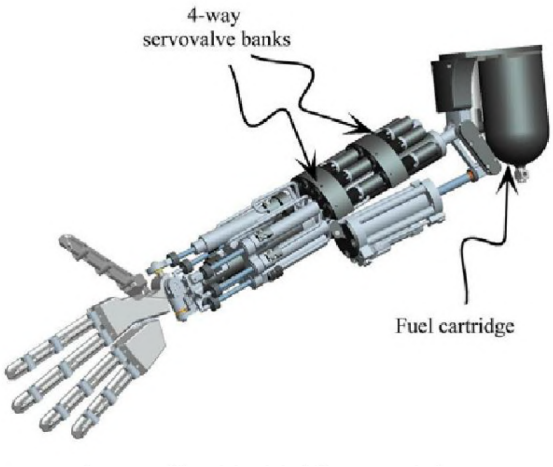


Fig. 20. CAD model of the full arm prosthesis of Fite et al. [63]. The fuel cartridge containing the $H_2O_2$, the $CO_2$ cartridge and the catalyst pack supplies pressurized gas to the 4-way servovalve banks, which determine the actuators that are pressurized.

*2) Dual-Mode:* The act of grasping an object can be divided into two phases: the prehension and the pinching phase. The prehension phase is when the fingers are moving towards the object, but do not touch it. The pinching phase is when the fingers touch the object and apply a force to it. Most conventional hand prostheses use the same actuation for both phases of grasping. The motion and force characteristics of both phases are, however, very different; In the prehension phase a large stroke is needed to move the fingers to the object, however, almost no force is needed, as the fingers do not touch the object yet. In the pinching phase it is the other way around; Almost no stroke is needed, as the fingers already touch the object, but a large force is needed to hold the object. Therefore, using the same combination of actuation and transmission for both phases is very inefficient, as both phases require very different actuation characteristics. Kim et al. [66] and Plettenburg [68], therefore, suggest to use different actuators for both of the phases, to make sure that each phase uses an actuator with optimized characteristics. This will, therefore, result in a higher energy efficiency of the hand prosthesis, and in turn a lower gas consumption and longer usage time.

In his dissertation Plettenburg [68] details the design of a pneumatic hand prosthesis using dual-mode operation. Figure 21 shows a schematic drawing of this prosthesis.

The figure shows the hand in its rest position, where it it closed and locked in place by the locking mechanism, which resists reaction forces from an object inside the hand. To grasp an object, the pinching motor is pressurized first, followed by unlocking the locking mechanism and pressurizing the prehension motor. Next the opened hand is moved around an object and the prehension motor is depressurized, thus moving the fingers to the object by the weak closing spring. Then the locking mechanism is engaged, followed by depressurizing the pinching motor, which results in a pinching force by the strong pinching spring.

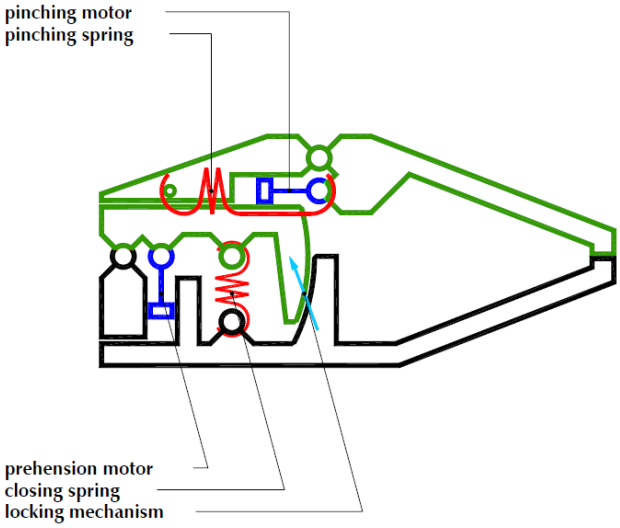


Fig. 21. Schematic drawing of the pneumatically powered dual-mode hand prosthesis in [5], consisting of a thumb and finger, actuated by respectively a pinching motor/spring and a prehension motor/spring, including a locking mechanism.

Table I shows an overview of the masses and operating cycle of the hand. Furthermore, it shows the same specifications for a comparable commercial myoelectric hand prosthesis. As can be seen in the table, not only the mass of the hand prosthesis itself is much lower for the pneumatic dual-mode prosthesis, also the mass of the pneumatic energy storage is much lower than that of a commercial myoelectric device, eventhough both have an energy storage that lasts one full day. Moreover, the operating cycle (the time it takes to open en close it) of the pneumatic dual-mode prosthesis is much faster than that of the myoelectric device. Both the low mass and fast operating cycle make the pneumatic dual-mode prosthesis a very attractive option for future hand designs.

TABLE I
COMPARISON OF DUAL-MODE HAND.

| | Hand prosthesis | |
|---|---|---|
| | Plettenburg | Myoelectric Bock |
| Mass hand | 60 g | 130 g |
| Mass energy storage | 36 g | 60 g |
| Mass complete prosthesis | 250 g | 340 g |
| Operating cycle | <1 s | >2.5 s |

*3) Pressure:* Pneumatic pressure is something that has varied widely among hand prostheses; There has not been a standard pressure level. The pressure depended on factors like the available compressors, storage cartridge pressure, maximum pressure ratings of parts, or the results of tests with different pressure levels used to operate the hand prosthesis. More recently researchers started looking into the supply pressure for pneumatically powered hand prostheses [46], [69], [72].

With the emergence of soft pneumatic actuators, researchers have started looking at how to actuate the prostheses with a pressure level that is as low as possible. The reason for this is that a low pressure level lowers the chance of rupture of the soft materials, is safer when used in the presence of humans and makes it easier to refill. However, a low pressure level commonly results in a lower gripping force and heavily reduced usage time. Tsujiuchi et al. [43], however, were able to develop a pneumatic actuator, using a lower pressure level, that has a similar performance to conventional pneumatic actuators. Their hand prosthesis has a movable range similar to that of a human hand and can lift objects with a mass up to 400 g. This is enough to pick up many everyday objects, however, it will not be able to lift heavier objects, such as a water bottle, a laptop, a pan, etc. The usage of low pressure in soft pneumatic actuators therefore has aspects that seem promising, however, more research should be done into increasing the actuation forces before it becomes an attractive option for prosthesis users.

Other research focuses on the ideal supply pressure for pneumatical devices in general. Doedens [71] did research on the optimal $CO_2$ pressure for a pneumatic system. Based upon previous research, theoretical work and experiments, an ideal pressure level of 1.2 MPa was found. Using this level of $CO_2$ pressure in a pneumatic system, such as a pneumatically powered hand prosthesis, would result in a minimum gas-consumption and, thus, a prolonged usage time before needing to refill.

*4) Energy Recovery:* Pneumatic actuation generally relies on letting pressurized gas flow into a previously depressurized chamber. This gas expands in the chamber and performs work, which means the actuator exerts a force, e.g. a PAM used to close the fingers of a hand prosthesis. When the actuator needs to release the force, e.g. to open the hand prosthesis again, the gas in the chamber is released into the surrounding, returning the chamber to a depressurized state. The releasing of this gas into the surrounding means that energy is lost during the usage of the pneumatically actuated hand. Furthermore, energy is lost when the pressure of the gas is reduced from the saturation pressure in the supply to the pressure allowed for operation of the hand prosthesis. This results in a loss of approximately 60% of the total energy in a gas cartridge and results in a higher gas consumption and, therefore, a lower usage time. Energy recovery methods aim to reduce the amount of lost energy and, therefore, the gas consumption, letting the prosthesis be used longer [12], [69], [77].

Verga [69] designed a small free-piston expander-compressor, that is able to recover energy from the system, when the $CO_2$ pressure is lowered from saturation to operation level. The device can be used to lower the pressure from the $CO_2$ at the saturation pressure to the pressure that is required for operating the hand prosthesis. While this expansion is performed by the free-piston of the device, work is recovered from the expansion by at the same time compressing air from the surrounding. This compressed air can then be used in the prosthetic hand, reducing the amount of energy that is lost

and decreasing the gas consumption, which in turn increases the usage time. Figure 22 shows a cross section of the design in two different positions.

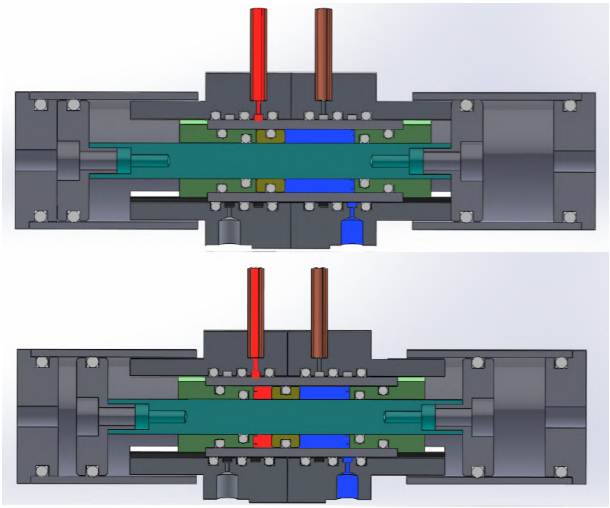

Fig. 22. Schematic overview of the free-piston expander-compressor designed by Verga [69]. Red is used to indicate the high pressure $CO_2$ and blue to indicate air. In the top figure the $CO_2$ inlet on the left is opened, which causes the piston to slide to the right and the $CO_2$ to expand, as can be seen in the bottom figure. At the same time that the $CO_2$ is expanded, the air is compressed by the same piston.

The design of Verga [69] is still a very early prototype and therefore its specifications do not yet meet the requirements set at the beginning of the design stage. The prototype has a mass of 100 g, which is 76 g more than required. Furthermore, there is no data available yet on the actual energy recovery, as during the testing an o-ring failed, preventing further testing. The concept of recovering energy from the pressure changes, however, seems very promising and would be an interesting concept for further research, which should show how well it actually works.

### D. Fabrication

*1) Casting:* Casting is not a new fabrication method. However, its usage in casting entire hand prostheses is. With the emergence of soft pneumatics, casting is used to create full hand prostheses or complete pneumatic finger actuators. Furthermore, casting can be combined with 3D printed molds, to create customized prostheses and allow rapid prototyping.

A big advantage of casting is that it is a relatively cheap and easy process for large quantities, as a single cast can be used to create many parts. On the downside, however, casting does not allow for a very high level of detail in the cast parts and, therefore, the parts that it is used for can not have a too complex geometry. However, soft pneumatic actuators are generally simple enough to be cast without a problem [13], [16], [21], [28], [31].

As shown before in figure 6, Fras and Althoefer [25] used a 3D printed mold, based on a 3D scan of a human hand, to cast the entire exoskeleton structure for a soft pneumatic hand prosthesis.

*2) 3D Printing:* 3D printing is a relatively new technology that allows parts to be printed layer-by-layer from a vast array of materials, such as plastics and metals. This technology allows prostheses or parts thereof to be directly printed from a CAD model. A computer program is used to 'slice' the 3D model of the object to be printed into separate layers, which can then be used by a 3D printer.

A big advantage of 3D printing is the high degree of customizability and rapid prototyping it allows, as objects can be printed straight from the CAD model. Furthermore, the printing in thin layers allows a high complexity of parts and enables one to print entire systems, such as a hand prosthesis, in a single print. Furthermore, 3D printing is relatively cheap for a low number of products, which makes it ideal for customized parts and prostheses. A disadvantage is, however, that 3D printing is rather expensive and slow when a large amount of prints is needed, which makes it less suitable for mass fabrication. Furthermore, 3D printing results in parts with non homogeneous material due to the printing in layers, which affects the physical properties of the part [16]–[19], [22], [24], [27]–[31], [67], [75], [78]–[83].

Cuellar et al. [80] developed a hand prosthesis, that can entirely be 3D printed in only two parts. Figure 23 shows the CAD model of the full hand prosthesis and a 3D printed prototype of one of the two parts of the prosthesis.

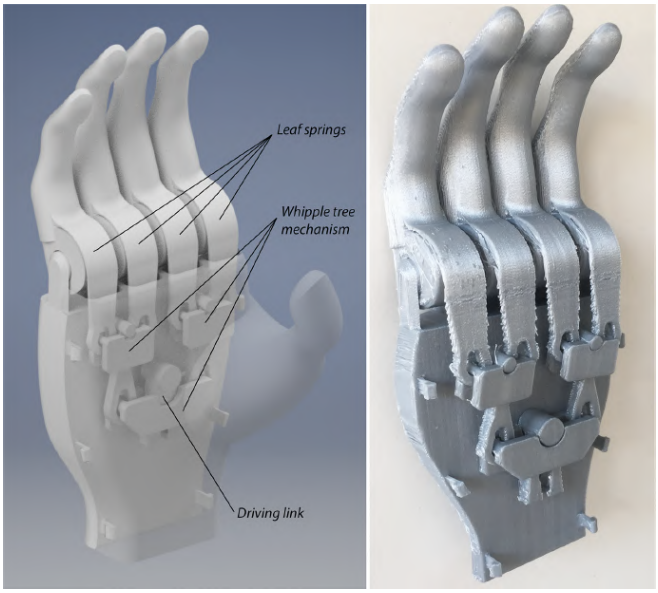


Fig. 23. CAD model and a 3D printed prototype of one of the two parts of the prosthetic hand in [80]. The hand is actuated by a cable that pulls on the driving link of the whippletree mechanism and leaf springs return the fingers to their neutral, opened position.

The hand prosthesis is designed in such a way that its fingers are actuated, eventhough it is printed as a single part. The four fingers can be actuated using a single cable, meaning that the hand is underactuated. The elasticity of the material acts as the return spring to keep the hand open when no force is

exerted on the cable. This hand prosthesis is intended to be body powered by attaching the cable to a harness, however, the same principle could be used for a 3D printed pneumatic hand prosthesis, where instead of a harness a pneumatic cylinder would be used.

The 3D printed prototype is able to exert a force up to 6 N at the tip of the fingers. Compared to commercially available body powered hand prostheses the prototype is able to exert a larger force at relatively low user input forces, but a lower force at relatively high user inputs. Therefore, this prosthesis would be attractive for cases where it will be used for lighter tasks. Moreover, the energy needed to operate the prototype is low compared to the commercially available hands. The elasticity of the 3D printed material and cable result in hysteresis in the opening and closing of the hand, however, not too much to bother the user. The life time of the 3D printed hand prototype is on average 2446 $\pm$ 499 operating cycles. This life time is very short, considering a person opens/closes his hand several hundred times a day. The 3D printed hand was, however, not designed for life time, but to be able to be used by persons in areas where normal prostheses are not available or too expensive. The 3D printed hand therefore offers a cheap and quick option for users that otherwise would have no access to prostheses at all. For future research, however, it would be interesting to see whether the life time, and grip forces for higher user inputs can be increased, in order to see if 3D printing is also an attractive solution for producing prostheses in places where access to prostheses is not an issue.

*3) Advanced Materials:* Besides the fabrication processes, more attention is also being paid to the materials that are used to create hand prostheses or parts thereof [16].

Krishnan et al. [54] designed and tested a PAM made with silk fibers instead of the conventionally used synthetic fibers, such as nylon. The advantage of using silk over other fibers is that it is naturally stronger than fibers such as nylon or even steel. Furthermore, silk is a soft and natural fiber which makes it ideal for usage in bio-compatible devices and prostheses. Nothing is reported on the actual performance of the silk PAMs, except that they contract like conventional PAMs, therefore, it is uncertain whether it is an attractive solution for future hand prosthesis designs.

Wang [81] focuses on the usage of self healing polymers in combination with 3D printing. A big problem with 3D printed hand prostheses, or pneumatic finger actuators, is that they suffer from fatigue and will start tearing or cracking with use. The advantage of self healing polymers over conventional polymers, is that they repair themselves when damaged. This means that a crack or tear will be fixed automatically and recovers about 97% of its original strength after 24 hours. Using self healing polymers to 3D print soft pneumatic hand prostheses will, therefore, allow them to last much longer before they need to be replaced.

## E. Ergonomics

*1) Miniaturization:* The first generations of pneumatically powered hand prostheses were very heavy and bulky, as it was simply not possible to create smaller and lighter prostheses with the technology at the time. Throughout the years hand prostheses have become lighter and smaller, as their components could be made smaller using new technologies, and better materials could be used to decrease the weight even further. The lower weight and smaller volume, make the hand easier to operate and allow it to be fit within the shape of a human hand. In the last two decades even more focus has come on the miniaturization of the components of hand prostheses. Miniaturization does not only change the size and weight of the hand. but also the characteristics of the components, as different physical properties have different scaling factors. Therefore, miniaturization runs into physical limitations, preventing further miniaturization. However, components of hand prostheses are still becoming smaller and smaller [29], [49], [51], [61], [72].

De Volder, Moers and Reynaerts [49] detail the development of a miniature PAM. Figure 24 shows a schematic overview of the design and pictures of the prototype.

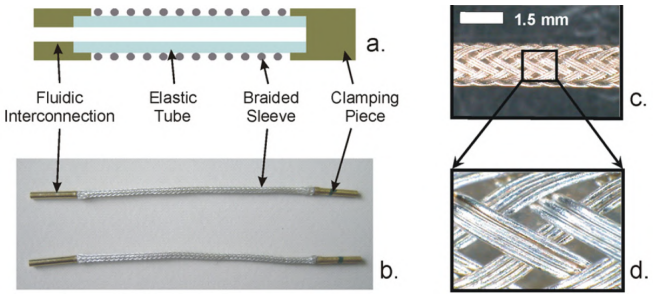


Fig. 24. Schematic overview (a) and a prototype (b) of the miniature PAM in [49], including an image showing the scale of the PAM (c) and an image showing the braided mesh (d). The PAM has a diameter of 1.5 mm and is 82 mm long.

Despite its small size, the miniature PAM is able to create a tension force of 6 N at a supply pressure of 1 MPa, which is around an order of magnitude higher than conventional pneumatic actuators of comparable or even larger sizes. Furthermore the miniature PAM has an actuation speed of more than 350 mm/s, which means it could be used in a prosthesis design with a fast operating cycle. The stroke of the miniature PAM is limited, however; It contracts up to 15% of its original length, compared to 30% for conventional PAMs.

Miniaturization seems like an attractive solution for components of future hand prostheses, as it decreases both the size and weight of the hand. However, the miniaturization should not lead to a decrease in performance. Therefore, it would be beneficial to look further into the effects of scaling down components, and how their performance can be maintained simultaneously.

*2) Customization:* A large focus of recent research has been the customization of prostheses. Customization of hand pros-

theses allows them to be tailored specifically for the intended user, making them more comfortable and more cosmetically appealing. The emergence of 3D printing has allowed the prostheses to be customized for each user and to be modelled after real human hands. Furthermore, the modular design of hand prostheses, allows users to build a hand prosthesis from separate modules to exactly fit their individual needs.

An advantage of this customization is that hand prostheses are becoming much more personalised, resulting in a higher acceptance rate by the user and making them a better fit for the task. A downside, however, of customization is that for each user a different design has to be made, which makes production more expensive, although new technologies, such as 3D printing, are making such customized production cheaper than ever before [11], [17]–[19], [22], [24], [27], [29]–[31], [67], [75]–[85].

Almeida et al. [17] designed a hand prosthesis using soft pneumatic actuators. The whole hand prosthesis is modelled after a 3D scan of a real human, as can be seen in figure 25.


Fig. 25. 3D printed soft prosthetic hand of Almeida et al. [17] based on the 3D scans of the adjacent human hand. The segmentation of the fingers allows them to bend similarly to a human hand.

The hand is entirely 3D printed from semi-flexible plastic and has internal air chambers. The fingers are segmented, which means that they will bend once pressurized. Figure 26 shows the deformation of one segmented finger, under increasing pressure levels.

An electro-pneumatic control system is used to control the movements of the hand. The pneumatic part of the system consists of a pneumatic piston pump that is used for pressurizing the hand, and four solenoid valves. The thumb is controlled by itself and the four other fingers are controlled together. Therefore, two of the solenoid valves act as an inlet for pressurization of respectively the thumb and the fingers, and the other two valves act as an outlet for depressurizing. The electric part of the system consists of a control board (Arduino) connected to an amplifying circuit, relay, battery and three sensors.

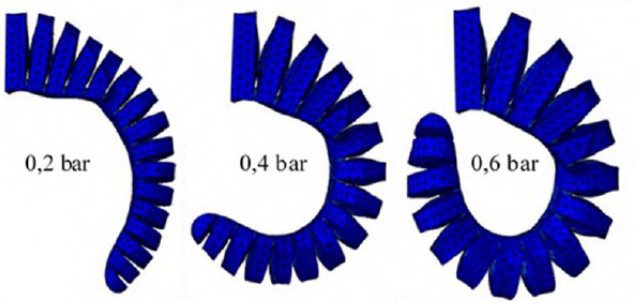


Fig. 26. Simulation of the gradual pressurization of the segmented soft pneumatic finger actuators of Almeida et al. [17], showing their bending behavior.

Tests performed by Almeida et al. [17] show that the bending angles achieved by controlling the soft pneumatic fingers are much lower than were predicted using simulation software. They attribute this to faults in 3D printing and the material. Furthermore, they do not report on the forces, operating cycle and energy usage of the prosthetic hand. These are all very interesting and important specifications of the performance of the hand prosthesis that could determine whether this is an attractive direction to go for future designs. More research is therefore needed to be able to determine if this design will be feasible, but the concept of 3D printing a cosmetically identical human hand seems very promising.

## IV. Discussion

In this section the results that were shown in section III will be discussed. Subsection IV-A will highlight the promising advances that were found. Next, subsection IV-B will look back on the mayor drawbacks of pneumatic hand prostheses from the past, in the light of the aforementioned advances. Hereafter, subsection IV-C will give recommendations for future research. Finally, subsection IV-D will discuss the commercialisation of the pneumatically powered hand prostheses described within this paper.

### A. Promising directions

The research as shown in section III, shows that there have been many advancements in the field of pneumatically powered hand prostheses;

The prostheses have become more human-like, both in their appearance as in their movements, due to technologies such as 3D printing, soft pneumatic actuators and PAMs. The prosthetic hands developed by Fras and Althoefer [25], and Almeida et al. [17], for example, used 3D printing combined with soft pneumatic actuators to become cosmetically very similar to real human hands. These advancements show a lot of promise as cosmetics are a very important aspect of a hand prosthesis for a user thereof.

The prostheses are also becoming much more energy efficient, meaning they can be used longer consecutively, and require smaller gas cartridges. The pneumatically powered dual-mode hand prosthesis of Plettenburg [68], for example, divided grasping into two separate stages, which allowed for the

selection of optimized actuators for both tasks. This not only resulted in a lowered energy consumption, which subsequently lead to a more lightweight energy storage, but the overall mass of the hand prosthesis was more than 26% lower than a commercial myoelectric competitor. Furthermore, the dual-mode hand is also more than twice as fast as its competitors. The work of Doedens [71], furthermore, showed how careful selection of gas pressures can reduce the amount of energy needed to actuate a hand prosthesis. These advancements show a lot of promise as energy efficiency, and consequently the mass of the energy storage and the usage time, play important factors when selecting a hand prosthesis.

Furthermore, the advances in the control of the prostheses makes them easier to operate by the user, due to more natural and accurate control methods. The myoelectric controller designed by Feng et al. [21], for example, uses electrodes to measure electrical signals in the muscles in the residual limb that would be used to control a real hand. This means that the user uses the same (feed forward) control for the hand prosthesis as he would use for a real hand. Using a pattern recognition model, the myoelectric model is able to convert the muscle signals to prosthetic hand movement with an accuracy of 93.2%. These advancements show a lot of promise as intuitive and accurate control are very important to a prosthesis user, as they want the prosthesis to do what they want without having to do too much effort.

Finally, fabrication methods such as 3D printing and casting, allow the prostheses to be produced much cheaper than before, making them affordable for a much larger part of the population. The prosthetic hand designed by Cuellar et al. [80], for example, is entirely 3D printed in just two parts. Therefore, the cost of this prosthesis is virtually the same as the 3D printing material cost, which comes down to only a couple of euros. This is a fraction of what a conventional commercial hand prosthesis costs and makes it accessible to a much larger part of the population, that now is able to afford a hand prosthesis, albeit a very simple one.

### B. Troubles of the past

As described in section I, pneumatic actuation for hand prostheses never became popular in the past due to their unmanageable control, the bulkiness of the gas storage and the difficulty of refilling the gas storage. The aforementioned research shows, however, that the recent developments in the field of pneumatically powered hand prostheses have overcome these problems; The research of Feng et al. [21] showed how myoelectric control can be used to intuitively control a hand prosthesis with an accuracy of 93.2%. Next, the design of the pneumatically powered dual-mode hand prosthesis of Plettenburg [68] showed that careful design of components and focusing on energy efficiency, resulted in a gas storage with a mass that is almost half that of a commercially available competitor. Finally, sub-subsection III-C1 showed that nowadays gas cartridges, that can be used in pneumatic hand prostheses, are widely available and can be easily replaced when depleted.

Due to the advances in pneumatically powered hand prostheses, pneumatic actuation is becoming a very attractive option for hand prostheses, as besides overcoming the mayor drawbacks from the past, it also offers advantages over body powered or electrically powered prostheses, such as:

- High operating speeds, as could be seen in the design of Plettenburg [68].
- Large forces, as could be seen in the PAM of De Volder, Moers and Reynaerts [49].
- Low weight, as could be seen in the design of Plettenburg [68].

### C. Future research

The results show that it is not only rewarding to improve existing technologies, such as the miniaturisation of a PAM by De Volder, Moers and Reynaerts [49], but that looking into fundamentally different principles can result into advances that lead to even better performance than already existing technologies. An example of this is the pneumatically powered dual-mode hand prosthesis of Plettenburg [68], that by dividing grasping into two stages is able to achieve a much higher energy efficiency than conventional hand prostheses. For future research it may, therefore, be interesting to not only focus on improving existing technologies, but also to try to come up with completely new ideas.

Furthermore, ideas that were discarded in the past, due to not being feasible at the time, might become attractive again, due to advances in technology that allow the idea to become feasible. This is, for example, visible in the development of an advanced hand prosthesis using PAMs by Honda, Miyazaki and Nishikawa [39], whilst PAMs were already developed in the 1950s, but never became popular in hand prostheses. For future research it may, therefore, be interesting to revisit old technologies or ideas that were discarded at the time for not (yet) being feasible.

Moreover, it is wise to not just think of the prosthesis as a device, but also of its intended user, as the device can be perfect from an engineering point of view, but if the user does not like it the prosthesis will not be used. As stated in section I many people reject their prosthesis as they find it inconvenient to use, eventhough it might be very well engineered. Advances in hand prostheses, such as the improved myoelectric controller of Feng et al. [21], make the prosthesis easier to operate and thus more appealing to users. During future research it is, therefore, important to not only focus on the engineering aspects of the prosthesis, but to also keep in mind the intended user thereof.

Finally, the results show that advances in the field of pneumatically powered hand prostheses go hand in hand with the advances in the whole field of engineering. An example of this are the prosthetic hands developed by Fras and Althoefer [25], and Almeida et al. [17] that use 3D printing, which is a relatively new technology, to make the prostheses cosmetically similar to real human hands. For future research it is, therefore, wise to keep an eye on the developments in the whole field of engineering in order to see if there are new technologies that may be applied in the design of a hand prosthesis.

### D. Commercialisation

All examples of prosthetic hands or parts thereof given in this paper are not (yet) commercially available. For most of the prostheses this is because they are still in an early stage of development, and the designs that were fabricated were prototypes. Before becoming commercially viable these designs will first need to be thoroughly tested and iteratively adjusted in order to get a performance that is attractive to prosthesis users. Once the prosthesis performs well, comfort and cosmetics play an important role too. These should already be taken into account in an early design stage, however, once the technical design of the hand is optimized, there is room to improve the appearance of the hand, by for example fitting it with a cosmetic glove, and to improve the comfort of the hand, by ensuring a good fit to the residual limb and distribute the weight and forces on it. After all this is done the prosthesis should still undergo a clinical trial to see what the actual users think of the hand prosthesis and whether or not it can be successfully commercialized. For most of the prostheses within this paper there is still a long way to go, however, the early prototypes show promising aspects and further research and development could lead to new commercial pneumatic hand prostheses.

On the the other hand there were also examples within this paper that do not (yet) seem like designs that could lead to a commercial product. For example the foot controller of Vorob'ev, Mikheev and Morgunenko [60] does not seem like the most practical form of prosthesis control, especially when compared to other technologies such as myoelectric control. Furthermore, the authors do not give any test results or specifications of the controller which raises the suspicion that either it did not work as intended or that a lot more research is needed in order to make it work. Together these points give the impression that this is not a commercially attractive direction to continue in, and that the effort is better spend on other advancements.

## V. Conclusion

Pneumatically powered hand prostheses have come a long way since 2000. Advances in the areas of actuation, control, energy, ergonomics and fabrication significantly increased both the performance and the appearance of the hand prostheses that have been developed. Although the pneumatic hand prostheses presented in this paper are not yet ready for commercialisation, the current designs show numerous promising aspects, and further development could result in commercial pneumatic hand prostheses that perform better than their competitors. As the major drawbacks of using pneumatic actuation from the past, i.e. unmanageable control, bulkiness of gas storage and difficulty of refilling the gas storage, have now been overcome, pneumatics has now become a very attractive actuation method when designing a new hand prosthesis. Furthermore, more and more advantages are becoming apparent which could increase the popularity and performance of pneumatically powered hand prostheses even further during the coming years.

## Acknowledgment

The author would like to thank Dick Plettenburg for his guidance and input throughout the process of creating this review. Furthermore, the author would like to thank Frans van der Helm for his feedback on the draft report. Moreover, the author would like to thank Alexis Cuevas Landeros, Arie Hoek, Leo Hoek and Leonor Arrebola Aranda for their support and motivation.

## References

[1] *Standards for Prosthetics and Orthotics Service Provision,* World Health Organization, Geneva, Sep. 4, 2015

[2] P. Herberts, L. Korner, K. Caine and L. Wensby, "Rehabilitation of unilateral below-elbow amputees with myoelectric prostheses," *Scandinavian Journal of Rehabilitation Medicine*, vol. 12, no. 3, pp. 123-128, 1980.

[3] S. F. Burrough and J. A. Brook, "Patterns of Acceptance and Rejection of Upper Limb Prostheses," *Orthotics and Prosthetics*, vol. 39, no. 3, pp. 40-47, 1985.

[4] Science Museum, *Thalidomide*, Science Museum's History of Medicine. Accessed on: Feb. 5, 2020. [Online]. Available: http://broughttolife.sciencemuseum.org.uk/broughttolife/themes/controversies/thalidomide

[5] D. H. Plettenburg, *Pneumatically Powered Prostheses: An Inventory.* Delft, Netherlands: Delft University of Technology, 2002.

[6] D. H. Plettenburg, "Electric versus pneumatic power in hand prostheses for children," *Journal of Medical Engineering and Technology*, vol. 13, no. 1/2, pp. 124-128, 1989. Available doi: 10.3109/03091908909030211

[7] J. Monestier, "Total hand prostheses," US4685929A, Aug. 11, 1987

[8] H. K. Yap, W. K. Ang, J. H. Lim, J. C. H. Goh and C. H. Yeow, "A fabric-regulated soft robotic glove with user intent detection using EMG and RFID for hand assistive application," *2016 IEEE International Conference on Robotics and Automation*, 2016. Available doi: 10.1109/ICRA.2016.7487535

[9] H. K. Yap et al., "A Fully Fabric-Based Bidirectional Soft Robotic Glove for Assistance and Rehabilitation of Hand Impaired Patients," *IEEE Robotics and Automation Letters*, vol. 2, no. 3, pp. 1383-1390, 2017. Available doi: 10.1109/LRA.2017.2669366

[10] M. A. Devi, G. Udupa and P. Sreedharan, "A novel underactuated multi-fingered soft robotic hand for prosthetic application," *Robotics and Autonomous Systems*, vol. 100, pp. 267-277, 2017. Available doi: 10.1016/j.robot.2017.11.005

[11] J. J. Huaroto, E. Suarez, H. I. Krebs, P. D. Marasco and E. A. Vela, "A Soft Pneumatic Actuator as a Haptic Wearable Device for Upper Limb Amputees: Toward a Soft Robotic Liner," *IEEE Robotics and Automation Letters*, vol. 4, no. 1, pp. 17-24, 2019. Available doi: 10.1109/LRA.2018.2874379

[12] D. Kim, "Compliant motion control for a compliant rehabilitation system," *2015 IEEE International Conference on Rehabilitation Robotics*, pp. 422-427, 2015. Available doi: 10.1109/ICORR.2015.7281236

[13] J. H. Low, A. Marcelo and C. H. Yeow, "Customizable soft pneumatic finger actuators for hand orthotic and prosthetic applications," *2015 IEEE International Conference on Rehabilitation Robotics*, pp. 380-385, 2015. Available doi: 10.1109/ICORR.2015.7281229

[14] H. K. Yap, F. Sebastian, C. Wiedeman and C. H. Yeow, "Design and characterization of low-cost fabric-based flat pneumatic actuators for soft assistive glove application," *2017 International Conference on Rehabilitation Robotics*, pp.1465-1470, 2017. Available doi: 10.1109/ICORR.2017.8009454

[15] K. Nishikawa, M. Shakutsui, K. Hirata and M. Takaiwa, "Development of pneumatic myoelectric hand with simple motion selection," *International Conference on Intelligent Robotics and Applications*, pp. 147-157, 2016. Available doi: 10.1007/978-3-319-43518-3_15

[16] B. Gorissen, D. Reynaerts, S. Konishi, K. Yoshida, J. W. Kim and M. De Volder, "Elastic Inflatable Actuators for Soft Robotic Applications," *Advanced Materials*, vol. 29, no. 43, 2017. Available doi: 10.1002/adma.201604977

[17] H. D. Almeida, P. Almeida, T. Charters and M. J. G. C. Mendes, "Electro-pneumatic control of soft robotic hand prosthesis actuators," *2019 IEEE 6th Portuguese Meeting on Bioengineering*, 2019. Available doi: 10.1109/ENBENG.2019.8692563

[18] S. S. Yun, B. B. Kang K. J. Cho, "Exo-glove PM: An easily customizable modularized pneumatic assistive glove," *IEEE Robotics and Automation Letters*, vol. 2, no. 3, pp. 1725-1732, 2017. Available doi: 10.1109/LRA.2017.2678545

[19] Y. Nemoto, K. Ogawa and M. Yoshikawa, "F3Hand: A Five-Fingered Prosthetic Hand Driven with Curved Pneumatic Artificial Muscles," *2018 40th Annual International Conference of the IEEE Engineering in Medicine and Biology Society*, pp. 1668-1671, 2018. Available doi: 10.1109/EMBC.2018.8512692

[20] J. C. Cool and G. J. O. Van Hooreweder, "Hand prosthesis with adaptive internally powered fingers," *Medical & biological engineering*, vol. 9, no. 1, pp. 33-36, 1971. Available doi: 10.1007/BF02474402

[21] N. Feng, H. Wang, F. Hu and J. Gong, "Humanoid Soft Hand Design Based on sEMG Control," *2018 9th International Conference on Information Technology in Medicine and Education*, pp. 187-191, 2018. Available doi: 10.1109/ITME.2018.00050

[22] E. Thompson-Bean, R. Das and A. McDaid, "Methodology for designing and manufacturing complex biologically inspired soft robotic fluidic actuators: Prosthetic hand case study," *Bioinspiration and Biomimetics*, vol. 11, 2016. Available doi: 10.1088/1748-3190/11/6/066005

[23] D. F. Schmidt, G. S. Lowe and A. P. Paplinski, "On the design of a hydraulically actuated finger for dextrous manipulation," *Proceedings of the 2004 IEEE International Conference on Robtics and Automation*, pp. 1239-1244, 2004. Available doi: 10.1109/ROBOT.2004.1307994

[24] M. Sekine, K. Kawamura and W. Yu, "Optimizing body thickness of watchband-type soft pneumatic actuator for feedback of prosthesis grasping force," *Biosystems and Biorobotics*, vol. 22, pp. 425-429, 2019. Available doi: 10.1007/978-3-030-01887-0_82

[25] J. Fras and K. Althoefer, "Soft Biomimetic Prosthetic Hand: Design, Manufacturing and Preliminary Examination," *2018 IEEE/RSJ International Conference on Intelligent Robots and Systems*, pp. 6998-7003, 2018. Available doi: 10.1109/IROS.2

[26] J. Fras and K. Althoefer, "Soft pneumatic prosthetic hand," *Lecture Notes in Computer Science*, vol. 10965, pp. 112-120, 2018. Available doi: 10.1007/978-3-319-96728-8_10

[27] K. Panayiotis, "3D Printed Soft Fluidic Actuator for an Assistive Hand Exoskeleton Device," M.S. thesis, 3mE, TU Delft, Netherlands, 2018.

[28] R. A. Bos et al., "A structured overview of trends and technologies used in dynamic hand orthoses," *Journal of NeuroEngineering and Rehabilitation*, vol. 13, pp. 1-25, 2016. Available doi: 10.1080/17483107.2016.1253117

[29] B. Smit, "Control of Pneumatic Soft Robotics. Design of a miniature 3D printed integrated valve, actuated by Shape Memory Alloy Wires," M.S. thesis, IDE, TU Delft, Netherlands, 2017.

[30] R. Scharff, "Soft Robotics: 3D-printing air pressure sensors and actuators," M.S. thesis, IDE, TU Delft, Netherlands, 2015.

[31] D. Van den Akker, "The development of a hybrid manufacturing system combining multimaterial 3D-printing and silicone casting, to create soft robotic parts," M.S. thesis, IDE, TU Delft, Netherlands, 2017.

[32] B. G. Gerberich, B. Mosadegh and G. M. Whitesides, "Portable prosthetic hand with soft pneumatic fingers," US2015351936A1, Dec. 10, 2015

[33] J. Belter, J. Segil, A. Dollar and R. Weir, "Mechanical design and performance specifications of anthropomorphic prosthetic hands: A review," *Journal of rehabilitation research and development*, vol. 50, no. 5, pp. 599-618, 2013. Available doi: 10.1682/JRRD.2011.10.0188

[34] D. Plettenburg, "Pneumatic actuators: A comparison of energy-to-mass ratio's," *Proceedings of the 2005 IEEE 9th International Conference on Rehabilitation Robotics*, pp. 545-549, 2005. Available doi: 10.1109/ICORR.2005.1502022

[35] A. P. Tjahyono, K. C. Aw, H. Devaraj, W. Surendra and E. Haemmerle, "A five-fingered hand exoskeleton driven by pneumatic artificial muscles with novel polypyrrole sensors," *Industrial Robot: An International Journal*, vol. 40, no. 3, pp. 251-260, 2013. Available doi: 10.1108/01439911311309951

[36] S. D. Prior, A. S. White, R. Gill, J. T. Parsons and P. R. Warner, "A novel pneumatic actuator," *Proceedings of IEEE Systems Man and Cybernetics Conference*, pp. 418-422, 1993. Available doi: 10.1109/ICSMC.1993.384779

[37] M. Ouerfelli, V. Kumar and W. Harwin, "An inexpensive pneumatic manipulator for rehabilitation robotics," *Proceedings IEEE International Conference on Robotics and Automation*, pp. 636-641, 1993. Available doi: 10.1109/ROBOT.1993.292050

[38] J. Szkopek and G. Redlarski, "Artificial-hand technology-current state of knowledge in designing and forecasting changes," *Applied Sciences*, vol. 9, no. 19, 2019. Available doi: 10.3390/app9194090

[39] Y. Honda, F. Miyazaki and A. Nishikawa, "Control of pneumatic five-fingered robot hand using antagonistic muscle ratio and antagonistic muscle activity," *Proceedings of the 2010 3rd IEEE RAS & EMBS International Conference on Biomedical Robotics and Biomechatronics*, pp. 337-342, 2010. Available doi: 10.1109/BIOROB.2010.5627770

[40] S. Ide and A. Nishikawa, "Bioinspired control of a multifingered robot hand with musculoskeletal system," *Smart Textiles and Their Applications*, pp. 185-195, 2016. Available doi: 10.1016/B978-0-08-100574-3.00010-2

[41] D. G. Caldwell and N. Tsagarakis, "Biomimetic actuators in prosthetic and rehabilitation applications," *Technology and Health Care*, vol. 10, no. 2, pp. 107-120, 2002. Available doi: 10.3233/THC-2002-10203

[42] M. Sekine, K. Kita and W. Yu, "Designing and testing lightweight shoulder prostheses with hybrid actuators for movements involved in typical activities of daily living and impact absorption," *Medical Devices: Evidence and Research*, vol. 8, pp. 279-294, 2015. Available doi: 10.2147/MDER.S83756

[43] N. Tsujiuchi, T. Koizumi, S. Shirai, T. Kudawara and Y. Ichikawa, "Development of a low pressure driven pneumatic actuator and its application to a robot hand," *IECON 2006 - 32nd Annual Conference on IEEE Industrial Electronics*, pp. 3040-3045, 2006. Available doi: 10.1109/IECON.2006.347883

[44] G. Bao, L. Zhang, Q. Yang and J. Ruan, "Development of flexible pneumatic spherical joint," *IEEE Conference on Robotics, Automation and Mechatronics*, pp. 381-384, 2004. Available doi: 10.1109/RAMECH.2004.1438949

[45] K. Kadota, M. Akai, K. Kawashima and T. Kagawa, "Development of Power-Assist Robot Arm using pneumatic rubber muscles with a balloon sensor," *The 18th IEEE International Symposium on Robot and Human Interactive Communication*, pp. 546-551, 2009. Available doi: 10.1109/ROMAN.2009.5326335

[46] H. Takeda, N. Tsujiuchi, T. Koizumi, H. Kan, M. Hirano and Y. Nakamura, "Development of prosthetic arm with pneumatic prosthetic hand and tendon-driven wrist," *31st Annual International Conference of the IEEE EMBS*, pp. 5048-5051, 2009. Available doi: 10.1109/IEMBS.2009.5333668

[47] B. Peerdeman, G. Smit, S. Stramigioli, D. Plettenburg and S. Misra, "Evaluation of pneumatic cylinder actuators for hand prostheses," *The Fourth IEEE RAS/EMBS International Conference on Biomedical Robotics and Biomechatronics*, pp. 1104-1109, 2012. Available doi: 10.1109/BioRob.2012.6290807

[48] M. V. Pawar, "Experimental Modelling of Pneumatic Artificial Muscle Systems Designing of Prosthetic Robotic Arm," *2018 3rd International Conference for Convergence in Technology*, 2018. Available doi: 10.1109/I2CT.2018.8529453

[49] M. De Volder, A. J. M. Moers and D. Reynaerts, "Fabrication and control of miniature McKibben actuators," *Sensors and Actuators A: Physical*, vol. 166, pp. 111-116, 2011. Available doi: 10.1016/j.sna.2011.01.002

[50] R. M. Robinson, C. S. Kothera, B. K. S. Woods, R. D. Vocke and N. M. Wereley, "High specific power actuators for robotic manipulators," *Journal of Intelligent Material Systems and Structures*, vol. 22, pp. 1501-1511, 2011. Available doi: 10.1177/1045389X11417653

[51] T. E. Pillsbury, R. M. Robinson and N. M. Wereley, "Miniaturized pneumatic artificial muscles actuating a bio-inspired robot hand," *Proceedings of the ASME 2013 Conference on Smart Materials, Adaptive Structures and Intelligent Systems*, 2013. Available doi: 10.1115/SMASIS2013-3262

[52] M. M. Gavrilovic and M. R. Maric, "Positional servo-mechanism activated by artificial muscles," *Medical and biological engineering*, vol. 7, no. 1, pp. 77-82, 1969. Available doi: 10.1007/BF02474672

[53] M. S. Sekine, K. Sugimori, T. V. J. Tarvainen and W. Yu, "Prototyping a parallel link arm driven by small pneumatic actuator for shoulder prostheses," *Proceedings of the 2012 IEEE International Conference on Robotics and Biomimetics*, pp. 1391-1396, 2012. Available doi: 10.1109/ROBIO.2012.6491163

[54] S. Krishnan, T. Nagarajan, A. M. A. Rani and T. V. V. L. N. Rao, "Silk Pneumatic Artificial Muscle (SPAM) construction for bio-medical engineering application," *2012 IEEE Business, Engineering and Industrial Applications Colloquium*, pp. 302-306, 2012. Available doi: 10.1109/beiac.2012.6226071

[55] M. Iwaki, Y. Hasegawa and Y. Sankai, "Study on wearable system for daily life support using McKibben pneumatic artificial muscle," *The 2010 IEEE/RSJ International Conference on Intelligent Robots and Systems*, pp. 3670-3675, 2010. Available doi: 10.1109/IROS.2010.5649881

[56] A. Polhemus, B. Doherty, K. Mackiw, R. Patel and M. Paliwal, "UGrip II: A novel functional hybrid prosthetic hand design," *2013 39th Annual*

*Northeast Bioengineering Conference*, pp. 303-304, 2013. Available doi: 10.1109/NEBEC.2013.148

[57] A. E. Comer, "Pneumatic muscle analogs for exoskeletal robotic limbs and associated control mechanisms," US2003018388A1, Jan. 23, 2003

[58] D. H. Plettenburg, "A myoelectrically-controlled, pneumatically-powered hand prosthesis for children," *Journal of Rehabilitation Research and Development*, vol. 28, no. 1, p. 21, 1990.

[59] H. J. B. Witteveen, "Tactile feedback for myoelectric forearm prostheses," Ph.D. dissertation, MIRA, University of Twente, Netherlands, 2014.

[60] E. I. Vorob'ev, A. V. Mikheev, and K. O. Morgunenko, "A Model Hand Prosthesis Controlled by Foot and Toe Movements," *Biomedical Engineering*, vol. 51, no. 2, pp. 142-146, 2016. Available doi: 10.1007/s10527-017-9702-y

[61] K. B. Fite, T. J. Withrow, X. Shen, K. W. Wait, J. E. Mitchell and M. Goldfarb, "A gas-actuated anthropomorphic prosthesis for transhumeral amputees," *IEEE Transaction on Robotics*, vol. 24, no. 1, pp. 159-169, 2008. Available doi: 10.1109/TRO.2007.914845

[62] K. B. Fite, T. J. Withrow, K. W. Wait, J. E. Mitchell and M. Goldfarb, "Liquid-fueled actuation for an anthropomorphic upper extremity prosthesis," *Proceedings of the 28th IEEE EMBS Annual International Conference*, pp. 5638-5642, 2006. Available doi: 10.1109/IEMBS.2006.259638

[63] K. B. Fite, T. J. Withrow, X. Shen, K. W. Wait, J. E. Mitchell and M. Goldfarb, "Progress towards the development of a highly functional anthropomorphic transhumeral prosthesis," *Proceedings of the 2007 IEEE 10th International Conference on Rehabilitation Robotics*, pp. 205-211, 2007. Available doi: 10.1109/ICORR.2007.4428428

[64] R. M. Crowder and D. R. Whatley, "Robotic gripping device having linkage actuated finger sections," US4834443A, May 30, 1989

[65] J. F. D. Marsh and R. D. McLeish, "A Self-Contained Hydraulic Power Source for Artificial Upper Limbs," *IEEE Transactions on Biomedical Engineering*, vol. BME-22, no. 4, pp. 322-326, 1975. Available doi: 10.1109/TBME.1975.324452

[66] K. R. Kim, S. H. Jeong, P. Kim and K. S. Kim, "Design of Robot Hand with Pneumatic Dual-Mode Actuation Mechanism Powered by Chemical Gas Generation Method," *IEEE Robotics and Automation Letters*, vol. 3, no. 4, pp. 4193-4200, 2018. Available doi: 10.1109/LRA.2018.2853763

[67] J. Ten Kate, G. Smit and P. Breedveld, "3D-printed upper limb prostheses: a review," *Assistive Technology*, vol. 12, no. 3, pp. 300-314, 2017. Available doi: 10.1080/17483107.2016.1253117

[68] D. H. Plettenburg, "A sizzling hand prosthesis. On the design and development of a pneumatically powered hand prosthesis for children," Ph.D. dissertation, 3mE, TU Delft, Netherlands, 2002.

[69] F. G. E. Verga, "Exergy saving pneumatically actuated autonomous systems," M.S. thesis, 3mE, TU Delft, Netherlands, 2016.

[70] D. Schelvis, "Increased Pinch Force of Body Powered Prosthetic Hand with Pneumatic Force Servo," M.S. thesis, 3mE, TU Delft, Netherlands, 2018.

[71] D. C. Doedens, "Optimal CO2 pressure for a pneumatic system," M.S. thesis, 3mE, TU Delft, Netherlands, 2015.

[72] J. Rob, "Ultralight Pressure Regulator for Application in Pneumatic Prostheses," M.S. thesis, 3mE, TU Delft, Netherlands, 2012.

[73] G. Puchhammer, "Hand prosthesis comprising two drive devices," US2008262634A1, Oct. 23, 2008

[74] G. Puchhammer, "Hand prosthesis and force transmission device," US2008319553A1, Dec. 25, 2008

[75] R. R. Dehoff, R. F. Lind, L. L. Love, W. H. Peter and B. S. Richardson, "Freeform fluidics," US2013331949A1, Dec. 12, 2013

[76] P. Ferrara et al., "Artificial finger," US10426636B2, Oct. 1, 2019

[77] F. Wijsman, "The Design of a Glove Compensated Hand Prosthesis," M.S. thesis, 3mE, TU Delft, Netherlands, 2010.

[78] N. Omarkulov, K. Telegenov, M. Zeinullin, A. Begalinov and A. Shintemirov, "Design of an anthropomorphic upper extremity prosthesis," *2015 37th Annual International Conference of the IEEE Engineering in Medicine and Biology Society*, pp. 2474-2477, 2015. Available doi: 10.1109/EMBC.2015.7318895

[79] M. W. M. Groenewegen, "Design of a Compliant, Multi-Phalanx Underactuated Prosthetic Finger," M.S. thesis, 3mE, TU Delft, Netherlands, 2014.

[80] J. S. Cuellar, G. Smit, P. Breedveld, A. A. Zadpoor and D. H. Plettenburg, "Functional evaluation of a non-assembly 3D-printed hand prosthesis," *Journal of engineering in medicine*, vol. 233, no. 11, pp. 1122-1131, 2019. Available doi: 10.1080/17483107.2016.1253117

[81] W. Y. Wang, "Explore Meaningful Applications for Self-healing Polymers through Additive Manufacturing," M.S. thesis, IDE, TU Delft, Netherlands, 2017.

[82] M. Moreo, "Parametric design of a 3D printable hand prosthesis for children in developing countries," M.S. thesis, 3mE, TU Delft, Netherlands, 2016.

[83] J. S. Cuellar, G. Smit, A. A. Zadpoor and P. Breedveld, "Ten guidelines for the design of non-assembly mechanisms," *Journal of Engineering in Medicine*, vol. 232, no. 9, pp. 962-971, 2018. Available doi: 10.1080/17483107.2016.1253117

[84] W. Jopek, M. Kucharski, M. Turow and M. Wasielewski, "Modular human hand prosthesis with modular, mechanically independent finger modules," US2013030550A1, Jan. 31, 2013

[85] A. Armienta Meza, O. E. Cazares Almaral, R. I. Esparza Gutiérrez and J. M. Herrera Hernández, "Modular prosthetic arm system," WO2019083349A1, May 2, 2019

# B

# Matlab code

## B.1. Concept Calculation

```
clear all
close all
clc

% Phalange length
AB = 45; %[mm]
BC = 20; %[mm]
CD = 20; %[mm]

% Pneumatic pressure
p = 1.2; %[MPa]

% Density CO2 at 1.2 MPa and 20 deg. Celcius
rho = 0.023200449229673584; %[mg/mm^3]

% Store concept values
ncycls = [];
Fds = [];


% Concept 1
% Pneumatic cylinder
d = 7; %[mm] diameter
L = 7; %[mm] length
n = 7; % number of cylinders in hand

% Derived from cylinder
Fcyl = 0.25*p*pi*d^2; %[N] force in cylinder
mco2 = 0.25*rho*pi*d^2*L; %[mg] gas used for filling whole cylinder
mco2t = n*mco2; %[mg] total co2 used per grasp
ncycl = 12*1000/mco2t; % total number of grasps on one cartridge
ncycls = [ncycls ncycl];

% Solve forces
Fd = Fcyl*3/4;
Fds = [Fds Fd];


%Concept 2
% Pneumatic cylinder
d = 7; %[mm] diameter
L = 7; %[mm] length
n = 4; % number of cylinders in hand

% Derived from cylinder
Fcyl = 0.25*p*pi*d^2; %[N] force in cylinder
mco2 = 0.25*rho*pi*d^2*L; %[mg] gas used for filling whole cylinder
mco2t = n*mco2; %[mg] total co2 used per grasp
ncycl = 12*1000/mco2t; % total number of grasps on one cartridge
ncycls = [ncycls ncycl];

% Solve forces
```

```
Fd = Fcyl/4;
Fds = [Fds Fd];


% Concept 3
% Concept rejected due to gear and band friction
ncycl = 0; % total number of grasps on one cartridge
ncycls = [ncycls ncycl];
Fd = 0;
Fds = [Fds Fd];


% Concept 4
% Pneumatic cylinder
d = 7; %[mm] diameter
L = 7; %[mm] length
n = 4; % number of cylinders in hand

% Derived from cylinder
Fcyl = 0.25*p*pi*d^2; %[N] force in cylinder
mco2 = 0.25*rho*pi*d^2*L; %[mg] gas used for filling whole cylinder
mco2t = n*mco2; %[mg] total co2 used per grasp
ncycl = 12*1000/mco2t; % total number of grasps on one cartridge
ncycls = [ncycls ncycl];

% Solve forces
Fd = Fcyl/8.5;
Fds = [Fds Fd];


% Concept 5
% Pneumatic cylinder
d = 7; %[mm] diameter
L = 6; %[mm] length
n = 7; % number of cylinders in hand

% Derived from cylinder
Fcyl = 0.25*p*pi*d^2; %[N] force in cylinder
mco2 = 0.25*rho*pi*d^2*L; %[mg] gas used for filling whole cylinder
mco2t = n*mco2; %[mg] total co2 used per grasp
ncycl = 12*1000/mco2t; % total number of grasps on one cartridge
ncycls = [ncycls ncycl];

% Solve forces
Fd = Fcyl*(1/4 + 1/(2*sqrt(5)));
Fds = [Fds Fd];


% Concept 6/7
% Pneumatic cylinder
d = 7; %[mm] diameter
L = 7; %[mm] length
n = 7; % number of cylinders in hand
```

```
% Derived from cylinder
Fcyl = 0.25*p*pi*d^2; %[N] force in cylinder
mco2 = 0.25*rho*pi*d^2*L; %[mg] gas used for filling whole cylinder
mco2t = n*mco2; %[mg] total co2 used per grasp
ncycl = 12*1000/mco2t; % total number of grasps on one cartridge
ncycls = [ncycls ncycl];
ncycls = [ncycls ncycl];

% Solve forces
Fd = Fcyl*(1/4 + 1/8.5);
Fds = [Fds Fd];
Fds = [Fds Fd];


% Concept 8
% Pneumatic cylinder
d = 7; %[mm] diameter
L = 7; %[mm] length
n = 11; % number of cylinders in hand

% Derived from cylinder
Fcyl = 0.25*p*pi*d^2; %[N] force in cylinder
mco2 = 0.25*rho*pi*d^2*L; %[mg] gas used for filling whole cylinder
mco2t = n*mco2; %[mg] total co2 used per grasp
ncycl = 12*1000/mco2t; % total number of grasps on one cartridge
ncycls = [ncycls ncycl];

% Solve forces
Fd = Fcyl*(1/2 + 1/4 + 1/8.5);
Fds = [Fds Fd];

% Plot normalized and combined results
Fdsn = Fds/norm(Fds);
ncyclsn = ncycls/norm(ncycls);
figure
bar([Fdsn.',ncyclsn.'])
title("Normalized concept performance")
xlabel("Concept number")
ylabel("Normalized performance")
legend("Tip force","Grasping cycles")

figure
bar(Fdsn+ncyclsn)
title("Combined concept performance")
xlabel("Concept number")
ylabel("Combined performance")
```

*Published with MATLAB® R2020a*

## B.2. Advanced Calculation

```
clear all
close all
clc

global AB BC CD h1 h2 p k

AB = 60; % [mm]
BC = 40; % [mm]
CD = 30; % [mm]

h1 = 15; % [mm]
h2 = 10; % [mm]

p = 1.2; % [MPa]

k = 0.2; % [N/mm] pen spring

% Density CO2 at 1.2 MPa and 20 deg. Celcius
rho = 0.023200449229673584; %[mg/mm^3]

% Start lengths
EF0 = AB - h1;
EG0 = sqrt(AB^2 + (h1-h2)^2);
GH0 = BC - h2;
GI0 = BC;

% Elongation cylinder 1
b = 0;
EFs = [];
EGs = [];
as = [];

for a = 0:0.01:pi/2
    coord = coordinates(a,b);
    dxef = coord(6,1)-coord(5,1);
    dyef = coord(6,2)-coord(5,2);
    EF = sqrt(dxef^2 + dyef^2)-EF0;
    EFs = [EFs, EF];

    dxeg = coord(7,1)-coord(5,1);
    dyeg = coord(7,2)-coord(5,2);
    EG = sqrt(dxeg^2 + dyeg^2)-EG0;
    EGs = [EGs, EG];

    as = [as, a];
end
% figure
% plot(as, EFs)
% title("Elongation cylinder 1")
% xlabel("alpha [rad]")
% ylabel("length [mm]")
%
```

```
% figure
% plot(as, EGs)
% title("Elongation spring 1")
% xlabel("alpha [rad]")
% ylabel("length [mm]")

% Elongation cylinder 2
a = 0;
GHs = [];
GIs = [];
bs = [];

for b = 0:0.01:pi/2
    coord = coordinates(a,b);
    dxgh = coord(8,1)-coord(7,1);
    dygh = coord(8,2)-coord(7,2);
    GH = sqrt(dxgh^2 + dygh^2)-GH0;
    GHs = [GHs, GH];

    dxgi = coord(9,1)-coord(7,1);
    dygi = coord(9,2)-coord(7,2);
    GI = sqrt(dxgi^2 + dygi^2)-GI0;
    GIs = [GIs, GI];

    bs = [bs, b];
end
% figure
% plot(bs, GHs)
% title("Elongation cylinder 2")
% xlabel("beta [rad]")
% ylabel("length [mm]")
%
% figure
% plot(bs, GIs)
% title("Elongation spring 2")
% xlabel("beta [rad]")
% ylabel("length [mm]")

max_cyl1 = max(EFs);
max_cyl2 = max(GHs);
max_sp1 = max(EGs);
max_sp2 = max(GIs);

a = 0;
b = 0;
d1 = 10;
d2 = 7;

vars = ["Fc1";"Fc2";"Fc3";"Fc4";"Fc5";"Fc6";"Fc7";"Fc8";...
    "Fs1";"Fs2";"Fs3";"Fs4";"Fs5";"Fs6";"Fs7";"Fs8";...
    "FAx";"FAy";"FBx";"FBy";"FCx";"FCy";"FDy";"MA";"FM"];%;"FM"];

units = ["N";"N";"N";"N";"N";"N";"N";"N";"N";"N";"N";...
    "N";"N";"N";"N";"N";"N";"N";"N";"N";"N";"N";...
```

```
    "Nmm";"N"];

Fdss = [];
Fmss = [];
as = [];
for a = 0:pi/32:pi/2
    Fds = [];
    Fms = [];
    as = [as;a];
    bs = [];
    for b = 0:pi/32:pi/2
        Y = force_eqn_solver(a, b, d1, d2);
        Fds = [Fds,Y(23)];
        Fms = [Fms,Y(25)];
        bs = [bs,b];
    end
    Fdss = [Fdss;Fds];
    Fmss = [Fmss;Fms];
end

figure
surf(bs,as,Fdss)
title("Tip force [N]")
xlabel("beta [rad]")
ylabel("alpha [rad]")
zlabel("F_{D,y} [N]")

figure
surf(bs,as,Fmss)
title("Middle phalange force [N]")
xlabel("beta [rad]")
ylabel("alpha [rad]")
zlabel("F_{M,y} [N]")

max_spf1 = k*max_sp1;
max_spf2 = k*max_sp2;

p1 = max_spf1/(0.25*pi*d1^2);
p2 = max_spf2/(0.25*pi*d2^2);

rho1 = 0.0005244330531298777; % [mg/mm^3]
rho2 = 0.0010341224677548285; % [mg/mm^3]

gas_usage_maxf = (0.25*pi*d1^2*max_cyl1+0.25*pi*d2^2*max_cyl2)*rho; %
 [mg]
gas_usage_minf =
 (0.25*pi*d1^2*max_cyl1)*rho1+(0.25*pi*d2^2*max_cyl2)*rho2; % [mg]
ncycles_maxf = 12*1000/(4*gas_usage_maxf) % Cycles maximum stroke,
 maximum force
ncycles_minf = 12*1000/(4*gas_usage_minf) % Cycles maximum stroke,
 maximum force
```

*Published with MATLAB® R2018b*

## B.3. Advanced Dual-Mode Calculation

# Table of Contents



```
clear all
close all
clc

global AB BC CD h1 h2 p k

AB = 45; % [mm]
BC = 40; % [mm]
CD = 30; % [mm]

h1 = 10; % [mm]
h2 = 8; % [mm]

p = 1.2; % [MPa]

k = 0.2; % [N/mm] pen spring

% Density CO2 at 1.2 MPa and 20 deg. Celcius
rho = 0.023200449229673584; %[mg/mm^3]

% Start lengths
EF0 = AB - h1;
EG0 = sqrt(AB^2 + (h1-h2)^2);
GH0 = BC - h2;
GI0 = BC;

% Elongation cylinder 1
b = 0;
EFs = [];
EGs = [];
as = [];

for a = 0:0.01:pi/2
    coord = coordinates(a,b);
    dxef = coord(6,1)-coord(5,1);
    dyef = coord(6,2)-coord(5,2);
    EF = sqrt(dxef^2 + dyef^2)-EF0;
    EFs = [EFs, EF];

    dxeg = coord(7,1)-coord(5,1);
    dyeg = coord(7,2)-coord(5,2);
    EG = sqrt(dxeg^2 + dyeg^2)-EG0;
    EGs = [EGs, EG];
```

```
    as = [as, a];
end

% Elongation cylinder 2
a = 0;
GHs = [];
GIs = [];
bs = [];

for b = 0:0.01:pi/2
    coord = coordinates(a,b);
    dxgh = coord(8,1)-coord(7,1);
    dygh = coord(8,2)-coord(7,2);
    GH = sqrt(dxgh^2 + dygh^2)-GH0;
    GHs = [GHs, GH];

    dxgi = coord(9,1)-coord(7,1);
    dygi = coord(9,2)-coord(7,2);
    GI = sqrt(dxgi^2 + dygi^2)-GI0;
    GIs = [GIs, GI];

    bs = [bs, b];
end

max_cyl1 = max(EFs);
max_cyl2 = max(GHs);
max_sp1 = max(EGs);
max_sp2 = max(GIs);

a = 0;
b = 0;
d1 = 10;
d2 = 7;

vars = ["Fc1";"Fc2";"Fc3";"Fc4";"Fc5";"Fc6";"Fc7";"Fc8";...
    "Fs1";"Fs2";"Fs3";"Fs4";"Fs5";"Fs6";"Fs7";"Fs8";...
    "FAx";"FAy";"FBx";"FBy";"FCx";"FCy";"FDy";"MA";"FM"];%;"FM"];

units = ["N";"N";"N";"N";"N";"N";"N";"N";"N";"N";"N";...
    "N";"N";"N";"N";"N";"N";"N";"N";"N";"N";"N";...
    "Nmm";"N"];

clc

d3 = 25; % [mm] palm cylinder max diameter

max_spf1 = k*max_sp1;
max_spf2 = k*max_sp2;
max_cyl1 = max(EFs);
max_cyl2 = max(GHs);

p1 = max_spf1/(0.25*pi*d1^2);
p2 = max_spf2/(0.25*pi*d2^2);
```

```
p_min = max(p1,p2);

V1 = 0.25*pi*d1^2*max_cyl1;
V2 = 0.25*pi*d2^2*max_cyl2;
V_tot = 4*(V1+V2);

A_hs = 0.25*pi*d3^2;
L_hs = V_tot/A_hs;

d_hs_co2 = 25; % [mm]
A_hs_co2 = 0.25*pi*d_hs_co2^2;
V_hs_co2 = A_hs_co2*L_hs;

p_hs_co2 = p_min*A_hs/A_hs_co2; % [MPa]

rho_p_min = 0.0010341224677548285; % density co2 at 0.0571 MPa and 20
 celcius.

m1 = rho_p_min*V_hs_co2; % [mg]

L_f = 0.3; % [mm] force stroke cylinders
L_hf = 1;
V_tot_f = 4*0.25*pi*(d1^2+d2^2)*L_f;
A_hf = V_tot_f/L_hf;
d_hf = sqrt(A_hf/(0.25*pi));

p_max = p*A_hs_co2/A_hf;

m2 = rho*L_hf*A_hs_co2;

% Calculate minimum wall thickness
sigma_y = 350; % [MPa] yield strength AISI 1020 Steel
t1 = p_max*(d1/2)/sigma_y;
t2 = p_max*(d2/2)/sigma_y;

p = p_max;

Fdss = [];
Fmss = [];
as = [];
for a = 0:pi/32:pi/2
    Fds = [];
    Fms = [];
    as = [as;a];
    bs = [];
    for b = 0:pi/32:pi/2
        Y = force_eqn_solver(a, b, d1, d2);
        Fds = [Fds,Y(23)];
        Fms = [Fms,Y(25)];
        bs = [bs,b];
    end
    Fdss = [Fdss;Fds];
    Fmss = [Fmss;Fms];
end
```

```
figure
surf(bs,as,Fdss)
title("Tip force [N]")
xlabel("beta [rad]")
ylabel("alpha [rad]")
zlabel("F_{D,y} [N]")

figure
surf(bs,as,Fmss)
title("Middle phalange force [N]")
xlabel("beta [rad]")
ylabel("alpha [rad]")
zlabel("F_{M,y} [N]")
```

# Reaction forces

```
Fs = [];

a = 0;
b = a;
Y = force_eqn_solver(a, b, d1, d2);
Fs = [Fs;Y];
```

# Calculate lock

```
clc

dl = 10; % [mm]
Ll = 8.2; % [mm]
Vl = 0.25*pi*dl^2*Ll;
ml = rho_p_min*Vl; % [mg]
```

# Calculate regulator

```
clc

d_reg = 8; % [mm]
L_reg = 12; % [mm]
A_reg = 0.25*pi*d_reg^2;
V_reg = A_reg*L_reg;
mr = rho*V_reg;
mtot = m1+m2+ml+mr; % [mg]
cycles = 16*1000/mtot

% Springs
N_pre = p_min*A_reg;
k1 = 0.1; % [N\mm]
ks = 2*k1; % [N\mm]
L_pre = N_pre/ks % [mm]
L_step = 6; % [mm]
p_step1 = (N_pre+ks*L_step)/A_reg
```

```
p_step2 = (N_pre+2*ks*L_step)/A_reg
L_min = L_pre+2*L_step
```

*Published with MATLAB® R2018b*

## B.4. Coordinates

```
function coord = coordinates(a,b)
global AB BC CD h1 h2

A = [0, 0];
B = [AB, 0];
C = B + [BC*cos(a), -BC*sin(a)];
D = C + [CD*cos(a+b), -CD*sin(a+b)];
E = [0, h1];
g = B + [h1*sin(a), h1*cos(a)];
F = g + [-h1*cos(a), h1*sin(a)];
G = B + [h2*sin(a), h2*cos(a)];
I = C + [h2*sin(a+b), h2*cos(a+b)];
H = I + [-h2*cos(a+b), h2*sin(a+b)];

coord = [A;B;C;D;E;F;G;H;I];
end
```

*Published with MATLAB® R2018b*

## B.5. Spring force equations

```
function F = sp_force_eqn(x, a, b)
global AB BC h1 h2 k

% Get coordinates
coord = coordinates(a,b);

dyeg = coord(7,2) - coord(5,2);
dxeg = coord(7,1) - coord(5,1);

dygi = coord(9,2) - coord(7,2);
dxgi = coord(9,1) - coord(7,1);

dxgia = dxgi*cos(a) - dygi*sin(a);
dygia = -dxgi*sin(a) - dygi*cos(a);

% Spring forces
Fs1 = abs(x(1)); Fs2 = -abs(x(2)); Fs3 = abs(x(3)); Fs4 = x(4);
Fs5 = abs(x(5)); Fs6 = -abs(x(6)); Fs7 = abs(x(7)); Fs8 = abs(x(8));

F(1) = Fs1^2 + Fs2^2 - (Fs3^2 + Fs4^2);
F(2) = Fs5^2 + Fs6^2 - (Fs7^2 + Fs8^2);
F(3) = (Fs3*cos(a) + Fs4*sin(a))*dyeg - ((Fs4*cos(a) -
 Fs3*sin(a))*dxeg);
F(4) = -(Fs7*cos(b) + Fs8*sin(b))*dygia - ((Fs8*cos(b) -
 Fs7*sin(b))*dxgia);

% Force directions
F(5) = Fs2*dxeg - (dyeg*Fs1);
F(6) = -Fs6*dxgia - (dygia*Fs5);

% Spring force equations
EG0 = sqrt(AB^2 + (h1-h2)^2);
GI0 = BC;
EG = sqrt(dxeg^2 + dyeg^2);
GI = sqrt(dxgi^2 + dygi^2);
dEG = EG - EG0;
dGI = GI - GI0;
F(7) = sqrt(Fs1^2 + Fs2^2) - k*dEG;
F(8) = sqrt(Fs5^2 + Fs6^2) - k*dGI;
end
```

*Published with MATLAB® R2018b*

## B.6. Cylinder force equations

```
function F = cyl_force_eqn(x, a, b, d1, d2)
global p

% Get coordinates
coord = coordinates(a,b);

dyef = coord(6,2) - coord(5,2);
dxef = coord(6,1) - coord(5,1);

dygh = coord(8,2) - coord(7,2);
dxgh = coord(8,1) - coord(7,1);

dxgha = dxgh*cos(a) - dygh*sin(a);
dygha = dxgh*sin(a) + dygh*cos(a);

dygi = coord(9,2) - coord(7,2);
dxgi = coord(9,1) - coord(7,1);

% declare variables
% Cylinder forces
Fc1 = -abs(x(1)); Fc2 = -abs(x(2)); Fc3 = -abs(x(3)); Fc4 = -
abs(x(4));
Fc5 = -abs(x(5)); Fc6 = -abs(x(6)); Fc7 = -abs(x(7)); Fc8 = -
abs(x(8));

% Cylinder force equations
F(1) = 4*sqrt(Fc1^2 + Fc2^2) - (p*pi*d1^2);
F(2) = 4*sqrt(Fc5^2 + Fc6^2) - (p*pi*d2^2);

% Force relations
F(3) = Fc1^2 + Fc2^2 - (Fc3^2 + Fc4^2);
F(4) = Fc5^2 + Fc6^2 - (Fc7^2 + Fc8^2);
F(5) = (Fc3*cos(a) + Fc4*sin(a))*dyef - ((Fc4*cos(a) -
 Fc3*sin(a))*dxef);
F(6) = (Fc7*cos(b) + Fc8*sin(b))*dygha - ((Fc8*cos(b) -
 Fc7*sin(b))*dxgha);

% Force directions
F(7) = Fc2*dxef - (dyef*Fc1);
F(8) = Fc6*dxgha - (dygha*Fc5);
end
```

*Published with MATLAB® R2018b*

## B.7. FBD force equations

```
function F = force_eqn(x, a, b, Fcyl, Fsp)
global AB BC CD h1 h2

% declare variables
% Joint forces
FAx = x(1); FAy = x(2); FBx = x(3); FBy = x(4); FCx = x(5);
FCy = x(6); FDy = abs(x(7)); MA = x(8);FM = abs(x(9));% FM =
 abs(x(9));
% Cylinder forces
Fc1 = Fcyl(1); Fc2 = Fcyl(2); Fc3 = Fcyl(3); Fc4 = Fcyl(4);
Fc5 = Fcyl(5); Fc6 = Fcyl(6); Fc7 = Fcyl(7); Fc8 = Fcyl(8);
% Spring forces
Fs1 = Fsp(1); Fs2 = Fsp(2); Fs3 = Fsp(3); Fs4 = Fsp(4);
Fs5 = Fsp(5); Fs6 = Fsp(6); Fs7 = Fsp(7); Fs8 = Fsp(8);

% Force and moment equilibrium equations
F(1) = FAx + Fc1 + Fs1 + FBx;
F(2) = FAy + Fc2 + Fs2 + FBy;
F(3) = MA + AB*FBy - (h1*(Fc1 + Fs1));

F(4) = Fc5 + Fs5 + FBy*sin(a) + FCx - (Fc3 + Fs3 + FBx*cos(a));
F(5) = Fc6 + Fs6 + FCy + FM - (Fc4 + Fs4 + FBx*sin(a) + FBy*cos(a)); %
  + FM
F(6) = h2*(Fc5 + Fs5) - (h2*Fs3 + h1*(Fc3 + Fc4) + BC*FCy +
 0.5*BC*FM); % + 0.5*BC*FM

F(7) = FCy*sin(b) - (Fc7 + Fs7 + FCx*cos(b));
F(8) = FDy - (Fc8 + Fs8 + FCy*cos(b) + FCx*sin(b));
F(9) = CD*FDy + h2*(Fc7 + Fs7 + Fc8);
end
```

*Published with MATLAB® R2018b*

## B.8. Force equations solver

```
function Y = force_eqn_solver(a, b, d1, d2)
fun1 = @(x) cyl_force_eqn(x, a, b, d1, d2);
fun2 = @(x) sp_force_eqn(x, a, b);
x01 = [30,30,30,30,30,30,30,30];
x02 = [2,2,2,2,2,2,2,2];
options=optimset('TolX', 1E-10, 'MaxIter', 100000, 'MaxFunEvals',
 100000);
Fcyl = fsolve(fun1,x01,options); % Solve cylinder
Fsp =  fsolve(fun2,x02,options); % Solve spring

% Correct signs cylinder
Y(1) = -abs(Fcyl(1)); Y(2) = -abs(Fcyl(2)); Y(3) = -abs(Fcyl(3));
Y(4) = -abs(Fcyl(4)); Y(5) = -abs(Fcyl(5)); Y(6) = -abs(Fcyl(6));
Y(7) = -abs(Fcyl(7)); Y(8) = -abs(Fcyl(8));
% Correct signs spring
Y(9) = abs(Fsp(1)); Y(10) = -abs(Fsp(2)); Y(11) = abs(Fsp(3));
Y(12) = Fsp(4); Y(13) = abs(Fsp(5)); Y(14) = -abs(Fsp(6));
Y(15) = abs(Fsp(7)); Y(16) = abs(Fsp(8));

fun3 = @(x) force_eqn(x, a, b, Y(1:8), Y(9:16));
x03 = [1,1,1,1,1,1,1,1,1,1];
Fr = fsolve(fun3,x03,options); % Solve reaction/external forces

% Correct signs reaction/external
Y(17) = Fr(1); Y(18) = Fr(2); Y(19) = Fr(3); Y(20) = Fr(4);
Y(21) = Fr(5); Y(22) = Fr(6); Y(23) = abs(Fr(7)); Y(24) = Fr(8);
Y(25) = abs(Fr(9));
end
```

*Published with MATLAB® R2018b*

## B.9. O-ring calculator

```
d1 = 2;
d2 = 4;

d3 = 4.7;
d4 = 8;

syms b

t = (d4-d3)/2;

R0 = d2/2+d1/2;

V0 = 2*(pi^2)*R0*(d1/2)^2;

R1 = d3/2+t/2;

V1 = pi*((d4/2))^2*b - pi*(d3/2)^2*b + 2*pi^2*R1*(t/2)^2;

b1 = double(solve(V1==V0))
```

*Published with MATLAB® R2018b*

# B.10. High force measurement

```
clear all
close all
clc

press1 = [0;1;2;3;4;5.2;6.3;7.3;8;10;12];
press2 = [2;2.5;2.5;3.3;4;5.2;6.3;7;7.5;10;12];

figure
plot(press1,press2,'r*-')
hold on
plot(press1,press1,'b-')
axis([0 12 0 17],'square')
title('Supply pressure vs. outlet pressure')
xlabel('Pneumatic supply pressure [bar]')
ylabel('Hydraulic outlet pressure [bar]')
legend('Measurements', 'Theoretical')
```

*Published with MATLAB® R2018b*

## B.11. Full system measurement

```
clear all
close all
clc

press1 = [0;0.5;1;1.5;2;2.5;3;3.5];
press2 = [1.5;3;3.5;4;4.8;14.8;16;17.3;];

a = polyfit(press1(2:5),press2(2:5),1);
b = polyfit(press1(6:8),press2(6:8),1);

press3 = a(1)*press1+a(2);
press4 = b(1)*press1+b(2);

figure
plot(press1,press2,'r*-')
hold on
plot(press1,press3,'b--')
hold on
plot(press1,press4,'g--')
axis([0 4 0 18],'square')
title('Supply pressure vs. outlet pressure')
xlabel('Pneumatic supply pressure [bar]')
ylabel('Hydraulic outlet pressure [bar]')
legend('Measured', 'Regression low', 'Regression
 high', 'Location', 'northwest')

maxp = b(1)*12 + b(2);
```

*Published with MATLAB® R2018b*

# C

# Technical drawings

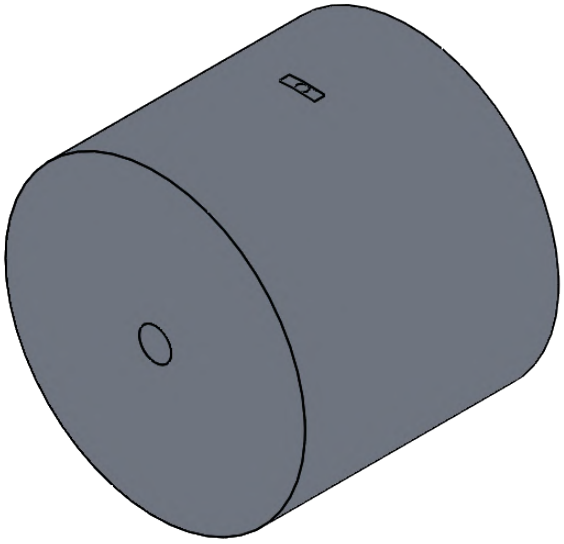

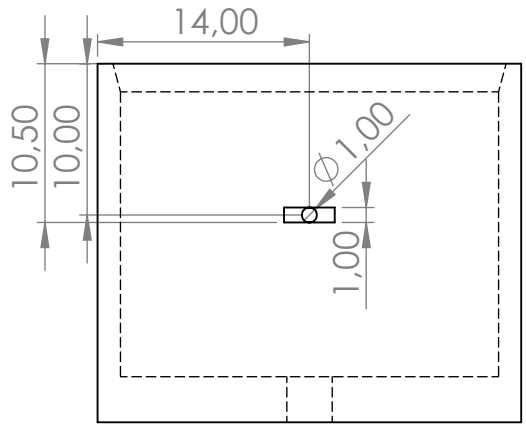


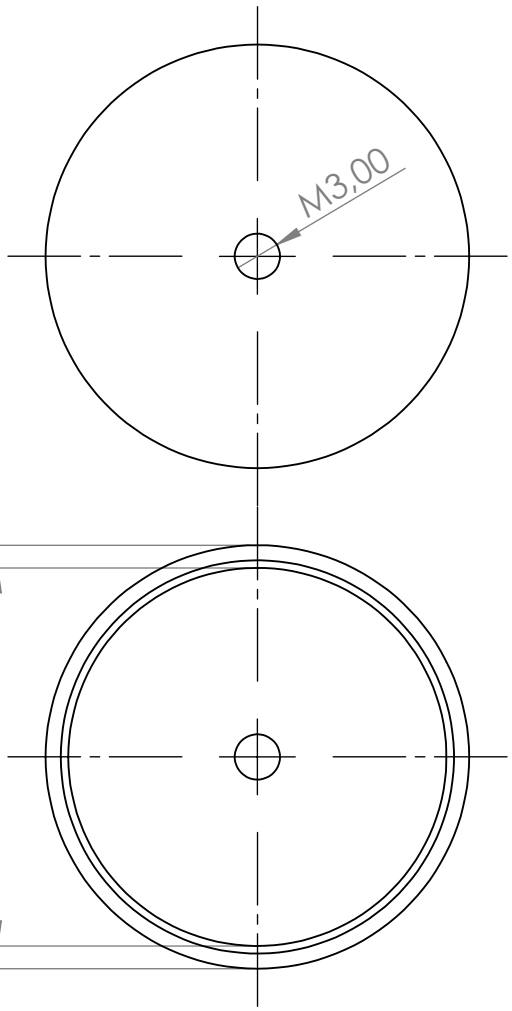


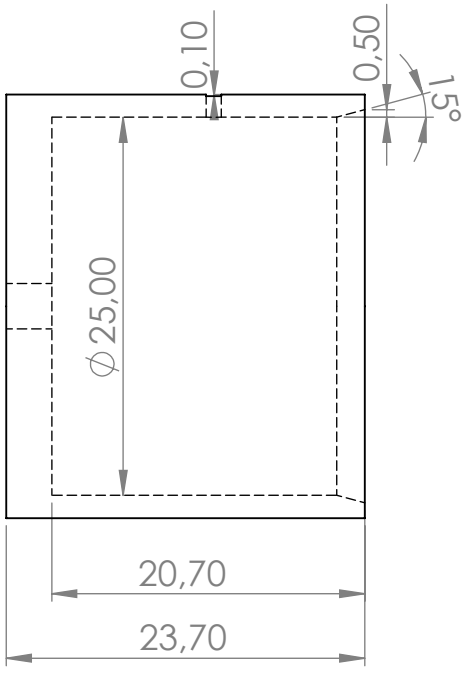


DO NOT SCALE DRAWING

AUTHOR: Ad Hoek 4445058

TITLE: Cylinder_HF_cap_co2

MATERIAL: 7075-T6

A4

SCALE: 2:1

SHEET 1 OF 1

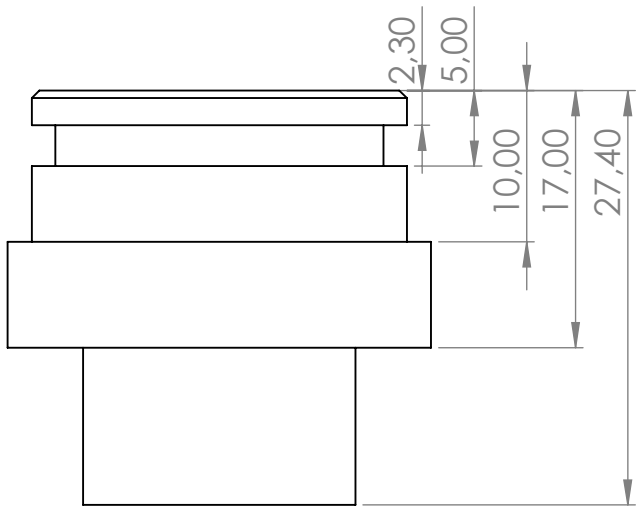


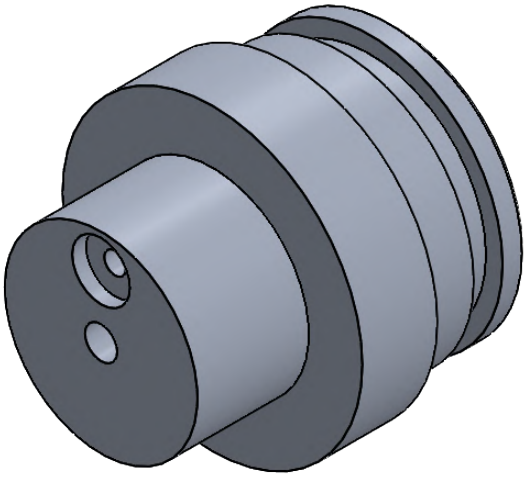

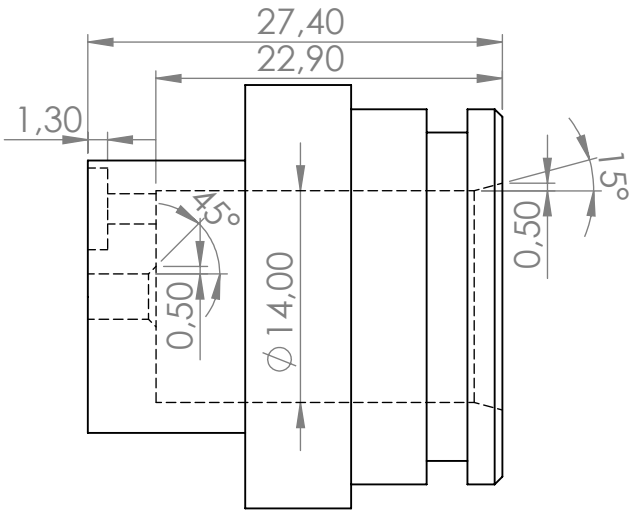


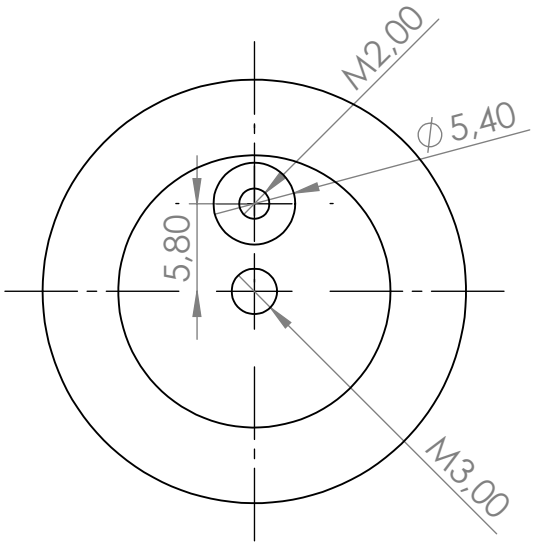


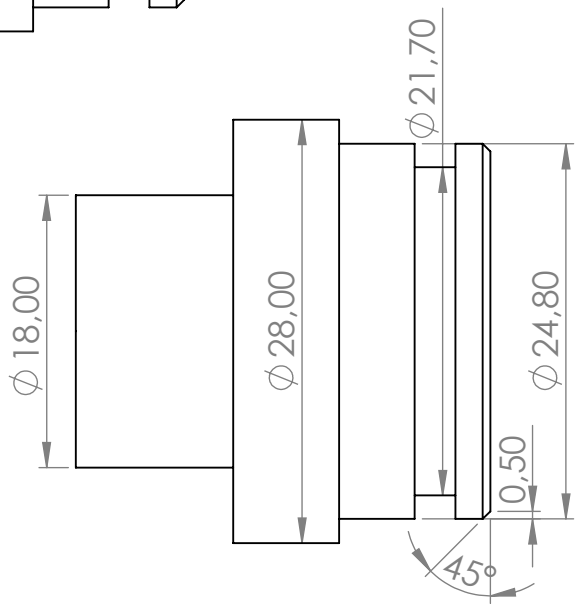


DO NOT SCALE DRAWING

AUTHOR: Ad Hoek 4445058

TITLE: Cylinder_HF_cap_h2o

MATERIAL: 7075-T6

A4

SCALE: 2:1

SHEET 1 OF 1

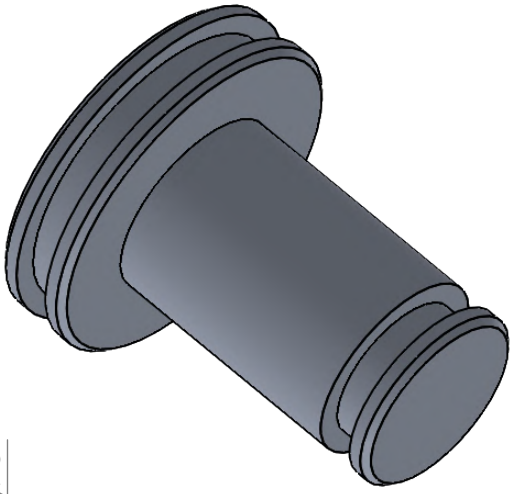

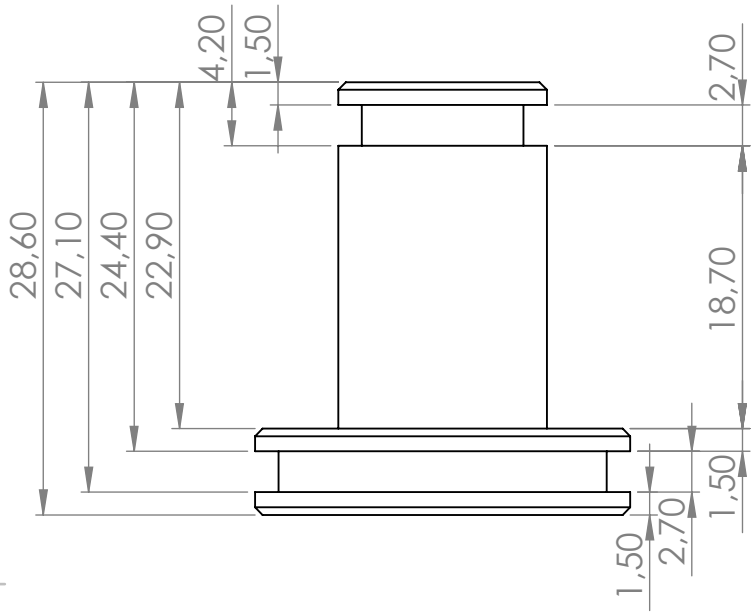


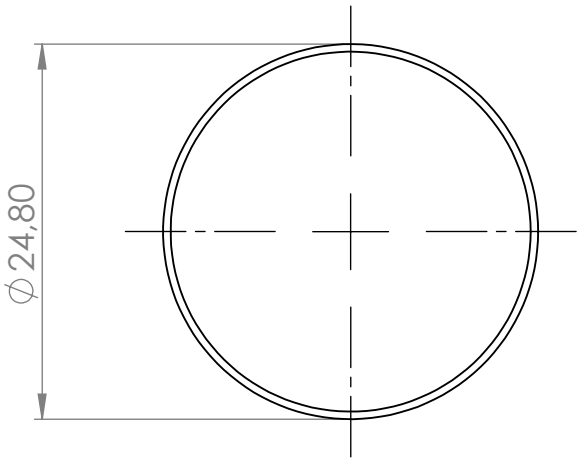


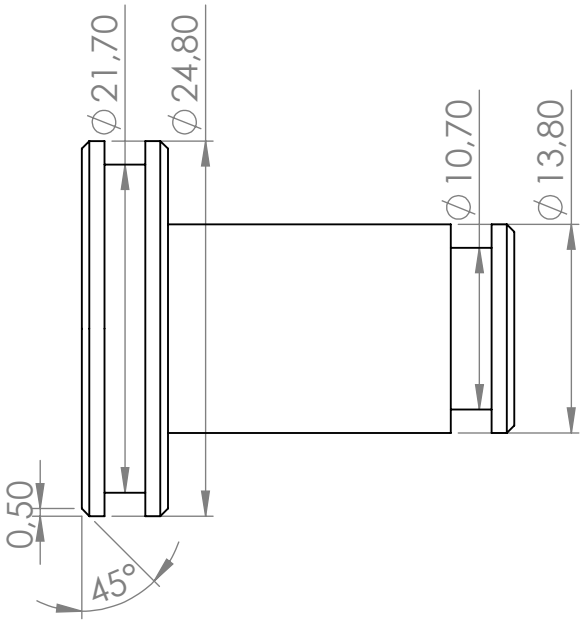


| | |
|---|---|
| DO NOT SCALE DRAWING | |
| AUTHOR: Ad Hoek 4445058 | |
| TITLE: Cylinder_HF_slide | |
| MATERIAL: 7075-T6 | A4 |
| SCALE: 2:1 | SHEET 1 OF 1 |

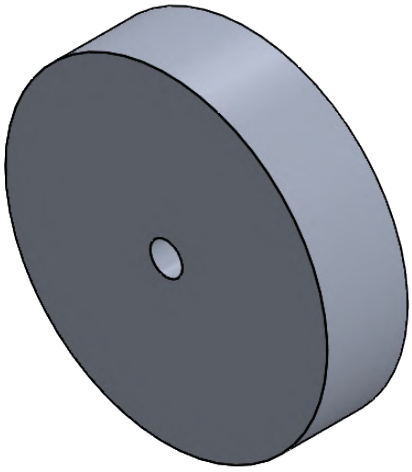

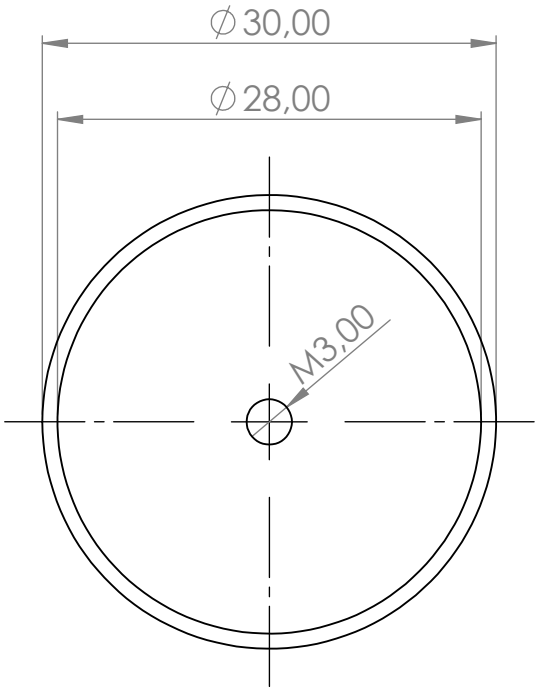


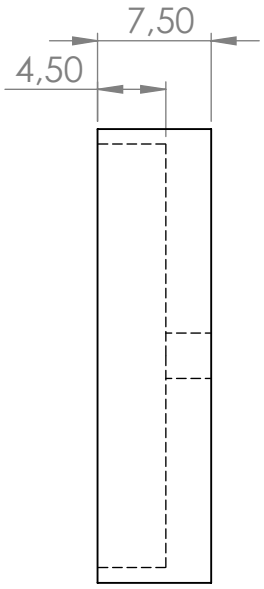


DO NOT SCALE DRAWING

AUTHOR: Ad Hoek 4445058

TITLE: Cylinder_HS_cap_co2

MATERIAL: 7075-T6

A4

SCALE: 2:1

SHEET 1 OF 1

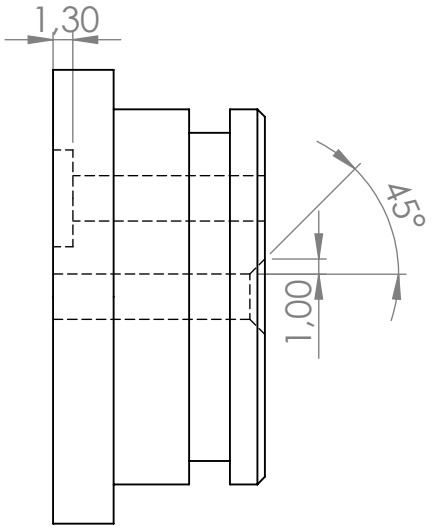


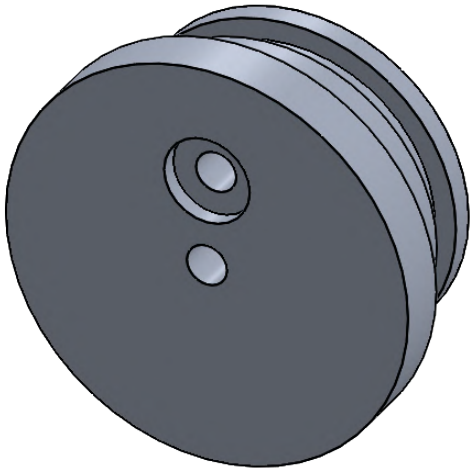

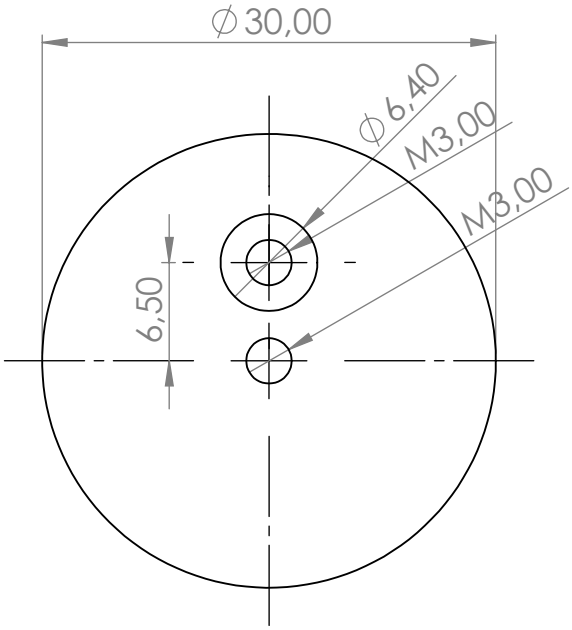


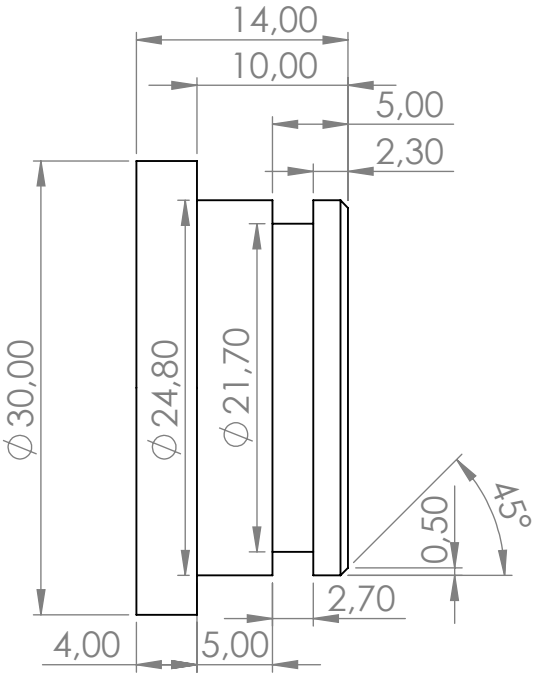


| | |
|---|---|
| DO NOT SCALE DRAWING | |
| AUTHOR: Ad Hoek 4445058 | |
| TITLE: Cylinder_HS_cap_h2o_inside | |
| MATERIAL: 7075-T6 | A4 |
| SCALE: 2:1 | SHEET 1 OF 1 |

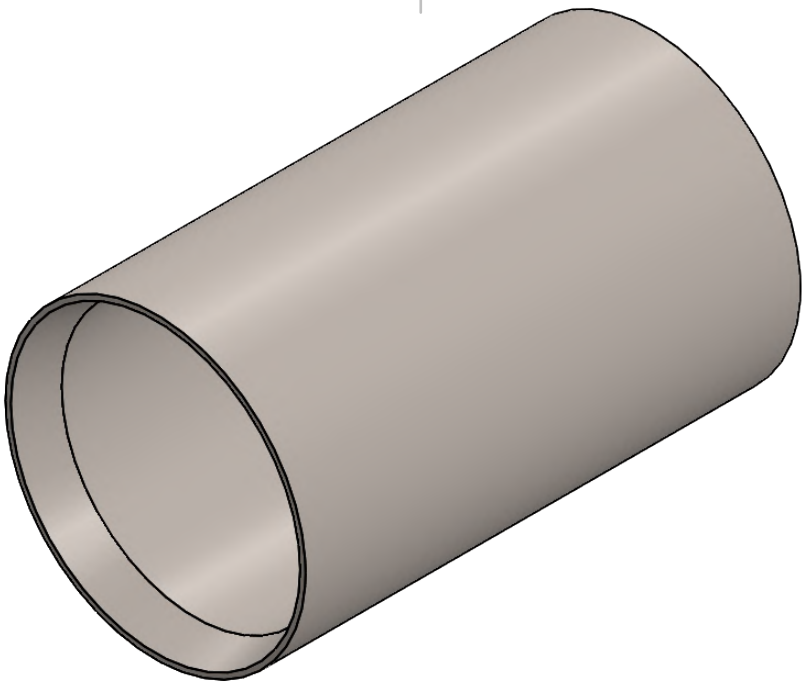

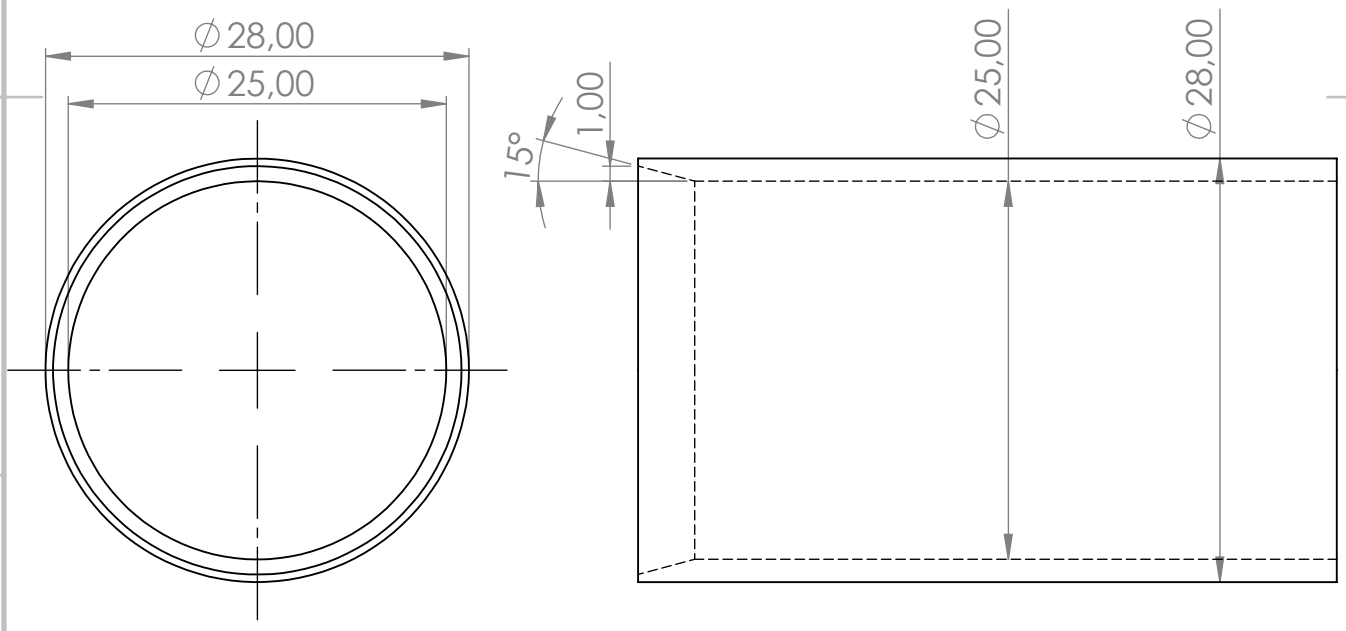


Salomon's metalen: 316(L) naadloze buis
28,00 x 1,50 mm

| | |
|---|---|
| DO NOT SCALE DRAWING | |
| AUTHOR: Ad Hoek 4445058 | |
| TITLE: Cylinder_HS_mid | |
| MATERIAL: RVS 316(L) | A4 |
| SCALE: 2:1 | SHEET 1 OF 1 |

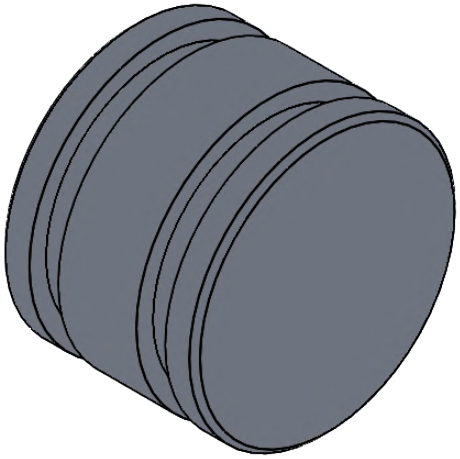

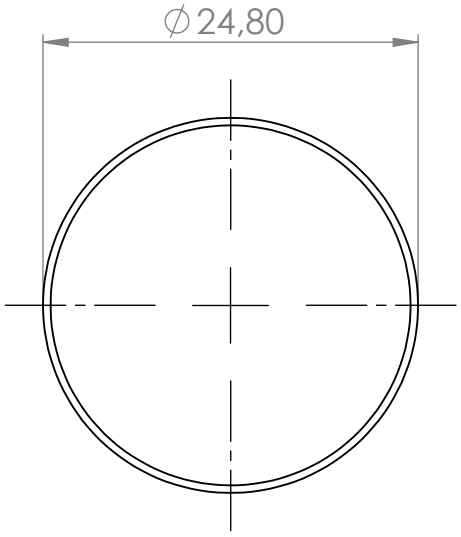


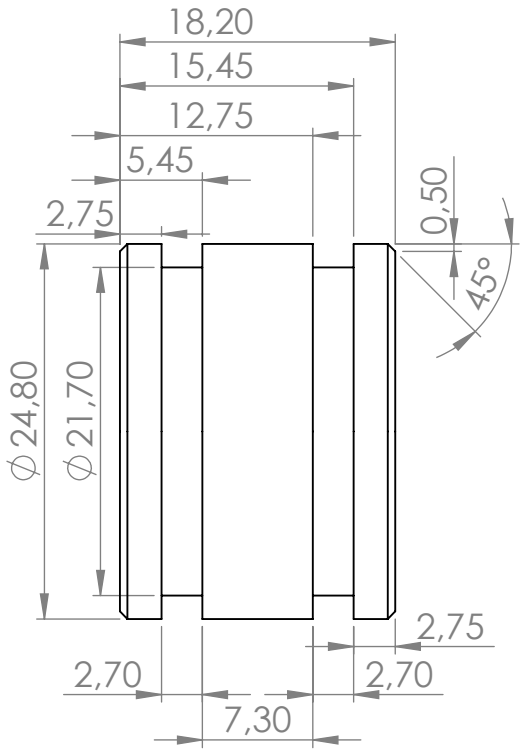


| | |
|---|---|
| DO NOT SCALE DRAWING | |
| AUTHOR: Ad Hoek 4445058 | |
| TITLE: Cylinder_HS_slide | |
| MATERIAL: 7075-T6 | A4 |
| SCALE: 2:1 | SHEET 1 OF 1 |

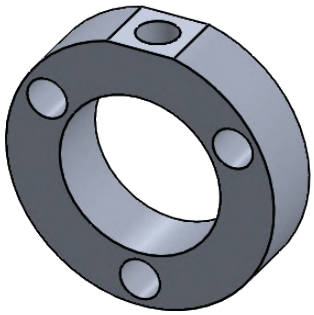

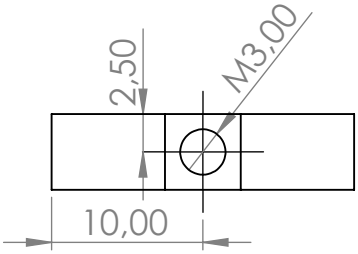


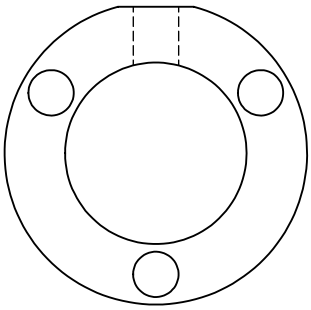

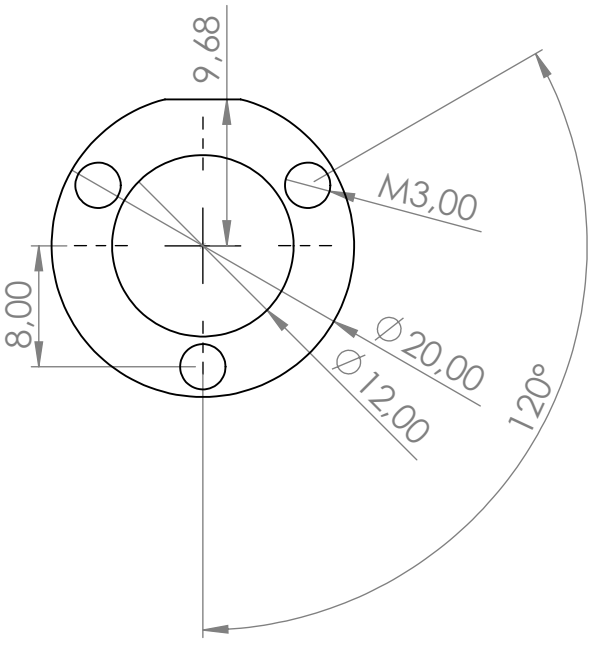


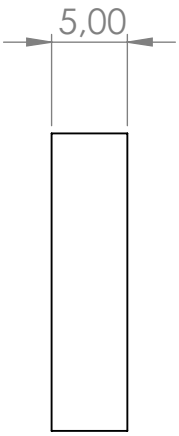


| | |
|---|---|
| DO NOT SCALE DRAWING | |
| AUTHOR: Ad Hoek 4445058 | |
| TITLE: Lock_connector | |
| MATERIAL: 7075-T6 | A4 |
| SCALE: 2:1 | SHEET 1 OF 1 |

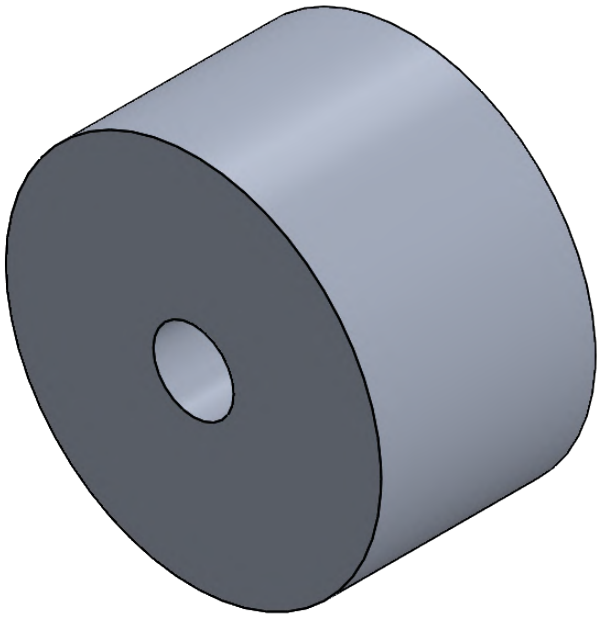

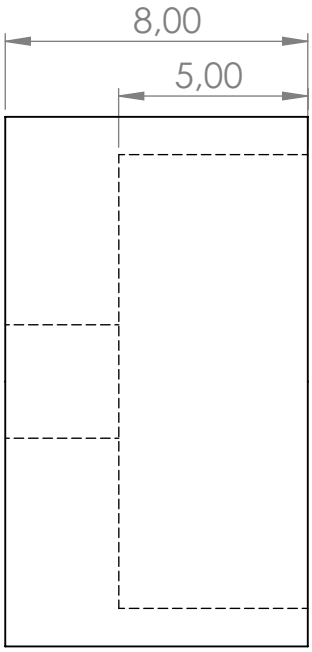


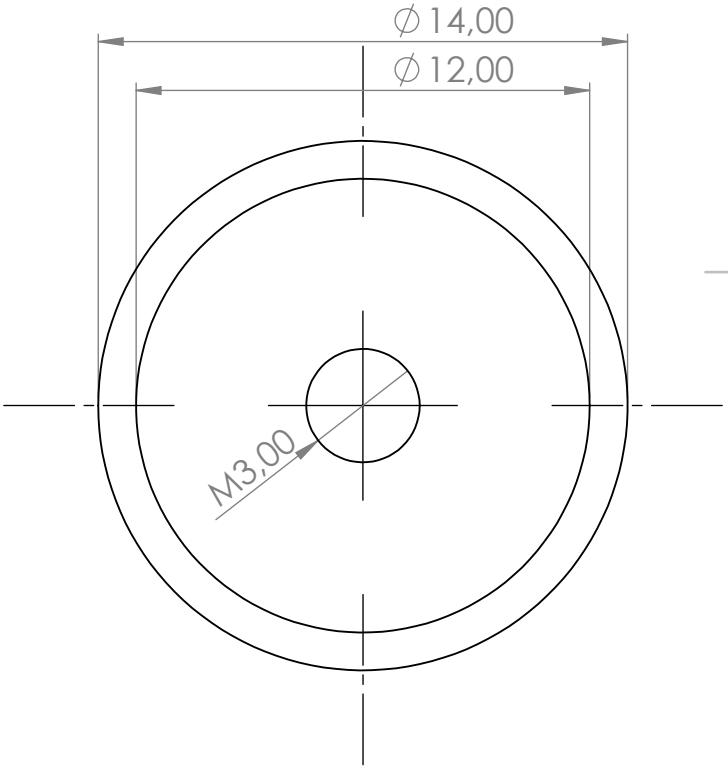


| | |
|---|---|
| DO NOT SCALE DRAWING | |
| AUTHOR: Ad Hoek 4445058 | |
| TITLE: Lock_cylinder_cap_co2 | |
| MATERIAL: 7075-T6 | A4 |
| SCALE: 5:1 | SHEET 1 OF 1 |

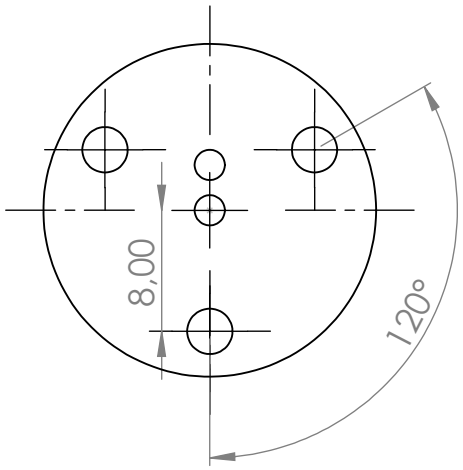


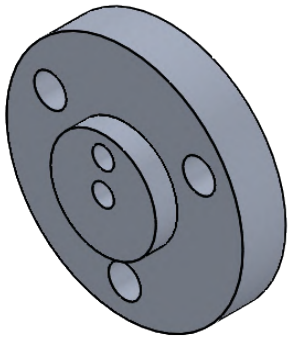

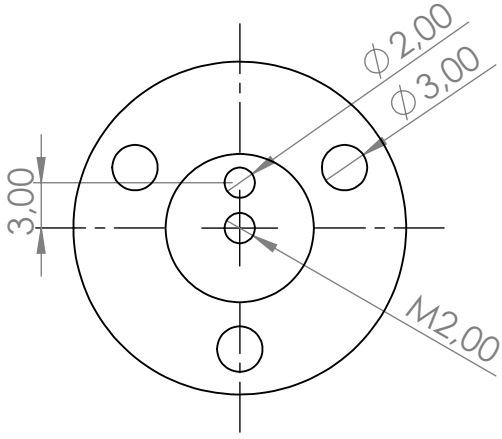


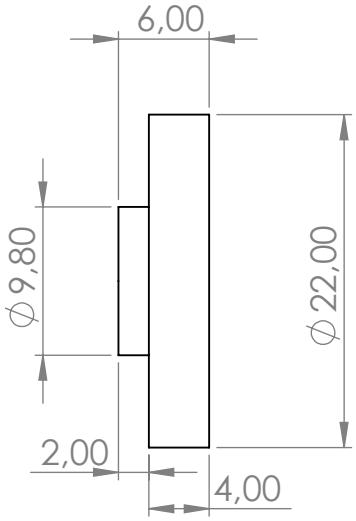


DO NOT SCALE DRAWING

AUTHOR: Ad Hoek 4445058

TITLE: Lock_cylinder_cap_inside

MATERIAL: 7075-T6

A4

SCALE: 2:1

SHEET 1 OF 1

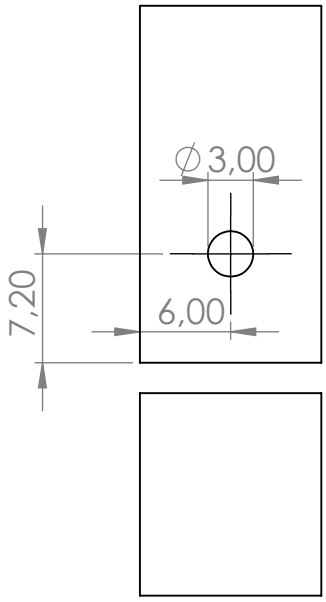


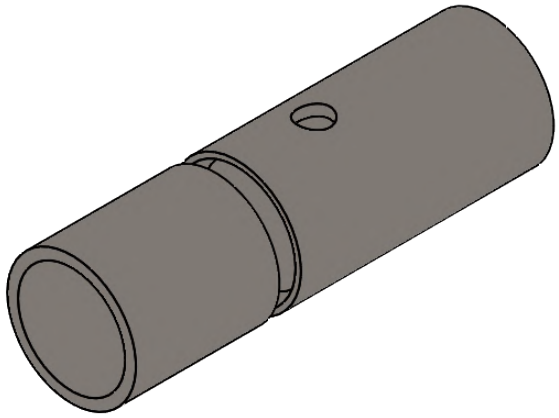

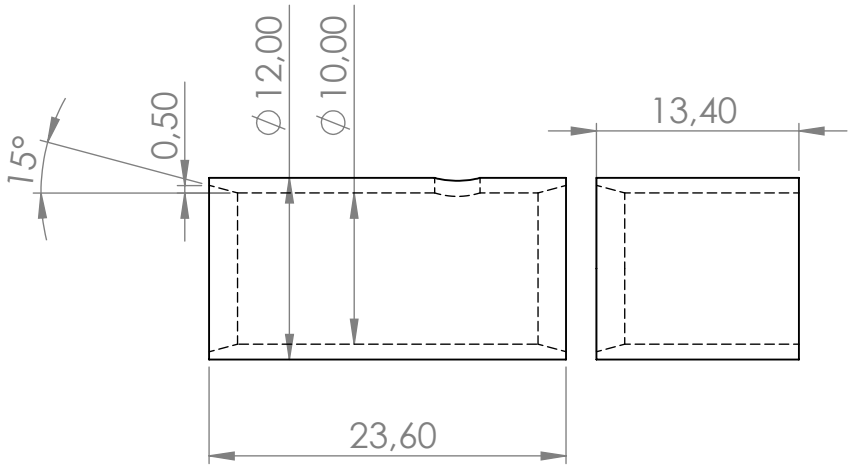


Salomon's metalen: 316(L) naadloze buis
12,00 x 1,00 mm

| | |
|---|---|
| DO NOT SCALE DRAWING | |
| AUTHOR: Ad Hoek 4445058 | |
| TITLE: Lock_cylinder_mid | |
| MATERIAL: RVS 316(L) | A4 |
| SCALE: 2:1 | SHEET 1 OF 1 |

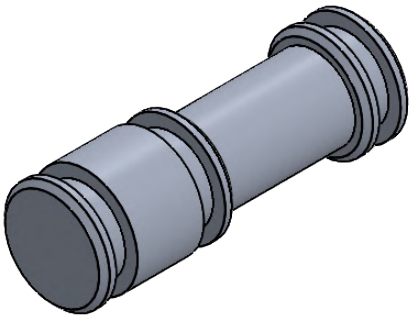

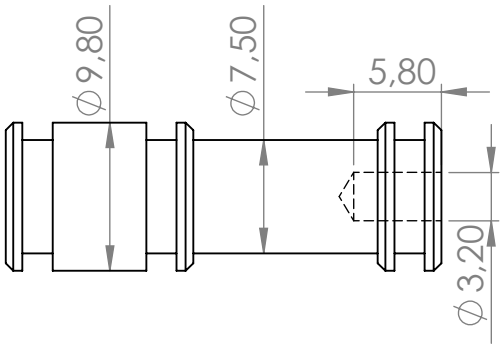


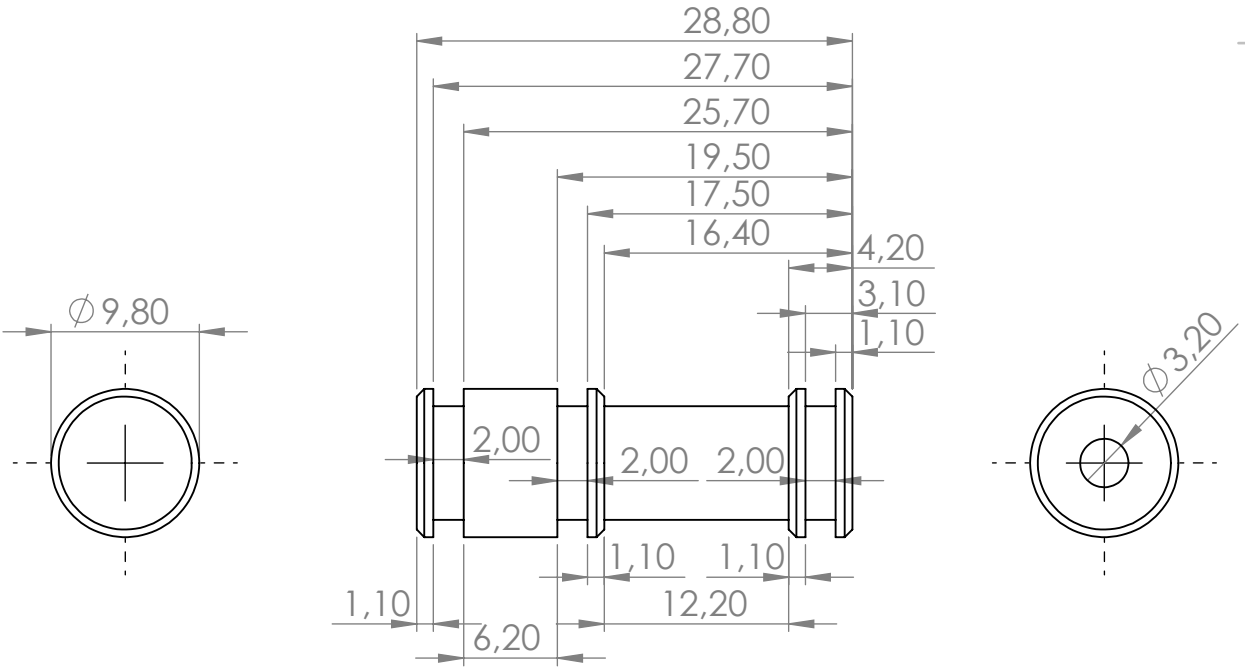


| | |
|---|---|
| DO NOT SCALE DRAWING | |
| AUTHOR: Ad Hoek 4445058 | |
| TITLE: Lock_cylinder_slide | |
| MATERIAL: 7075-T6 | A4 |
| SCALE: 2:1 | SHEET 1 OF 1 |

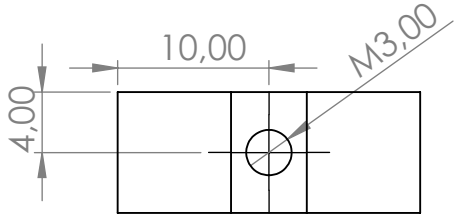


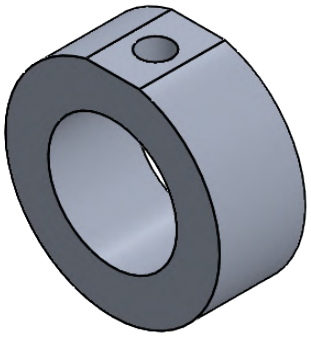

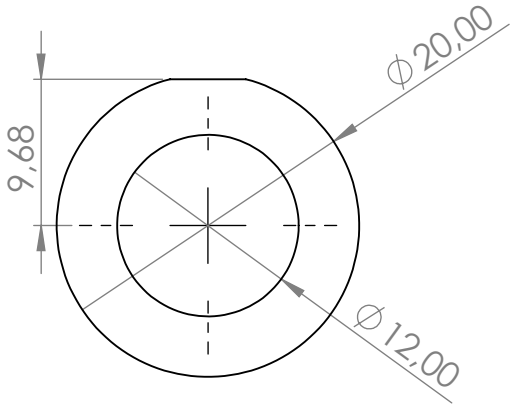


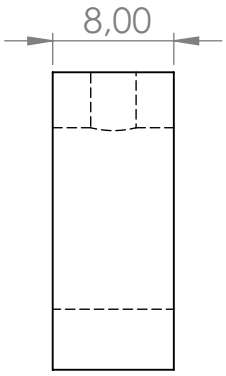


| | |
|---|---|
| DO NOT SCALE DRAWING | |
| AUTHOR: Ad Hoek 4445058 | |
| TITLE: Lock_pipe_connector | |
| MATERIAL: 7075-T6 | A4 |
| SCALE: 2:1 | SHEET 1 OF 1 |

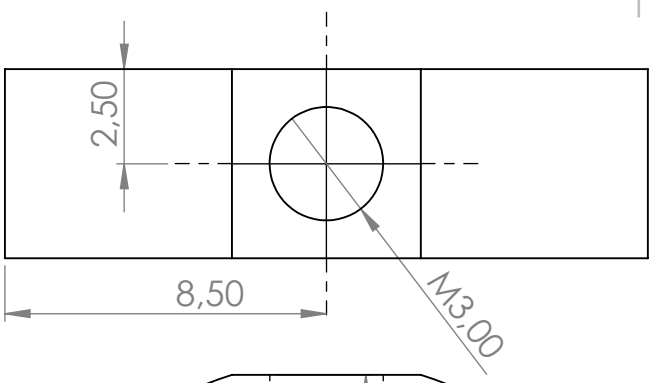


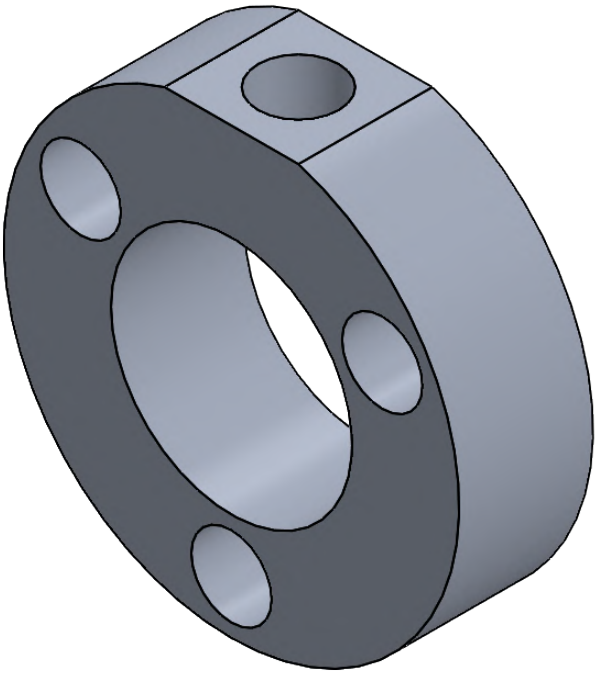

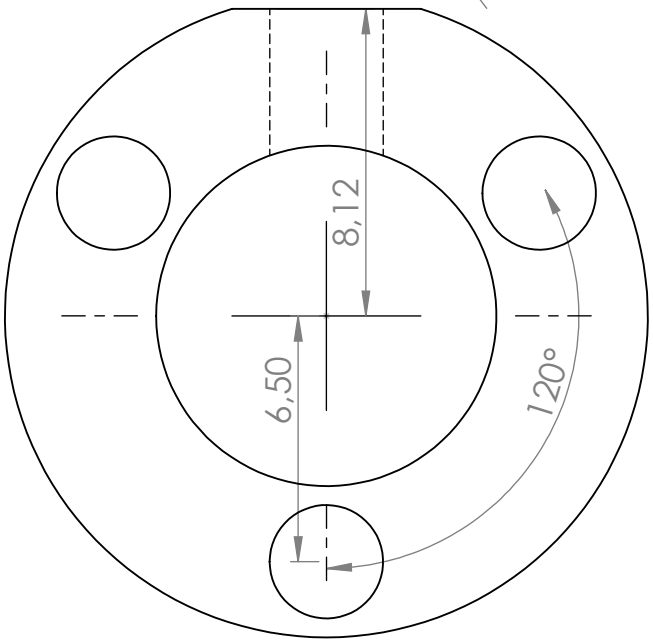


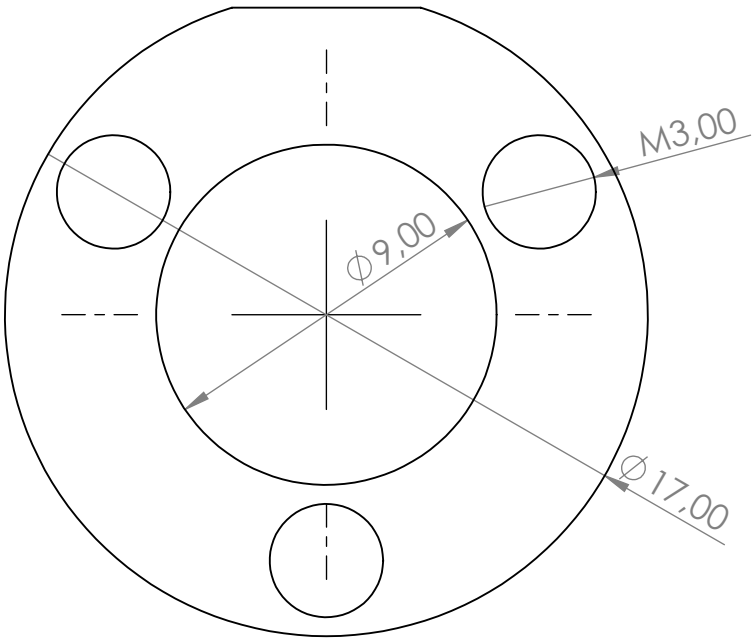


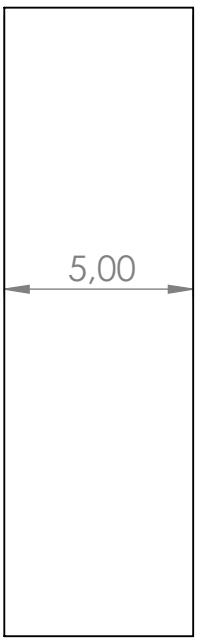


DO NOT SCALE DRAWING

AUTHOR: Ad Hoek 4445058

TITLE: Reg_connector

MATERIAL: 7075-T6

A4

SCALE: 5:1

SHEET 1 OF 1

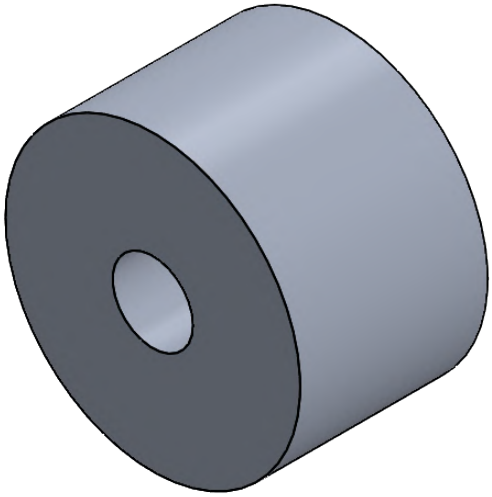

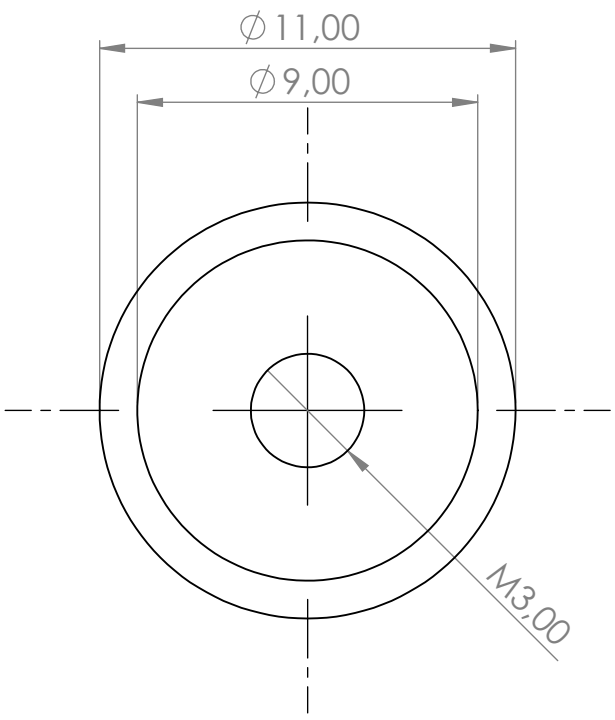


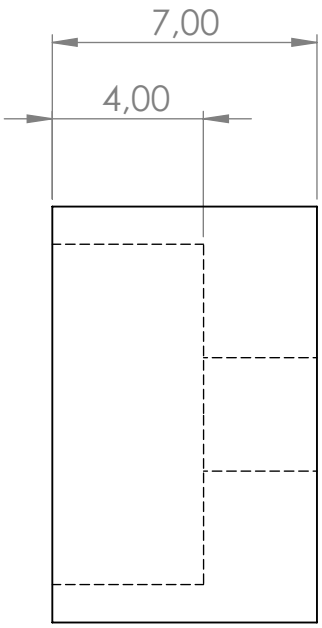


| | |
|---|---|
| DO NOT SCALE DRAWING | |
| AUTHOR: Ad Hoek 4445058 | |
| TITLE: Reg_cylinder_cap_co2 | |
| MATERIAL: 7075-T6 | A4 |
| SCALE: 5:1 | SHEET 1 OF 1 |

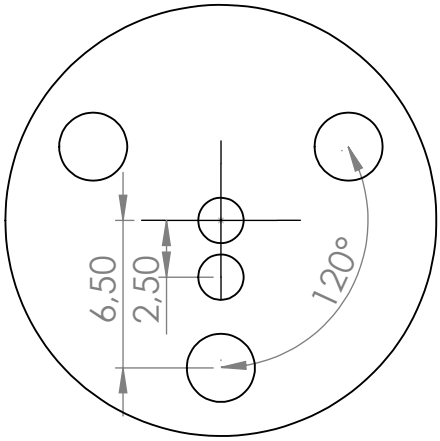


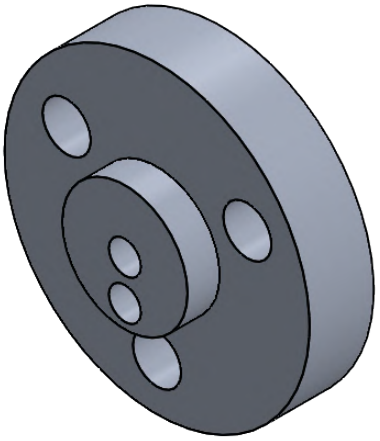

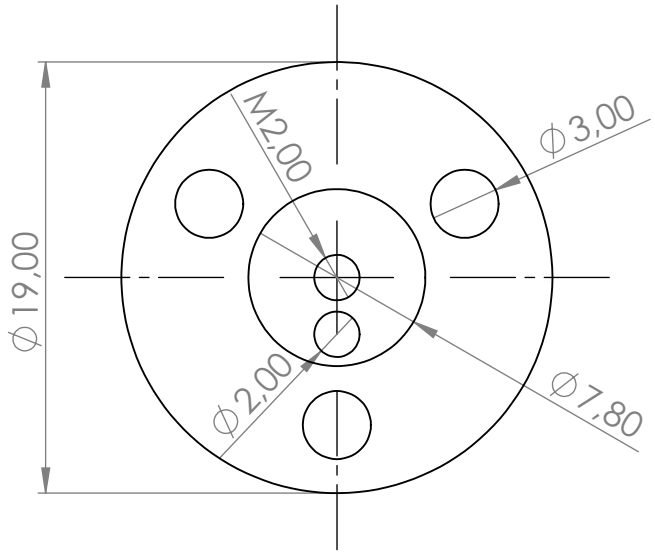


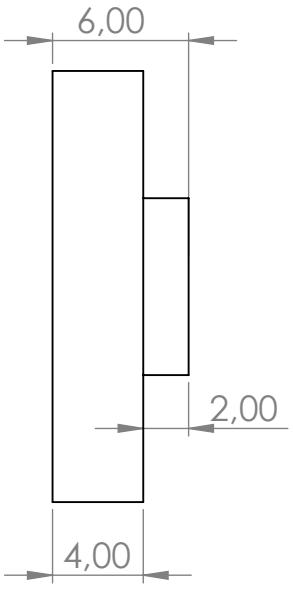


DO NOT SCALE DRAWING

AUTHOR: Ad Hoek 4445058

TITLE: Reg_cylinder_cap_inside

MATERIAL: 7075-T6

A4

SCALE: 3:1

SHEET 1 OF 1

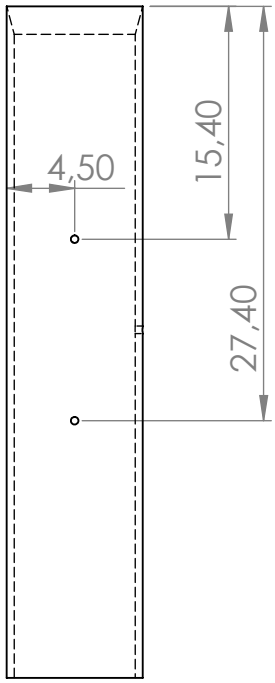


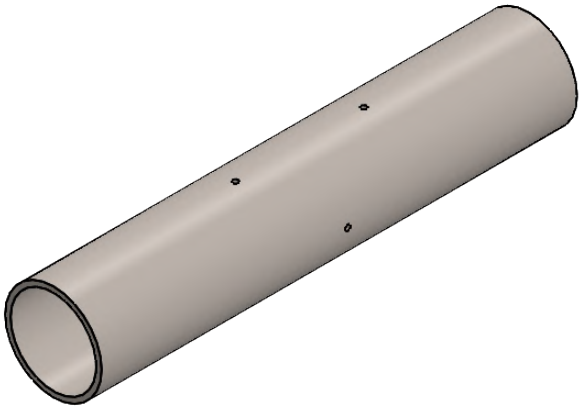

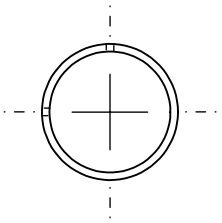

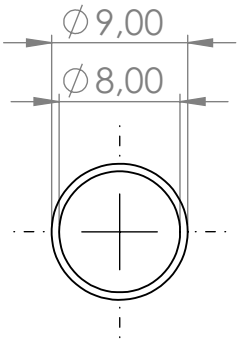


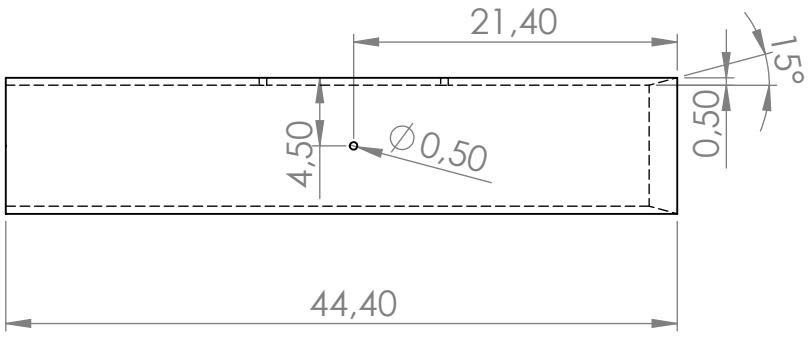


Salomon's metalen: 316(L) naadloze buis
9,00 x 0,50 mm

| | |
|---|---|
| DO NOT SCALE DRAWING | |
| AUTHOR: Ad Hoek 4445058 | |
| TITLE: Reg_cylinder_mid | |
| MATERIAL: RVS 316(L) | A4 |
| SCALE: 2:1 | SHEET 1 OF 1 |

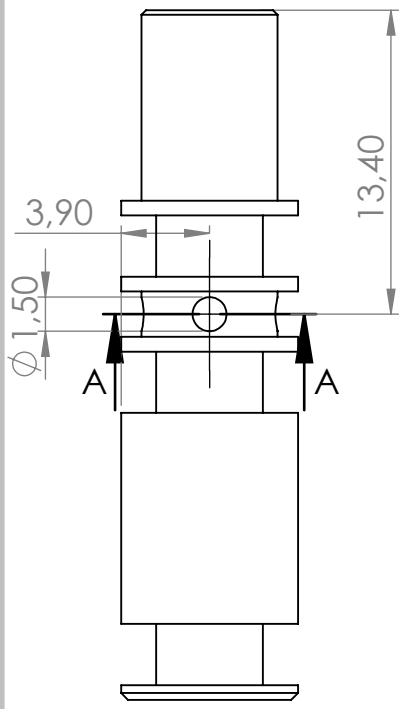


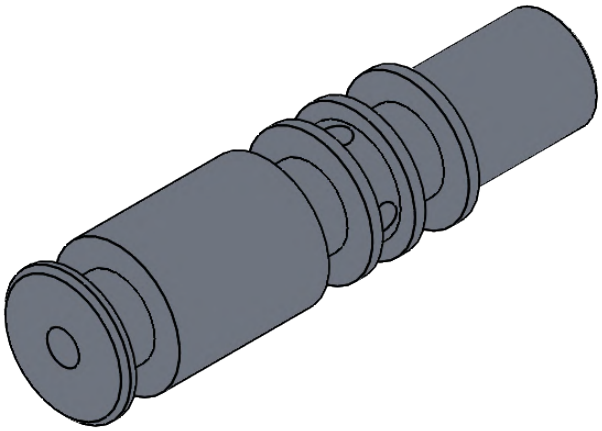

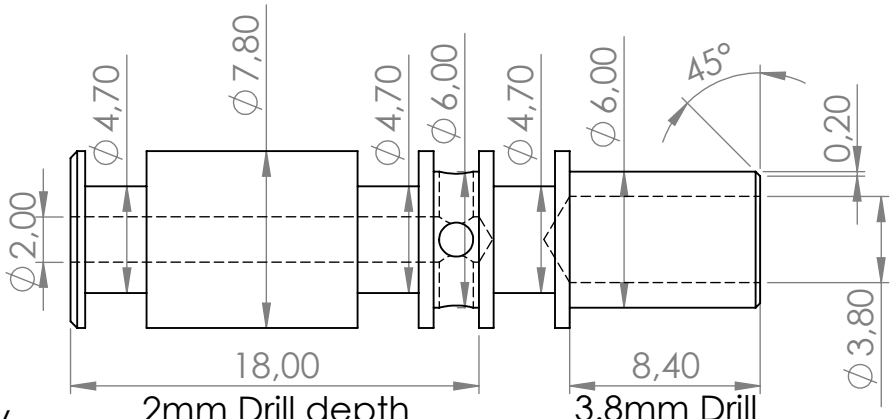


1.5mm Drill through twice perpendicularly

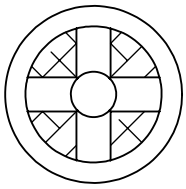

SECTION A-A
SCALE 3 : 1

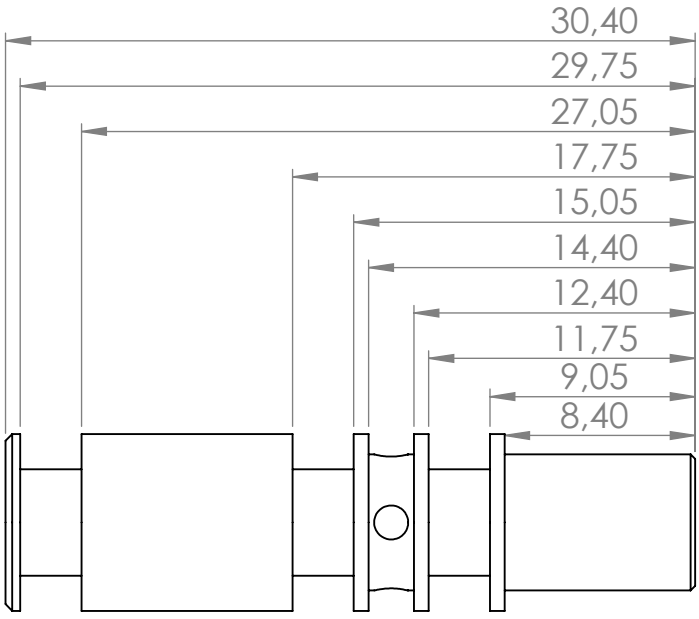


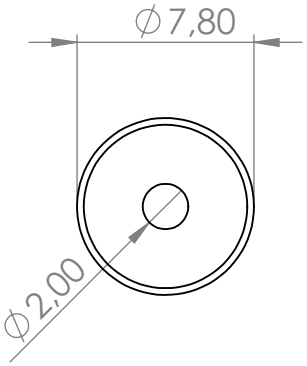


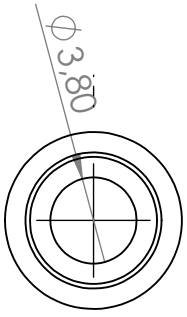


DO NOT SCALE DRAWING

AUTHOR: Ad Hoek 4445058

TITLE: Reg_cylinder_slide

MATERIAL: 7075-T6

A4

SCALE: 3:1

SHEET 1 OF 1

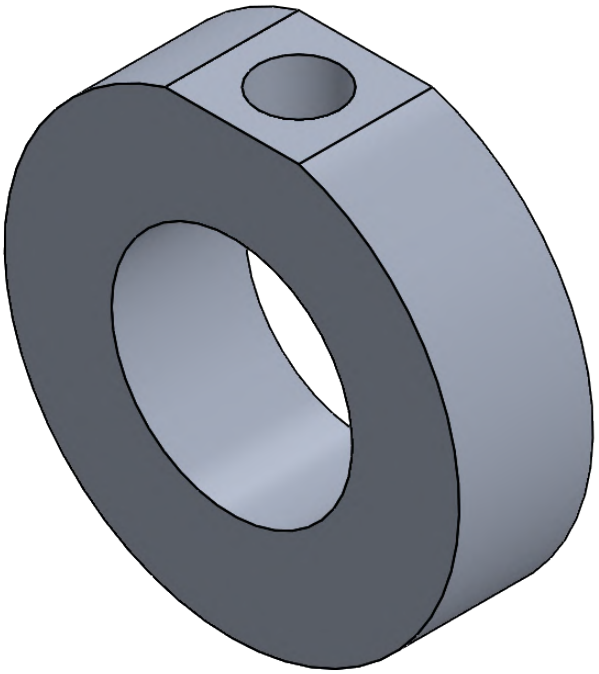

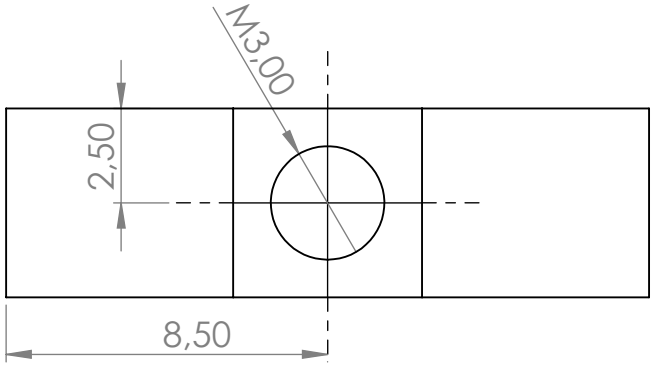


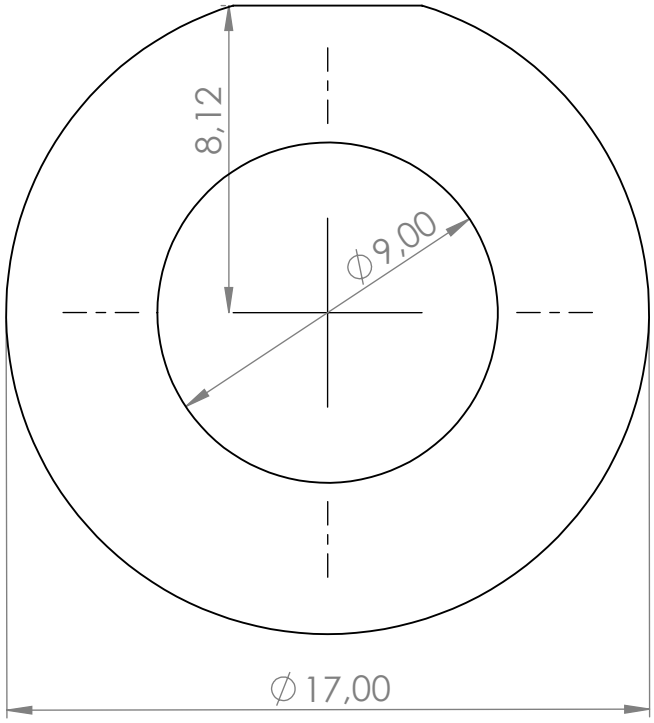


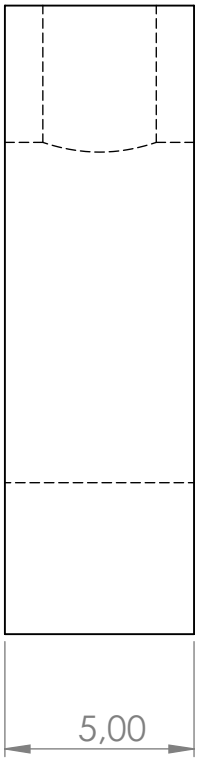


# Make 2 times

| | |
|---|---|
| DO NOT SCALE DRAWING | |
| AUTHOR: Ad Hoek 4445058 | |
| TITLE: Reg_pipe_connector_TWICE | |
| MATERIAL: 7075-T6 | A4 |
| SCALE: 5:1 | SHEET 1 OF 1 |

# D

# Laser cutting drawings

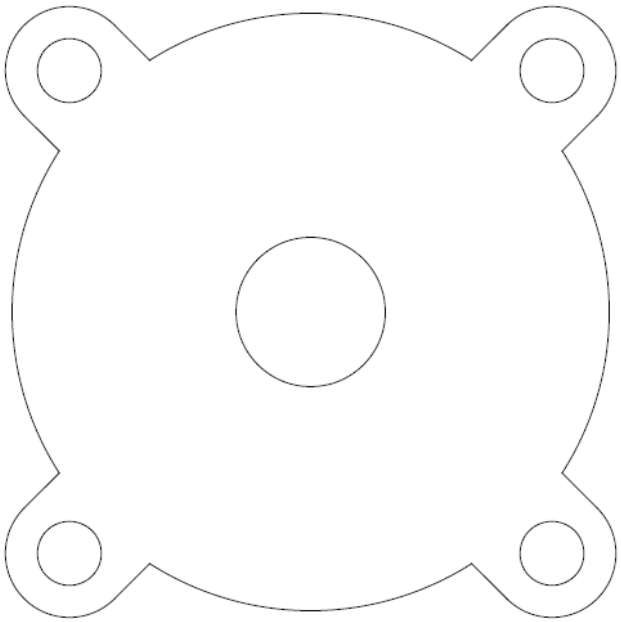

Cylinder_HF_clamp_co2 Scale 4:1

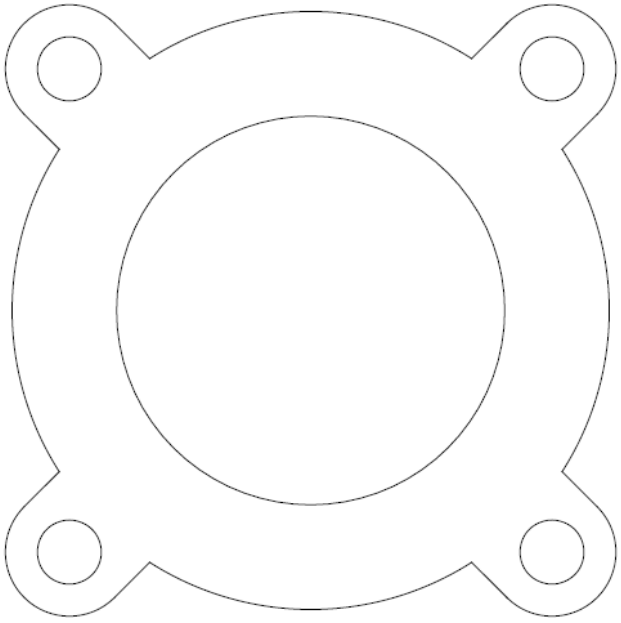

Cylinder_HF_clamp_h2o Scale 4:1

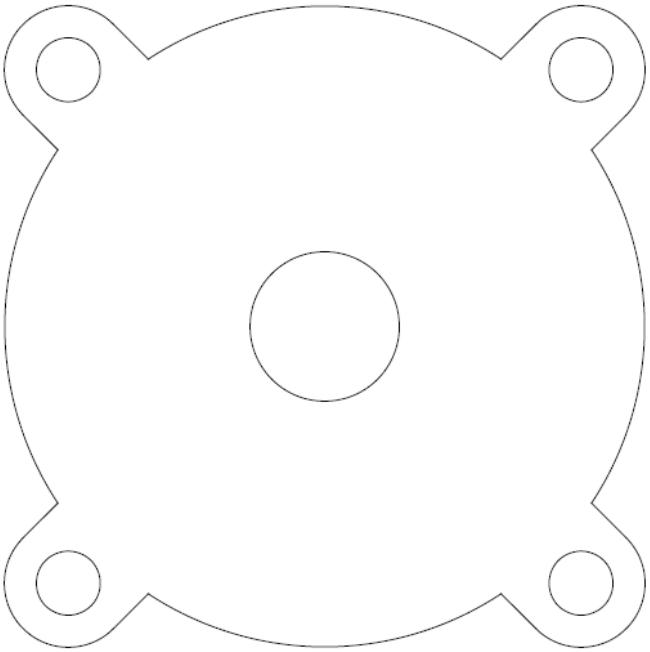

Cylinder_HS_clamp_co2 Scale 4:1

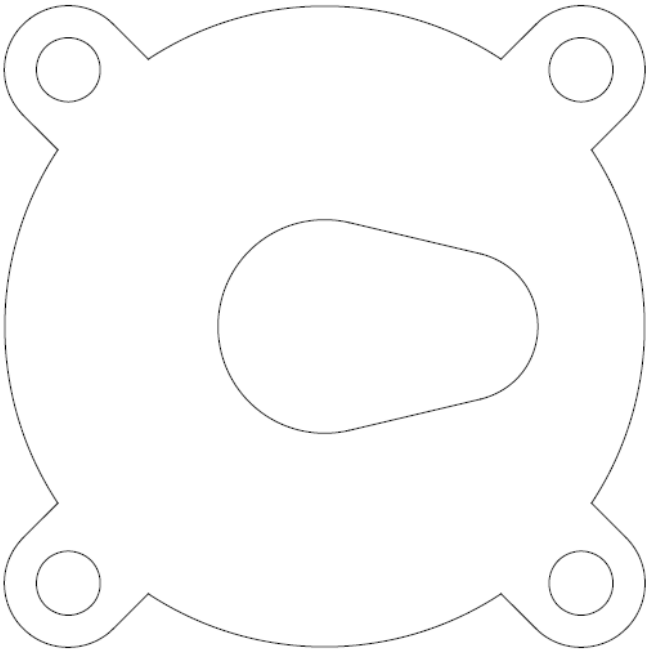

Cylinder_HS_clamp_h2o Scale 4:1

# E

# Prototype parts

Cylinder_HF_cap_co2

Cylinder_HF_cap_h2o (1/2)

Cylinder_HF_cap_h2o (2/2)

Cylinder_HF_slide

Cylinder_HS_cap_co2

Cylinder_HS_cap_h2o_inside (1/2)

Cylinder_HS_cap_h2o_inside (2/2)

Cylinder_HS_mid

Cylinder_HS_slide

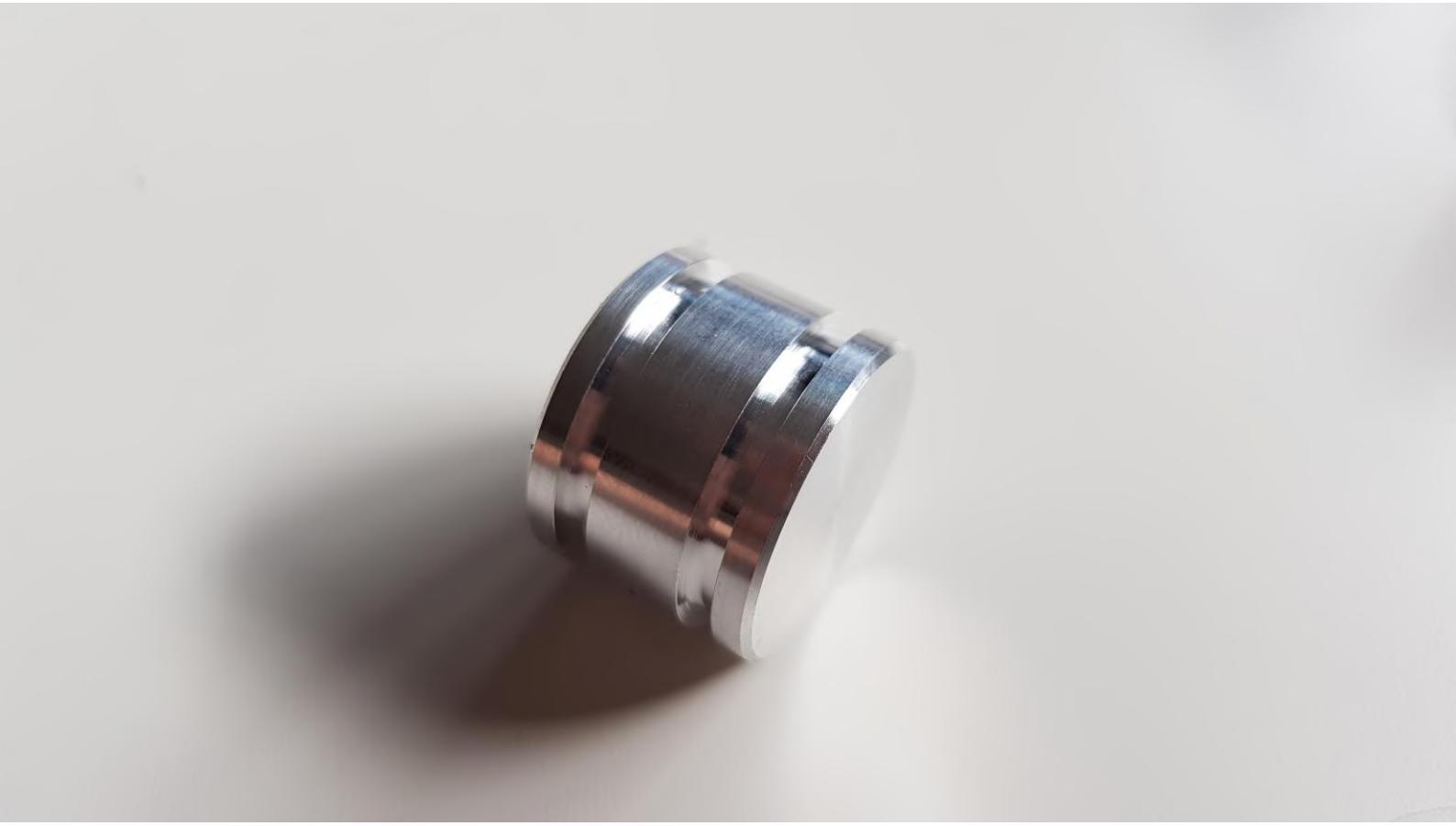

Lock_connector

Lock_cylinder_cap_co2

Lock_cylinder_cap_inside

Lock_cylinder_mid

Lock_cylinder_slide

Lock_pipe_connector

Reg_connector

Reg_cylinder_cap_co2

Reg_cylinder_cap_inside

Reg_cylinder_mid

Reg_cylinder_slide (1/2)

# Reg_cylinder_slide (2/2)

# Reg_pipe_connector_TWICE

Cylinder_HF_clamp_(co2 & h2o)

Cylinder_HS_clamp_(co2 & h2o)